THE DEVELOPMENT AND EVALUATION OF THE SUNSCREEN PRODUCT FOR UV-VISIBLE PROTECTION

ONJIRA CHUNNAWONG

A Thesis Submitted to the Graduate School of Naresuan University
in Partial Fulfillment of the Requirements
for the Master of Science in (Cosmetic Sciences)
2019

THE DEVELOPMENT AND EVALUATION OF THE SUNSCREEN PRODUCT FOR UV-VISIBLE PROTECTION

ONJIRA CHUNNAWONG

A Thesis Submitted to the Graduate School of Naresuan University
in Partial Fulfillment of the Requirements
for the Master of Science in (Cosmetic Sciences)
2019

Thesis entitled "The development and evaluation of the sunscreen product for UV-Visible protection"
By ONJIRA CHUNNAWONG
has been approved by the Graduate School as partial fulfillment of the requirements
for the Master of Science in Cosmetic Sciences of Naresuan University

Oral Defense Committee

.... Chair
(Assistant Professor Walaisiri Muangsiri, Ph.D.)

.... Advisor
(Associate Professor Tasana Pitaksuteepong, Ph.D.)

.... Internal Examiner
(Associate Professor Srisagul Sungthongjeen, Ph.D.)

.... Internal Examiner
(Assistant Professor Anothai Tangsumranjit, Ph.D.)

Approved

....
(Professor Paisarn Muneesawang, Ph.D.)

for Dean of the Graduate School

Title	THE DEVELOPMENT AND EVALUATION OF THE SUNSCREEN PRODUCT FOR UV-VISIBLE PROTECTION
Author	ONJIRA CHUNNAWONG
Advisor	Associate Professor Tasana Pitaksuteepong, Ph.D.
Academic Paper	Thesis M.S. in Cosmetic Sciences, Naresuan University, 2019
Keywords	Visible light Blue light Organic UV filter Inorganic UV filter Titanium dioxide Zinc oxide Iron oxide Particle size Surface coating Porphyrin protection factor

ABSTRACT

This study aimed to develop and evaluate the sunscreens protected against UV and visible light radiation. The development of sunscreens was started from the survey of the frequently used UV filters in the commercial products. The UV filter which showed high frequency of usage were selected for screening of UV and visible light protective ability. The selected inorganic UV filters/pigments were studied the effect of particle size and surface coating on UV and visible light protection. The filters having the maximum efficacy in UV and visible light protection were selected to incorporate in the sunscreen formulations. The colored sunscreens were developed and evaluated their efficacy based on the measurement of the UV and blue/visible light transmission through sunscreen film applied on a substrate. The indicated parameters were sun protection factor (SPF; UVB protection), UVA protection factor (UVAPF; UVA protection), and porphyrin protection factor (PPF; Blue light protection). The formulated sunscreens were again investigated the UV protective efficiency by internationally recognized methods. The selected UV and Vis filters were studied the effect on blue light protection in different types of base formulation. Finally, the developed color sunscreen was proved the blue light protection ability by the comparison with the commercial sunscreen products claimed to protect blue light radiation. From the survey, the selected UV filters were included in the study such as

Butyl methoxydibenzoylmethane (BMDM), Ethylhexyl methoxycinnamate (EHMC), Bis-ethylhexyloxyphenol methoxy-phenyl Triazine (BEMT), Octocrylene (OCR), Ethylhexyl salicylate (EHS), Homosalate (HMS), Diethylamino hydroxybenzoyl hexyl benzoate (DHHB), Ethylhexyl triazone (EHT), Methylene bis-benzotriazolyl tetramethyl-butylphenol (MBBT). The new generation UV filters such Tris-biphenyl triazine (TBPT), and Bis-ethylhexyloxy-phenol methoxyphenyl triazine (and) polymethyl methacrylate (BENT AQ) were also included. Among these filters, only TBPT could provide the absorptive efficiency covering from UV to visible light wavelength. The inorganic UV filters/pigments included in the study were titanium dioxide (TiO_2) and zinc oxide (ZnO). The effect of their particle size and surface coating on UV and visible light protection showed that, nanosize TiO_2 provided better UV protection than submicronsize TiO_2. Less significant different in UV protection was found between surface coated and uncoated nanosize TiO_2. The uncoated submicronsize TiO_2 showed the best protection in the blue/visible light wavelength, followed by coated submicronsize TiO_2 and nanosized TiO_2. The iron oxides having submicronsize showed better protection in both UV and visible light wavelengths, compared with those having micronsize. The addition of blended iron oxides to TiO_2 can enhance the protection against UV and visible light compared to TiO_2 alone. However, this was in the case only for uncoated and coated nanosized, coated submicronsize, not for uncoated submicronsize TiO_2. The combination of colored sunscreen with TBPT can improve both UVB, UVA and blue light protection in term of SPF, UVAPF, and PPF values respectively. In addition, the base formulations were greatly affected the protective ability against blue light radiation. The developed color sunscreen provided the SPF more than 50, UVAPF followed the requirement of European regulation, and PPF more than the commercial sunscreen products available on the market in protecting the blue light radiation. These studies were clear that different physicochemical properties of UV and Vis filters play a crucial role in their ability to protect against UV and blue/visible light radiation.

ACKNOWLEDGEMENTS

I would first like to express my sincere gratitude to my thesis advisor, Associate Professor Dr.Tasana Pitaksuteepong, who gave me an opportunity to do this thesis. I would like to thank for her continuous support of my master study, her patience and motivation since the thesis started until successful. Her guidance has been a great help in improvement of my thesis.

Besides my advisor, I would like to offer my special thanks to the thesis committees; Associate Professor Dr. Srisagul Sungthongjeen, Assistant Professor Dr. Anothai Tangsumranjit, and Assistant Professor Dr. Walaisiri Muangsiri for the advices and comments. All your kindness will always be remembered.

My grateful thanks are also extended to Ms. Supaporn Tuanthai at the research center for cosmetics and natural products (COSNAT) for her assistance and technical support during the UV protection measurement of sunscreens. And I also thank the other staffs at the faculty of Pharmaceutical Sciences for suggest the instruction of laboratory equipment.

I would also like to acknowledge the following suppliers; The Sun chemical Co., Ltd. (Bangkok, Thailand), Bonanzatech Co., Ltd. (Bangkok, Thailand), Green Leaf Chemical Co., Ltd. (Bangkok, Thailand) and Athena Corp Co. Ltd. (Samutprakarn, Thailand) for providing the organic UV filters, inorganic UV filters/pigments , and iron oxides samples.

Finally, my graduation would not be achieved without supporting from my parents, who always believing in me and providing the financial support. And the last gratefully thanks for all concerned whose names are not mentioned for their helps and supports until my thesis has done. Thank you.

ONJIRA CHUNNAWONG

TABLE OF CONTENTS

Page

List of tables

List of figures

Page

ABBREVIATIONS

4-MBC	4-methylbenzylidene camphor
λ_C	Critical wavelength
λ_{Vis}	Visible protection wavelength
˚C	Degree Celsius
A (1%, 1cm)	A One One
AUC	Area under the curve
BEMT	Bis-Ethylhexyloxyphenol Methoxyphenyl Triazine
BEMT AQ	Bis-Ethylhexyloxyphenol Methoxyphenyl Triazine (and) polymethyl methacrylate
BL	Blue light
BMDM	Butyl methoxydibenzoylmethane
BZ-3	Benzophenone-3
CAMKII	Calmodulin-dependent protein kinase
CAS number	Chemical Abstracts Service Registry Number
COLIPA	The European Cosmetic toiletry and Perfumery Association
CREB	Cyclic adenosine monophosphate response element binding protein
DHBT	Diethylhexyl butamido triazone
DHHB	Diethylamino hydroxybenzoyl hexyl benzoate
DTS	Drometrizole trisiloxane
EC	European Commission
EC Number	European Community number
EHMC	Ethylhexyl methoxycinnamate
EHS	Ethylhexyl salicylate
EHT	Ethylhexyl triazone
EPP	Erythropoietic protoporphyria
ERK1/2	Extracellular signal-related kinase
EU	European
GPCR	G-protein coupled receptor
HEV	High energy visible light

HMS	Homosalate
IL	Interleukin
INCI	International nomenclature cosmetic ingredient
IPD	Immediate pigment darkening
IR	Infrared light
ISO	International standard organization
JCIA	Japan cosmetic industry association
MBBT	Methylene bis-benzotriazolyl tetramethylbutylphenol
mg	Miligram
min	Minute
MITF	Microphthalmia associated transcription factor
mL	Milliliter
MMP	Matrix metalloproteinase
OCR	Octocrylene
OPN3	Opsin 3
p38 MAP	*p38* mitogen-activated protein kinase
PA	Protection grade of UVA
PBSA	Phyenylbenzimidazole sulfonic acid
PMMA	Polymethylmethacrylate
PPD	Persistent pigment darkening
PPF	Porphyrin protection factor
PPIX	Protoporphyrin IX
PS-15	Polysilicone-15
RI	Refractive index
ROS	Reactive oxygen species
SCCP	Scientific Committee on Cosmetic Products and Non-Food Products
SPF	Sun protection factor
TBPT	Tris-biphenyl triazine
TDSA	Terephthalylidend camphor sulfonic acid
TiO_2	Titanium dioxide
UV	Ultraviolet

UVAPF	UVA protection factor
USFDA	United States Food and Drug Administration
ZnO	Zinc oxide

CHAPTER I

INTRODUCTION

Statement of problem

The prevention of skin damages from ultraviolet (UV; 290-400 nm) radiation have been concerned for a long time. Currently, it is known that the other portions of solar spectrum aside from UV, particularly visible light can also induce the damaging effects to human skin. Visible light represents about 40% of the solar radiation reaching the earth’s surface. Visible light covers wavelengths ranging from 400 to 800, which are longer than UV. It can deeply penetrate into the hypodermis layer and can induce substantial effects to skin (4). In the study by Liebel et al. (5), showed that irradiation of visible light in human epidermis caused reactive oxygen species (ROS) generation, which was a primary factor in the release of proinflammatory cytokines and matrix metalloproteinases (MMPs). Activation of these mediators result in oxidative stress, which lead to skin photoaging. Multiple exposures to visible light in skin explants have also been shown to induce persistent pigmentation from increasing of tyrosinase and melanogenic activities (6). A clinical study by Mahmoud et al. (7), showed that visible light also induced dark and long-lasting hyperpigmentation in skin type IV-VI. Visible light induced the pigment formation through somewhat different pathway from UV induction (8). These effects can be induced by the wavelengths having highest energy of visible light spectrum, particularly blue light (400-450 nm). According to study of Nakashima et al. (9) and Duteil et al. (10), reported that blue light was main source for stimulating the oxidative stress and hyperpigmentation. The other impact of visible light has been implicated in photosensitivity such as solar urticaria, chronic actinic dermatitis, and porphyria (11). These skin disorders can limit the outdoor activity and decrease quality of life of photosensitivity patients. Blue light also called as digital pollution, because it always be found on digital screen, electronic devices, compact fluorescent, and LED light bulbs. Almost people spend time a day in front of these electronic equipment due to their daily routine or working. Prolonged exposure to blue light is increasingly associated with above described damaging effects.

As details above, exposure to blue/visible light can cause serious effects. The development of sunscreen products which could protect against these wavelengths are gaining interest as new generation sunscreen products. Schalka et al. (12), evaluated the efficacy of 13 colored sunscreens and 7 white sunscreens which were marketed in Brazil in the protection against visible light using a spectrophotometer and colorimetric measurements. The results showed that colored sunscreens gave better protection against visible light than white sunscreens. Almost of colored sunscreens investigated contained both organic non-particulate UV filters and opaque pigments. Castanedo-Cazares et al. (13) also demonstrated that a sunscreen containing BZ-3, EHMC, OCR, TiO_2, ZnO, and iron oxide (i.e. colored sunscreen) was shown to be better in the reduction of visible-light induced hyperpigmentation compared to that containing Mexoryl SX & XL, TiO_2, OCR, BEMT, BMDM, and EHT (i.e. white sunscreen). Both compared products contained organic and inorganic UV filters. Teramura et al. (11) demonstrated that the use of make-up base emulsion (containing EHMC, TiO_2, and iron oxide) together with powder foundation (containing EHMC, BZ-3, TiO_2, and iron oxide) or liquid foundation (EHMC, TiO_2, and iron oxide) could alleviate erythema and edema in Japanese patients with erythropoietic protoporphyria, a disease characterized by photosensitivity to visible light by 78.3% of patients. All three products contained both organic and inorganic UV filters. Recently, Martini & Maia Campos (14) showed that a sunscreen containing inorganic UV filters and pigment could provide better protection in the effect of visible light in cutaneous hyperchromias volunteers compared with a sunscreen containing inorganic UV filters only.

Although the protection of visible light using sunscreens has been studied as described above, none of these studies have been systematically investigated on the efficacy of these compounds in the protection of visible light. In addition, no detailed information about optimizing characteristics of TiO_2, ZnO, and iron oxides for maximum visible light protection was provided. The characteristics influencing the efficacy of these compounds in visible light protection are such as particle size and surface coating etc. These data are essential for the development of sunscreen products which could protect against visible light.

This study was therefore aimed to screen the efficacy of the organic and inorganic UV filters which were frequently used in commercial products in the protection of UV and visible light. The inorganic pigments, including TiO_2, ZnO and iron oxides were also investigated. Finally, the sunscreen formulations which could protect UV and visible light were aimed to obtain.

Objectives of the study

1. General objective

To develop and evaluate the protective efficiency of sunscreens against UV and visible light radiation

2. Specific objectives

2.1 To survey of UV filters used in the commercial sunscreens

2.2 To screen the UV and visible light protective efficiency of organic UV filters

2.3 To screen the UV and visible light protective efficiency of inorganic UV filters and pigments

2.4 To develop the sunscreen formulations and evaluate their efficacy on the protection of UV and visible light

CHAPTER II

LITEATURE REVIEW

Human skin

Skin is the largest organ of human body that is directly contacted to the outside environment. It acts as a barrier against harmful external influences, maintains the regulation of body temperature as well as prevents moisture loss. The structure of human skin is divided into three main layers, epidermis, dermis, and hypodermis (**Figure 1**).

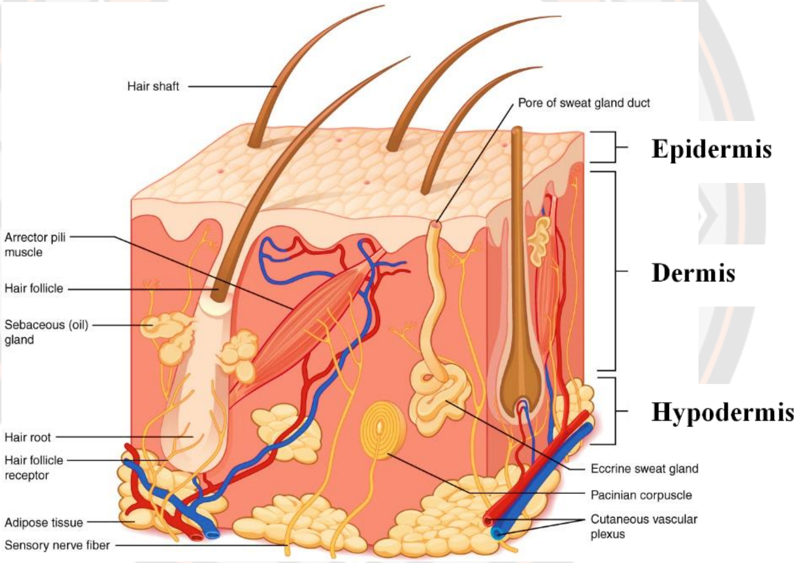

Figure 1 The structure of human skin *(*15*).*

Epidermis is the outermost layer of human skin with thickness about 0.05-1 mm depending on body part (16). Epidermis commonly is composed of five sublayers, from inner to outer layers as follows: stratum basal, stratum spinosum, stratum granulosum, stratum lucidum, and stratum corneum. The epidermis is composed of a variety of cells that have different morphology, shape, and function (**Figure 2**). The most abundant cells are keratinocytes, which account for 95% of total cells (17).

Stratum basal (Stratum germinativum, Basal cell layer) is a single sublayer that is in the deepest of epidermis. The basal layer is the primary location of mitotic divisions of keratinocyte stem cells that are constantly reproducing and pushing toward to replenish the epidermal cells above (18). These keratinocytes have cuboidal to columnar shape (19). Melanocyte is also found in this layer and it is responsible for the production of melanin pigment inside melanosome. The exposure to solar radiation stimulates the melanocytes to increase an melanogenesis and corresponding increase in melanin transfer to keratinocytes. The melanin functions by absorbing and blocking sunlight penetration into the skin. It is classified in two primary forms; eumelanin (black melanin) and pheomelanin (yellow melanin).

Stratum spinosum (Suprabasal cell layer, Squamous cell layer, prickle cell layer) lies on the stratum basal. The keratinocytes in this layer are polyhedral in shape with rounded nucleus. The cells are bridged with each other by desmosomes and communicated via chemical signal by gab junction. Langerhans also locate in this layer; it is a bone marrow-derived dendritic cell that serve antigen-processing and alloantigen stimulating functions.

Stratum granulosum (Granular cell layer) is a layer above stratum spinosum that containing living keratinocytes. These keratinocytes are composed of abundant keratohyalin granules in cytoplasm, which function in synthesis and modification of proteins involved in keratinization process.

Stratum lucidum (Stratum conjunctum, Clear layer) is thin and translucent layer that locates above from stratum granulosum. This layer could be found only in the palms of hands and soles of feet. The keratinocytes are transparent appearance due to they are densely packed with clear intercellular protein or eleidin that derive from keratohyalin.

Stratum corneum (Horny cell layer, Cornified layer) is the most superficial layer that provides mechanical protection to the underlying epidermis and a barrier to prevent water loss. The stratum corneum is the final layer of keratinization process that the keratinocytes are not alive, flattened shape, lost nuclei and cell organelles. The corneodesmosomes bridged between cells also undergo proteolytic degradation during desquamation, contributing to dead cell shedding from the surface of stratum corneum. These keratinocytes are known as corneocytes. The stratum corneum is described as brick (corneocytes) and motar (lipid-enriched intercellular matrix) structure; the corneocytes stack forming bilayers and is surrounded by a continuous intercellular matrix (16) and (20).

The period between the production of basal stem cells in the stratum basal, migration, differentiation to the upper layers and exfoliation from the outer surface of stratum corneum is called turnover time, which process approximately 4 weeks (28 days). However, the time varies depend on several factors including age, individual skin type, and environment.

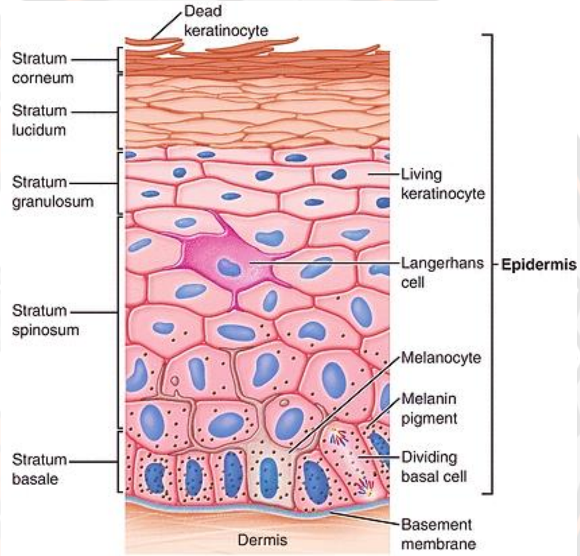

Figure 2 Schematic of epidermis–composed of five sublayers, from inner to outer layers as follows: stratum basal, stratum spinosum, stratum ganulosum, stratum lucidum, and stratum corneum (21). The keratinocyte stem cells at stratum basal are proliferated, differentiated and migrated towards to the stratum corneum (keratinization process).

Dermis is the middle layer of three main skin layers that is responsible for skin elastic and tensile strength. It is attached epidermis by the basement membrane and consists of three sublayers; papillary layer, subpapillary layer, and reticular layer. The dermis is an integral part of the body's connective tissue system that is composed of dermal extracellular matrix such as collagen fibers, elastin fibers, and ground substances. Collagen fibers especially type I and III are the most component of dermis (accounting for 80% of dermal extracellular matrix) that are synthesized by fibroblasts (19). The other cells reside in this layer including macrophages and mast cells. In addition, the dermis contains the hair follicles, nerves, sebaceous glands, apocrine glands, and sweat glands that can allow the sensation of pain and temperature.

Hypodermis (subcutaneous fat tissue, subcutis) is the deepest layer of the skin that functions as an energy reserve, thermogenesis, and protective padding and support. The hypodermis contains the lobules of fat cells that known as lipocytes. The thickness of hypodermis depends on the body site, particularly thick in organs such as cheeks, breasts, buttocks, palms, and soles (16).

Solar radiation

The sunlight emits a continuous spectrum of electromagnetic radiation including gamma rays, x-rays, ultraviolet (UV), visible light, infrared (IR), and radio waves. Only UV, visible light, and IR rays are able to reach the surface of the earth and the other rays will be absorbed by the atmosphere that envelops our planet (22). UV spectrum consists of 7% of the total solar radiation that reaching to human skin. A larger fraction is visible light spectrum (39%) and IR spectrum (54%) (23). This thesis focused on the UV and visible light radiations that are responsible for a variety of biological effects to the human skin.

Effects of ultraviolet radiation on the human skin

UV radiation (200-400 nm) can be divided into three main spectrum bands from the shorter to longer wavelengths; UVC, UVB, and UVA wavelengths. UVC rays (200-290 nm), the shortest wavelength, has the highest energy among UV radiation and normally blocked by stratospheric ozone layer. Therefore, it does not reach the earth’s surface. UVB rays (290-320 nm) is about 5% of UV spectrum that reaches the earth’s surface. It is completely absorbed by the epidermis layer of human skin (**Figure 3**). UVA rays (320-400 nm) comprises 95% of UV spectrum. It can be subdivided into UVAII (320–340 nm) and UVAI (340–400 nm) wavelength ranges. UVA radiation has less energy than UVB ray, but it can penetrate deeper into the dermis layers (4).

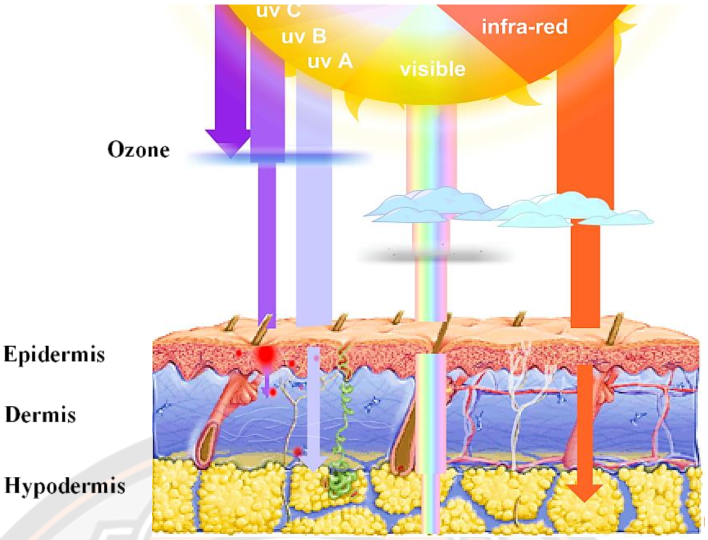

Figure 3 The penetration of ultraviolet, visible light, and infrared radiation to the human skin layers (Joanne loves science, (2014) from https://joanneloves-science.com/engineering/the-suns-rays-and-skin-damage/).

Exposure to UV radiation contribute in beneficial as well as detrimental effects to human skin. UV benefits to skin as follows;

- Synthesis of vitamin D
- Increasing of beta-endorphin during the sunbathing (22)
- Treating some skin disorder such as psoriasis vulgaris (24)

However, overexposure to UV radiation also cause in the undesirable damaging effects to human skin. UV radiation can induce both acute and chronic effects as follows;

Acute effects

Erythema is an acute inflammatory reaction. The excessive exposure of UVB radiation is an effective to induce erythema that causes from the vasodilatation of dermal blood vessels and increasing vascular permeability. Erythema can be associated with the clinical signs of inflammation, such as redness, tenderness, and edema. The severe erythema may result in blistering (25).

Pigmentation or tanning response is induced following exposure to UVA radiation, comprising three distinct phases as follows;

- **Immediate pigment darkening (IPD)** or immediate tanning reaction is a first transient phase that occurs and fades within minutes to a maximum of 2 hours after UVA exposure.

- **Persistent pigment darkening (PPD)** is a prolonged second phase that appears as a tan to brown color. It occurs within hours after UVA exposure and leaving some pigmentation that persists for 24 hours or longer.

- **Delayed tanning** is the last phase of pigmentation or skin tanning. Delayed tanning is caused from the increasing of number of melanocytes, melanosomes, and the production of new melanin transferred to keratinocytes. Delayed tanning typically appears brown dark color that occurs between 3-5 days after exposure to UVA ray and may persist for several day to week (25-27).

Sunburn is an inflammatory response that occurs from the keratinocytes receiving an UVB dose exceed a threshold damage, leading to activate apoptotic pathways or programmed cell death of keratinocytes. This is a protection mechanism for preventing the formation of skin cancer. These keratinocytes are known as sunburn cells (28, 29). The clinical symptoms include peeling or renewal of the skin.

DNA photodamage can be induced by UV radiation via both direct and indirect interactions. In directly, the excessive UVB radiation is absorbed by the major chromophore names genomic DNA, resulting in the formation of DNA photoproducts; cyclobutane pyrimidine dimers and 6,4-pyrimidine-pyrimidones. In contrast, indirect DNA damage occurs at UVA wavelength by the generation of ROS (singlet oxygen and hydrogen peroxide). The unrepaired of these DNA lesions may result in DNA mutation and contribute to the carcinogenesis (26).

Chronic effects

Photocarcinogenesis or skin cancer is the most common malignancies in Caucasian population and less common in Asian and black African races (30). Skin cancer can group into two categories; non-melanoma (basal cell carcinoma and squamous cell carcinoma) and melanoma. UVB radiation is primarily caused of the development of skin cancer that involves the combination of direct DNA damage as well as immune system modulation.

Photoaging is the result of the cumulative ROS production from long-term exposure to UV radiation. The generated ROS triggers the release of activator protein

1 (AP-1) and transforming growth factor-beta (TGF-β), which result to stimulate MMPs synthesis. These factors affect to degradation of collagen and inhibiting of procollagen I and III synthesis. The skin loss of strength and resilience, leading to development of deep wrinkles, atrophic skin, and multiple dark spots (31).

These damaging effects of UV radiation on the human skin depend on several factors including exposure dose, duration time, age, anatomical site, and skin type of individual person (32). The skin type responses to sunlight can classify by Fitzpatrick (29) (**Table 1**).

Table 1 Fitzpatrick classification of skin types according to response to solar radiation.

Skin type	**Phenotype**	**Reaction to solar radiation**
Type I	Very pale skin, freckles, Northern European/British	Always burns, never tans
Type II	White skin, Blonde hair, blue eyes, European/Scandinavian	Burns easily, tans slightly
Type III	Olive skin, Brown eyes, Dark hair	Burns moderately, tans moderately
Type IV	Light brown skin, Dark hair, Mediterranean, Asian or Latino	Burns minimally, tans easily
Type V	Dark brown skin, Dark hair, Indian, Native American	Rarely burns, tans easily
Type VI	Vary dark skin, African	Almost never burns, always Tans

Effects of visible light radiation on the human skin

The only portion of solar spectrum visible to human eye is visible light. It accounts for almost half of sunlight that reaching the earth’s surface. It can penetrate more deeply into the skin than UVB and UVA can, about 20% of visible light reaches the hypodermis layer (4) (**Figure 3**). Visible light is in the wavelength range from 400 to 800 nm. The portion of visible light spectrum having the highest energy and is referred to as blue light (400-450 nm) or high energy visible light (HEV). Visible light radiation was shown to influence the physiology of human skin as follow;

Oxidative stress and photoaging

Although, UV photons are higher energetic, visible light could also induce some of the same damaging effects to human skin as UV ray. Visible light was able to induce ROS (hydrogen peroxide), proinflammatory cytokines (IL-1α, IL-6, IL-8), and MMP-1, MMP-9-at doses equivalent to 15-90 min of the sunlight exposure (5). The cumulative all of which resulted in premature skin photoaging.

Exposure to blue light radiation can also influence the oxidative stress in human skin cells through the generation of ROS (9). The study of Oplander et al. (33) have been shown that the irradiation of blue light at wavelength 410 and 420 nm affected to oxidative stress in human fibroblasts, major cells in dermis and function in collagen synthesis. Blue light reduced the proliferation and antioxidative capacity of those cells.

Hyperpigmentation

A clinical study performed on human skin showed that visible light irradiation caused abnormal pigmentation. The pigmentation induced by visible light was more sustained dark and long-lasting in individuals, compared to that induced by UVAI radiation. In their study, the pigmentation was observed in subjects with Fitzpatrick skin type IV-VI but could not be observed in subjects with skin type II even at the highest irradiation dose (7). The study of Randhawa et al. (6) have been shown that the multiple exposure of visible light could induce the persistent pigmentation in darker skin as compared to the lighter skin (Caucasian). This effect was due to the increasing of tyrosinase enzyme and melanogenic activity including the type, size, and number of melanin produced in melanosome of darker melanocytes. However, the different wavelength range of visible light spectrum did not induce the similar effects on skin pigmentation. According to study of Duteil et al. (10), reported that the irradiation of blue light at wavelength 415 nm had more potential for stimulating the pronounced pigmentation on human skin, whereas the irradiation of red light (630 nm) induced very slightly modification of the pigmentation.

Chronic cumulative exposure to blue light is possibly associated with the worsening of some photo-induced hyperpigmentary disorders, especially melasma. Melasma is a melanogenesis dysfunction, resulting in an irregular brown or grayish-brown facial hypermelanosis and most commonly seen in Asian women (34, 35). Blue light induced melanogenesis through the membrane receptor names opsin 3 (OPN3), which is a G-protein coupled receptor (GPCR) of melanocytes (**Figure 4**). OPN3 functions as a sensor that activated by blue light, leading to increase calcium flux for the activation of CAMKII, followed by the phosphorylation of ERK1/2, CREB, p38 MAP kinase, and MITF. MITF control the expression of the main melanogenesis enzymes; tyrosinase and dopachrome tautomerase that have function in the synthesis of melanin pigments. In parallel, those enzymes have a role in formation the protein complex that comprises of multimeric tyrosinase (TYR) and tyrosinase-related protein (TYRP2/1). This protein complexes could lead to sustained tyrosinase activity in dark-skinned melanocytes (skin type III-VI), resulting in the long-lasting hyperpigmentation (8, 36).

Photodermatosis

The abnormal photosensitivity to visible light has also been implicated in some skin disorders such as solar urticaria, chronic actinic dermatitis, and erythropoietic protoporphyria (EPP). EPP is caused by the abnormal functioning of enzyme involved in heme biosynthesis names ferrochelatase. The deficiency of this enzyme results in overproduction of protoporphyrin IX that possess the maximum absorption spectrum in blue light wavelength (11). The clinical symptoms of EPP include swollen or blistering skin, a red itchy rash, and crusting that may appear during or after exposure to sunlight (37).

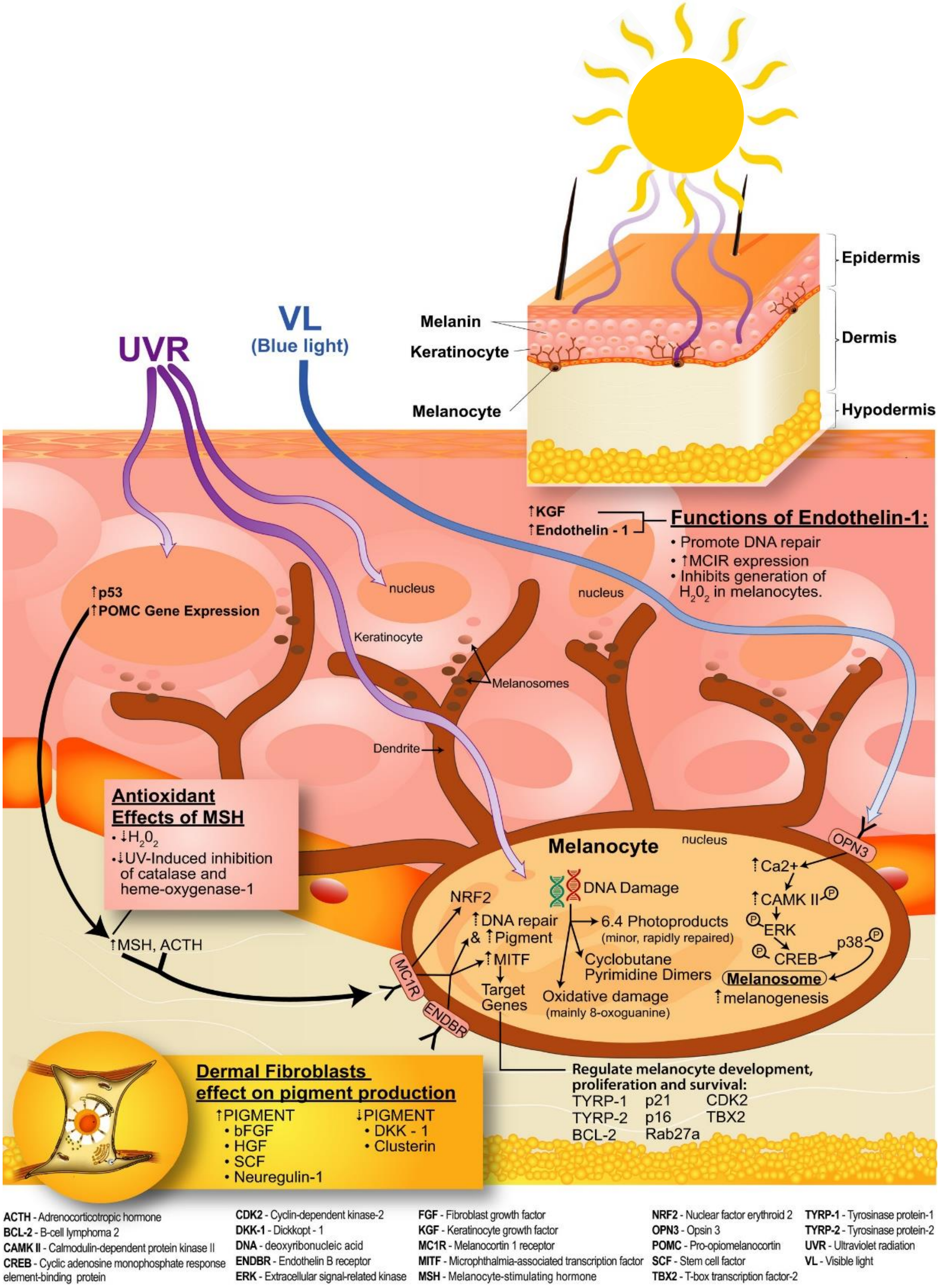

Figure 4 The different pathways of ultraviolet and blue light induced the melanin synthesis (melanogenesis) in human melanocytes (8).

The outdoor activities are exposed to the full solar spectrum, including both UV and visible light radiation. Prolonged exposure can produce those variety of damaging effects to human skin according to above described. These effects may impact on the quality of life of photosensitive patients. Therefore, it may be a need for using the sunscreens having the protective ability against both UV and visible light.

Protection of ultraviolet radiation

Many ways to protect the skin from the harmful effects induced by UV radiation, some of which include using umbrella, wearing protective clothing, hats or sunglasses. However, the direct way of UV protection is using the efficient sunscreens. Sunscreen is a cosmetic product containing UV filters as active ingredient in order to protect the skin from the deleterious UV or minimizing the amount of UV radiation that reaches the skin. UV filters are regulated globally as either over-the-counter (OTC) sunscreen drug products in United States and Australia or as cosmetics in Thailand, Europe, and Japan (38). The current UV filters are listed with INCI name, CAS number, EC number, and the maximum usage concentration of legislation, as show in **Table 2**. The UV filters can be classified into two groups depending on their different mechanisms, as illustrated below;

Organic UV filters

They function by absorbing UV radiation through their chromophores (azo, keto, nitro, nitroso, thio, ethylene etc.). The organic UV filters can be classified into three groups as follows; UVB filters, UVA filters, and UVB/A filters, based on their maximum absorption at specific range of wavelength.

Inorganic UV filters

These filters are able to attenuate UV radiation by reflection or scattering and absorption mechanisms (**Figure 5**). The inorganic UV filters widely used in sunscreens are titanium dioxide (TiO_2) and zinc oxide (ZnO). They have various physicochemical properties including crystalline structure, morphology, particle size, and surface coating. These properties are also importance factors influencing the efficacy of sunscreens in UV protection. European commission (EC) has authorized the specified properties of both TiO_2 (**Table 3**) and ZnO (**Table 4**) for selecting to use in the sunscreen formulations.

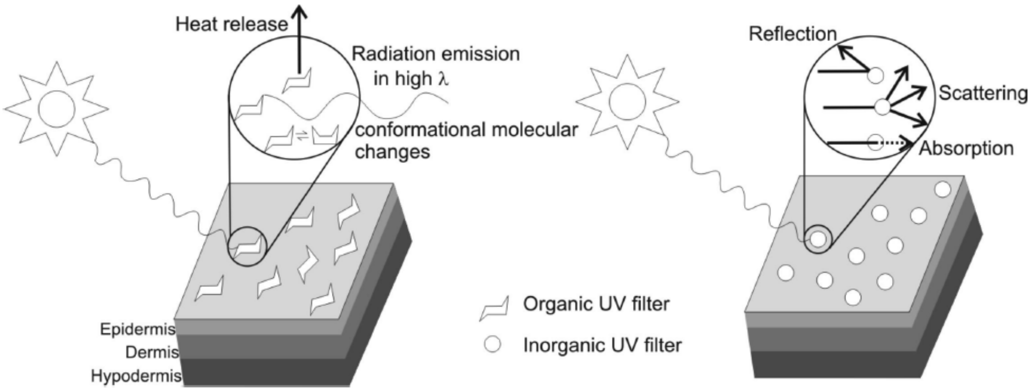

Figure 5 The UV attenuation of organic (left) and inorganic (right) UV filters in different mechanisms (39).

Factors affecting the efficacy of inorganic UV filters in ultraviolet protection

Crystalline form: TiO_2 occurs naturally in three crystalline forms including anatase, rutile, and brookite. Rutile is the most common form in sunscreen formulations due to its higher refractive index (RI) (2.700) and also lower photocatalytic activity than the other forms of TiO_2 (39). ZnO has two main crystalline form; wurtzite and zinc-blend. Wurtzite form is used in the most cases and stable form (40).

Particle size: TiO_2 and ZnO have various size ranges; nanosize (less than 100 nm), submicronsize (100-1000 nm), and micronsize (more than 1000 nm). The smaller particle size could provide greater UV absorption and also make more transparency formulations. This due to the smaller size have shown the higher band gap energy between the valence and conduction band, resulting to shift the absorption spectra from visible light to UV wavelength (41).

Surface coating: The photocatalytic activity of inorganic UV filters could be prevented by the surface coating. The coating lead to minimize the ROS formation by preventing direct contact between particle surface, oxygen, and surrounding medium (40). The surface treatment also improves the compatibility wettability, and dispersibility of TiO_2 and ZnO particles in medium, resulting to decrease the agglomeration of those particles.

Table 2 **Organic and inorganic UV filters are currently allowed to use in sunscreens and approved in Thailand, Europe, and Japan.**

INCI name	CAS Number	EC Number	Other name	Max Conc. (%)		
				Thai[a]	Europe[b]	Japan[c]
Organic UV filters						
4-methylbenzylidene camphor	36861-47-9 38102-62-4	253-242-6	Enzacamene	4	4	#
Camphor benzalkonium methosulfate	52793-97-2	258-190-8	-	6	6	#
Benzylidene camphor sulfonic acid	56039-58-8	-	-	6	6	#
Diethylhexyl butamido triazone	154702-15-5	-	Iscotrizinol	10	10	#
Ethylhexyl methoxycinnamate	5466-77-3	226-775-7	Octinoxate	10	10	20
Ethylhexyl dimethyl PABA	21245-02-3	244-289-3	Padimate O	8	8	10
Ethylhexyl salicylate	118-60-5	204-263-4	Octisalate	5	5	10
Ethylhexyl triazone	88122-99-0	402-070-1	Octyltriazone	5	5	5
Homosalate	118-56-9	204-260-8	-	10	10	10
Isoamyl p-methoxycinnamate	71617-10-2	275-702-5	Amiloxate	10	10	#
Octocrylene	6197-30-4	228-250-8	Octocrilene	10	10	10

Table 2 (Continued).

INCI name	CAS Number	EC Number	Other name	Max Conc. (%)		
				Thai[a]	Europe[b]	Japan[c]
Peg-25 PABA	116242-27-4	-	-	10	10	#
Phenylbenzimidazole sulfonic acid	27503-81-7	248-502-0	Ensulizole	8	8	3
Polyacrylamidomethyl benzylidene camphor	113783-61-2	-	-	6	6	#
Polysilicone-15	207574-74-1	426-000-4	-	10	10	10
Tris-biphenyl triazine	31274-51-8	-	-	10*	10*	10*
Butyl methoxy dibenzoylmethane	70356-09	274-581-6	Avobenzone	5	5	10
Diethylamino hydroxybenzoyl hexyl benzoate	302776-68-7	443-860-6	-	10	10	10
Disodium phenyl dibenzimidazole tetrasulfonate	180898-37-7	429-750-0	Bisdisulizole disodium	10	10	#
Menthyl anthranilate	134-09-8	205-129-8	Meradimate	5	-	#
Terephthalylidene dicamphor sulfonic acid	92761-26-7 90457-82-2	410-960-6	Ecamsule	10	10	10

Table 2 (Continued).

INCI name	CAS Number	EC Number	Other name	Max Conc. (%)		
				Thai^a	**Europe**^{b}	**Japan**^{c}
Benzophenone-3	131-57-7	205-031-5	Oxybenzone	10	6	5
Benzophenone-4	4065-45-6/ 6628-37-1	223-772-2	Sulisobenzone	5	5	10
Bis-ethylhexyloxyphenol methoxyphenyl triazine	187393-00-6	606-111-6	Bemotrizinol	10	10	3
Drometrizole trisiloxane	155633-54-8	-	-	15	15	15
Methylene bis-benzotriazolyl tetramethylbutylphenol	103597-45-1	403-800-1	Bisoctrizole	10*	10*	10*
Titanium dioxide	13463-67-7/ 1317-70-0/ 1317-80-2	236-675-5[1]/ 215-280-1[2]/ 215-282-2[3]	-	25	25	No limit
Zinc oxide	1314-13-2	215-222-5	-	25	25	No limit

Note: a is the maximum usage concentration of UV filters approved from Thailand FDA, 2017 (1),

b approved from European commission, 2020 (2) and c from Stiefel & Schwack, 2015 (3)

*Approval as active, #Not yet allowed to use in sunscreen

Table 3 The physicochemical properties of titanium dioxide are allowed to use in sunscreen products (European Commission, Reference number 27a, 2016).

Reference number	Chemical name	Name of common ingredients glossary	Conditions	
			Max Conc.	Other
27a	Titanium dioxide	Titanium Dioxide (nano)	25%	**Purity** ≥ 99 %
				Crystalline structure; rutile form or rutile with up to 5% anatase
				Morphology; clusters of spherical, needle or lanceolate shapes
				Median particle size; number size distribution ≥ 30 nm
				Aspect ratio from 1 to 4.5 and Volume specific surface area ≥ 460 m^2/cm^3
				Coating materials; Dimethicone, Triethoxycaprylylsilane, Hydrogen Dimethicone, Simethicone, Silica, Hydrated Silica, Stearic Acid, Aluminium hydroxide, Alumina, Aluminium Stearate
				Photocatalytic activity ≤ 10 % compared to corresponding non-coated or non-doped reference

Table 4 The physicochemical properties of zinc oxide are allowed to use in sunscreens (European Commission, Reference number 30a, 2016).

Reference number	Chemical name	Name of common ingredients glossary	Conditions	
			Max Conc.	Other
30a	Zinc oxide	Zinc oxide (nano)	25%	**Purity** ≥ 96%
				Crystalline structure; Wurtzite
				Morphology; Rod-like, star-like and/or isometric shapes
				Median diameter of the particle; number size distribution D50 (50% of the number below this diameter) > 30 nm and D1 (1% below this size) > 20 nm
				Water solubility<50 mg/L
				Coating materials; Dimethicone, Triethoxycaprylylsilane, Octyl Triethoxysilane, or uncoated

Methods to evaluate efficacy of sunscreens in ultraviolet protection

The performance of sunscreens against harmful effects from UV radiation are assessed by different methods, indicating UVB and UVA protection measurement.

UVB protection measurement

The most commonly used indicators for the classification of UVB protection levels afforded by sunscreens is sun protection factor (SPF). The SPF measurement exists for both *in vivo* and *in vitro* methods.

In vivo International standard organization (ISO) have published *in vivo* SPF standard method for determination of SPF value. In this method, the sunscreen was tested on the back of volunteers with the application rate of 2 mg/cm^2. The obtained SPF was calculated from the ratio between the minimal amount of UVB energy required to produce erythema or sunburn on the skin protected and unprotected by sunscreens (42). However *in vivo* SPF raises several ethical issues concerning the potential damage to skin volunteers. It is also time consuming, costly and not be practical for routine evaluation.

In vitro is developed for daily performing in the laboratory, but at present there is no official, harmonized published method accepted for SPF labelling. Several methods of *in vitro* SPF are based on the measurement of UVB transmission through sunscreen film spread on a substrate (43). The measured SPF could be categorized as low, medium, high and very high level, as show in **Table 5**. SPF values resulted greater than 50 should be specified "SPF 50+" on the label.

Table 5 Classification of sun protection factor (SPF) (44-47).

Protection category	European commission (2006)	USFDA final rule (2011)	Thai FDA (2017)	Standard Australia/ New Zealand (2012)
Low	6, 10	2 - < 15	6 - < 15	4, 6, 8, 10
Moderate	15, 20, 25	15 - < 30	15 - < 30	15, 20, 25
High	30, 50	30 - 50	30 - < 50	30, 40, 50
Very high	> 50	> 50	≥50	> 50

UVA protection measurement

The SPF values is not related to the overall UV protection of a sunscreen. This reason, the protection against UVA radiation must be evaluated. The measurement of UVA protection of sunscreens has been made through *in vivo* and *in vitro* methods.

In vivo has three methods including immediate pigment darkening (IPD), persistent pigment darkening (PPD), and UVA protection factor method. All three methods have somewhat similar procedure except their endpoints and expression of results;

- **Immediate pigment darkening method** determined the minimal amount of UVA dose required to produce pigmentation of the skin protected and unprotected by sunscreens. It evaluated the response immediately (60 second) after UVA exposure.
- **Persistent pigment darkening method** response evaluated at 2-24 hours after UVA exposure. This method has been officially adopted by Japan Cosmetic Industry Association (JCIA) for labelling UVA protection, that is according to ratings of PA plus sign, i.e. PA +, PA++, PA +++, and PA++++ (48).
- **UVA protection factor method** determined the minimal UVA dose required to produce erythema or tanning of the skin protected and unprotected by sunscreens. It is evaluated at 16-24 hours after exposure to UVA radiation (49).

In vitro is a method that based on the measurement of UVA transmission through a sunscreen film applied on a substrate, before and after exposure to a controlled UVA dose from source of solar-simulated radiation. The sunscreen sample is exposed to an irradiation dose proportional to the initial UVAPF before irradiation (50).

There are several *in vitro* UVA standard methods for the assessment of UVAPF values including methods from USFDA Final rule 2011 (45) , COLIPA 2011 (51), and ISO 24443:2012 (50). The different specification of these methods has been summarized in **Table 6**. In current, ISO24443:2012 *in vitro* UVA is a mostly used method in many countries worldwide including Europe, Canada, Mexico Mercosur, South Africa, Australia, and ASEAN (Brunei Darussalam, Cambodia, Indonesia, Laos, Malaysia, Myanmar, Philippines, Singapore, Thailand, and Vietnam) (38).

Table 6 Summary of the approved *in vitro* UVA test methods published by USFDA 2011, COLIPA 2011, and ISO 24443:2012.

	USFDA Final rule 2011	COLIPA 2011	ISO 24443:2012
Substrate	PMMA (2-7 microns)	PMMA (6 microns)	PMMA (6 microns)
Surface of substrate	Etched or Moulded	Moulded	Moulded
Minimum No. sample substrate	3	At least 4	At least 4
Application rate	0.75 mg/cm^2	1.3 mg/cm^2	1.3 mg/cm^2
Drying time	15 min	Minimum 15 min	30 min
Irradiation Dose (D)	D=8 J/cm^2	$D = UVAPF_0 \times 1.2$ J/cm^2	$D = UVAPF_0 \times 1.2$ J/cm^2
Characterization	λ_C	UVAPF, λ_C, UVA seal	UVAPF, λ_C, UVA seal

Note: $UVAPF_0$ = UVAPF value measured before irradiation
λ_C = Critical wavelength

The criteria for assessment of UVA protection of sunscreen products

Critical wavelength (λ_C) is defined as the wavelength at which the integral of the absorbance spectrum reached 90% of the total integral from wavelength 290-400 nm (3). USFDA requires that sunscreens offering a λ_C equal to or greater than wavelength 370 nm ($\lambda_C \geq 370$ nm), they can be specified “broad-spectrum” on the label.

The European commission (44) recommended that UVAPF value should have at least 1/3 of SPF and the λ_C should ≥ 370 nm to ensure that sunscreens can protect broad-spectrum covering UVB and UVA radiation. The sunscreens reach both requirements, they can be specified a logo “UVA seal” on the label (**Figure 6**).

Figure 6 UVA seal logo.

Protection of visible light radiation

The protection against harmful effects of blue/visible light is gaining interest in cosmetic industries. There are few studies focus on the efficacy of sunscreen products against these harmful rays. Schalka et al. (12) evaluated the efficacy of twenty sunscreen products which were marketed in Brazil in the protection against visible light by measuring absorbance value using the UV transmittance Analyzer (UV 1000®, Labsphere, New Hampshire, USA) and determining product's brightness and translucency using the chroma meter (CR-400, Minolta, Osaka, Japan). Among of these products, 13 products were colored sunscreens and 7 products were white sunscreens. They consisted of organic non-particulate UV filters and opaque pigments. The results showed that colored products gave better protection against visible light higher than white products. The conclusion of this study was in agreement with the study of Castanedo-Cazares et al. (13) who compared the efficacy of a broad-spectrum sunscreen containing iron (III) oxide or ferric oxide (red color) as an inorganic pigment with a regular broad-spectrum sunscreen in 68 melasma patients. All subjects received 4% hydroquinone as a depigmenting treatment. It was observed that the sunscreen containing BZ-3, EHMC, OCR, TiO_2, ZnO, and ferric oxide (i.e. colored sunscreen) was shown to be better in the enhancement of depigmenting efficacy of hydroquinone compared with the regular sunscreen containing Mexoryl SX & XL, TiO_2, OCR, BEMT, BMDM, and EHT (i.e. white sunscreen).

Teramura et al. (11) introduced a new parameter named porphyrin protection factor (PPF) for evaluating the protection of UVA and blue light based on protoporphyrin IX absorbance. Protoporphyrin IX is a compound found to be accumulated in erythropoietic protoporphyria (EPP) patients, a disease characterized by sensitivity to visible light. The researchers performed the *in vitro* PPF test for comparing the efficacy of combination of make-up base emulsion (containing EHMC, TiO_2, iron oxide; SPF 26.5 and PA 5.0) and either a powder (containing EHMC, BZ-3, TiO_2, iron oxide; SPF 15.0 and PA 6.7) or liquid foundation (containing EHMC, TiO_2, iron oxide; SPF 28.1 and PA 4.9) with a conventional sunscreen (containing ZnO, EHMC, PBSA; SPF 64.4 and PA 9.1). They concluded that combination of make-up was superior in protection of blue light based on the PPF parameter. They also performed the clinical study and demonstrated that the use of the make-up base emulsion together with powder foundation or liquid foundation could alleviate erythema and edema in 23 Japanese patients with EPP by 78.3% of the patients.

Recently, Martini and Maia Campos (14) evaluated the efficacy of two sunscreens. One product named “UV-only sunscreen” and contained TiO_2 and ZnO, UV filter grade. The other product named “UV-VIS sunscreen” and contained TiO_2 (UV filter), ZnO (UV filter) TiO_2 (pigment) as well as yellow, red, and black iron oxides. The results showed that UV-VIS sunscreen could reduce melanin index, epidermal pigmentation and hyperpigmented area in cutaneous hyperchromias (Sun-spot) subjects.

Methods to evaluate efficacy of sunscreens for visible light protection

Currently, there are no standardized method and official parameters to evaluate the efficacy of sunscreens in visible light protection. However, some studies have been evaluated the efficacy of sunscreens in blue/visible light protection by using the developed parameter and spectrophotometric measurements. For example, Moseley et al. (52) have evaluated the degree of visible light protection of developed colored sunscreens and commercial sunscreens through parameter named photosensitivity protection factor. In the measurement of this parameter, the sunscreen samples were applied on 3M Transpore tape at application rate 2 mg/cm^2 by using micropipette and gloved finger. The samples substrates were measured the transmission using Double grating Bentham spectroradiometer from 290 to 600 at 5 nm intervals. The obtained transmittance values were calculated the photosensitivity protection factor by the formula:

$$\text{Photosensitivity protection factor} = \frac{\sum E_{\lambda}\, S_{\lambda}\, \Delta\lambda}{\sum E_{\lambda}\, S_{\lambda}\, T_{\lambda}\, \Delta\lambda}$$

Where the summation interval is 290-600 nm, E_{λ} is a photosensitivity action spectrum from a patient with porphyria cutanea tarda, S_{λ} is solar spectral irradiance from the measurement in Australia at a solar zenith angle of 40°, T_{λ} is the transmittance values of the samples and $\Delta\lambda$ is a wavelength interval (5 nm).

The *in vitro* porphyrin protection factor (PPF) of Teramura et al. (11) was carried out by the measurement of the transmission of sunscreen applied on a substrate. The make-up base, powder, and liquid foundation were prepared on PMMA substrate and measured the transmittance values using integrating sphere spectrophotometer (UV-2000®, Labsphere, North Sutton, NH, USA) at wavelength between 300-450 nm. The calculation of PPF values was designed as the ratio of:

$$\text{Porphyrin protection factor (PPF)} = \frac{\int_{300\text{ nm}}^{450\text{ nm}} \mathrm{PP}(\lambda)\cdot \mathrm{I}(\lambda)\cdot \mathrm{d}(\lambda)}{\int_{300\text{ nm}}^{450\text{ nm}} \mathrm{PP}(\lambda)\cdot \mathrm{I}(\lambda)\cdot 10^{-\mathrm{Abs}(\lambda)}\cdot \mathrm{d}(\lambda)}$$

Where PP (λ) is the mean absorbance value of protoporphyrin IX solution, I (λ) is the standard spectral irradiance of the solar source based on an air mass of 1.5G (received from IEC60904-3), Abs (λ) is absorbance converted from the obtained transmittance at wavelength 300-450 nm, d (λ) is wavelength interval (1 nm).

Delamour et al. (53) have been developed the new *in vitro* method allowing the assessment of blue light protection of 25 sunscreen products from different companies. These products had SPF 6-50+ and different forms of formulation. The tested products were prepared on molded PMMA plates with an application rate 1.3 mg/cm^2 using syringe and automated spreading from device (HD-Spreadmaster, Helioscreen, France). The absorption of these products was measured using visible spectrophotometer (V770® UV-Visible/NIR spectrophotometer, Jasco, Japan) at wavelength 290-500 nm. The obtained absorbance values were used in the calculation of two blue light protection factors.

The first factor was the percentage of blue light absorbed or reflected by the tested products (%BL) which was calculated using the following equation:

$$\%\text{Transmittance BL} = \frac{\sum_{\lambda 1}^{\lambda 2} T_{1BL}}{n}$$

$$\%\text{BL} = 100 - \%\text{Transmittance BL}$$

Where T_{1BL} is the mean of the transmittance per plates, n is the number of measurements, λ_1=380 nm and λ_2=500 nm.

The second factor was the critical wavelength extended to blue light wavelength (BL-CW) that was equal to 90% of area under the absorbance curve at wavelength 290-500 nm and was calculated using the following equation:

$$\text{BL-CW} = 0.9 \cdot \int_{290\text{ nm}}^{500\text{ nm}} A_{1BL(\lambda)} \cdot d(\lambda)$$

Where A_{1BL} is the mean of absorbance, d (λ) is wavelength interval = 1 nm.

Schalka et al. (54) have been evaluated the effectiveness of 33 sunscreens formulation (17 products containing iron oxides and 16 products without iron oxides) marketed in Brazil for protecting visible light transmission. The measurement of this study followed the procedures of *in vitro* UVAPF standard (ISO24443:2012); the sunscreen sample was prepared on PMMA plates in the amount of 1.3 mg/cm^2 and measured the transmission using UVR transmittance analyzer (UV-2000®, Labsphere, New Hampshire, USA) at wavelength 290-450 nm, before and after irradiation. The evaluation of samples in visible light protection was determined by parameters named solar visible light protection factor (PF-VIS) and pigmentation protection factor.

$$\text{Solar visible light protection factor (PF-VIS)} = \frac{\int_{400\text{ nm}}^{450\text{ nm}} P(\lambda).I(\lambda).d(\lambda)}{\int_{400\text{ nm}}^{450\text{ nm}} P(\lambda).I(\lambda).10^{-A(\lambda)}.d(\lambda)}$$

Where P(λ) is immediate pigment darkening (IPD) spectrum proposed by Rosen (55), I(λ) is the radiation spectrum of the sun at the city of Sao Paulo, Brazil (23.3º S, 46.6º W), A (λ) is the average of the absorbance of the sunscreen after exposure, d(λ) is the wavelength interval (1 nm).

The pigmentation protection factor was calculated from the same equation of PF-VIS, but difference at wavelength 320-450 nm (54).

Although the protection of blue/visible light using sunscreens has been studied as described above, none of these studies have been systematically investigated on the efficacy of these compounds in the protection of blue/visible light. In addition, no detailed information about optimizing characteristics of TiO_2, ZnO, and iron oxides for maximum blue/visible light protection was provided. The characteristics influencing the efficacy of these compounds in blue/visible light protection were such as particle size and surface coating etc. These data were essential for the development of sunscreen products which could protect against blue/visible light.

This study was therefore aimed to screen the efficacy of the organic and inorganic UV filters which are frequently used in commercial products in the protection of UV and blue/visible light. The inorganic pigments, including TiO_2, ZnO, and iron oxides were also investigated. Finally, the sunscreen formulations which could protect UV and blue/visible light were aimed to obtain.

CHAPTER III

RESEARCH METHODOLOGY

Materials

1. Bis-Ethylhexyloxyphenol Methoxyphenyl Triazine (BEMT); Tinosorb S® (Cosmetic grade, BASF, Ludwigshafen, Germany)
2. Bis-Ethylhexyloxyphenol methoxyphenyl triazine (and) acrylates/c12-22 alkyl methacrylate copolymer (BEMT AQ); Tinosorb S®lite aqua (Cosmetic grade, BASF, Ludwigshafen, Germany) The aqueous suspension contains 18-22% BEMT, 17-21% acrylates/c12-22 alkyl methacrylate copolymer, 1.5-2.5% coco-glucoside, 0.3-0.8 disodium lauryl sulfosuccinate, 2.5-3.5 L-arginin.
3. Black iron oxide and triethoxycaprylylsilane (IBT-3000); Iron oxide black 3AS® (Cosmetic grade, K.S. pearl corporation, Incheon-city, Korea)
4. Black iron oxide and Triethoxycaprylylsilane (IBT-200); Ti-K black iron oxide AS® (Cosmetic grade, Athena Corp Co.Ltd., Samutprakarn, Thailand)
5. Butyl methoxydibenzoylmethane (BMDM); Eusolex 9020® (Cosmetic grade, Merck, Darmstadt, Germany)
6. C12-15 alkyl benzoate; Finsolv TN® (Cosmetic grade, Innospec Performance Chemicals, Colorado, United States)
7. Caprylic/Capric triglyceride; MCT oil® (Cosmetic grade, Natural Oleochemicals Sdn. Bhd., Johor, Malaysia)
8. Cetostearyl alcohol; Wax-s ceto stearyl alcohol® (Cosmetic grade, Kokyu Alcohol Kogyo CO., LTD., Chiba, Japan)
9. Diethylamino hydroxybenzoyl hexyl benzoate (DHHB); Uvinul A plus® (Cosmetic grade, BASF, Ludwigshafen, Germany)
10. Dimethyl sulfoxide (Analytical Reagent grade, Sigma-aldrich, Missouri, United States)
11. Ethanol (Analytical Reagent grade, RCI labscan limited, Bangkok, Thailand)
12. Ethylhexyl methoxycinnamate (EHMC); Uvinul MC 80® (Cosmetic grade, BASF, Ludwigshafen, Germany)

13. Ethylhexyl salicylate (EHS); Eusolex OS® (Cosmetic grade, Merck, Darmstadt, Germany)

14. Ethylhexyl triazone (EHT); Uvinul T 150® (Cosmetic grade, BASF, Ludwigshafen, Germany)

15. Homosalate (HMS); Eusolex HMS® (Cosmetic grade, Merck, Darmstadt, Germany)

16. Glycerin; Refined glycerin 99.5%®MIN USP (Cosmetic grade, Thai Oleochemicals company limited, Bangkok, Thailand)

17. Glyceryl stearate (and) PEG-100 Stearate; Lexemul 561® (Cosmetic grade, Inolex, Pennsylvania, United States)

18. Methylene bis-benzotriazolyl tetramethylbutylphenol (MBBT); Tinosorb M® (Cosmetic grade, BASF, Ludwigshafen, Germany). The aqueous suspension contains 50% MBBT, 7.5% decyl glucoside, 0.2% xanthan gum, 0.4% propylene glycol.

19. Octocrylene (OCR); Uvinul N 539 T® (Cosmetic grade, BASF, Ludwigshafen, Germany)

20. Protoporphyrin IX (free acid) (Cosmetic grade, Enzo life sciences, Inc., Farmingdale, New York)

21. Red iron oxide and Triethoxycaprylylsilane (IRT-1700); Iron oxide red 3AS® (Cosmetic grade, K.S. pearl corporation, Incheon-city, Korea)

22. Red iron oxide and Triethoxycaprylylsilane (IRT-200); Ti-K red iron oxide AS® (Cosmetic grade, Athena Corp Co. Ltd., Samutprakarn, Thailand)

23. Sorbitan monostearate; Span 60® (Cosmetic grade, Nof Corporation, Tokyo, Japan)

24. Stearic acid; Lalit stearic acid SA 1850® (Cosmetic grade, Pacific Oleochemicals Sdn. Bhd., Johor, Malaysia)

25. Titanium dioxide and aluminium hydroxide and triethoxycaprylylsilane (TT300); ALT-TSR-10® (Cosmetic grade, Tayca Corporation, Osaka, Japan)

26. Titanium dioxide and aluminium hydroxide and triethoxycaprylylsilane (TT60); Micro TiO2060 AS® (Cosmetic grade, K.S. Pearl Corporation, Incheon-city, Korea)

27.Titanium dioxide (T35); MT-500B® (Cosmetic grade, Tayca Corporation, Osaka, Japan)

28. Titanium dioxide and aluminium hydroxide and hydrated silica and dimethicone (TD35); SMT-500SAM® (Cosmetic grade, Tayca Corporation, Osaka, Japan)
29. Titanium dioxide and aluminium hydroxide (T250); CR-50® (Cosmetic grade, Daito Kasei Kogyo, Osaka, Japan)
30. Titanium dioxide and aluminium hydroxide and hydrogen dimethicone (TD250); SIO1-2 TiO2 CR-50® (Cosmetic grade, Daito Kasei Kogyo, Osaka, Japan)
31. Triethanolamine; Triethanolamine 99%® (Cosmetic grade, The Dow Chemical Company, Michigan, United States)
32. Tris-biphenyl triazine (TBPT); Tinosorb®A2B (Cosmetic grade, BASF, Ludwigshafen, Germany). The aqueous suspension contains 47-53% TBPT, 6.5-8.5% decyl glucoside, 0.2-0.6% disodium phosphate, 0.2-0.6% butylene glycol, 0.1-0.3% xanthan gum.
33. Yellow iron oxide and Triethoxycaprylylsilane (IYT-1500); Iron oxide yellow 3AS® (Cosmetic grade, K.S. pearl corporation, Incheon-city, Korea)
34. Yellow iron oxide and Triethoxycaprylylsilane (IYT-200); Ti-K yellow iron oxide AS® (Cosmetic grade, Athena Corp Co. Ltd., Samutprakarn, Thailand)
35. Zinc oxide and hydrogen dimethicone (ZnD100); ZnO-610Si(4)G® (Cosmetic grade, Sumitomo Osaka Cement, Chiba, Japan)
36. Zinc oxide and triethoxycaprylylsilane (ZnT20); SF-15-OTS® (Cosmetic grade, Sakai Chemical Industry, Sakai, Japan)
37. Zinc oxide and triethoxycaprylylsilane (ZnT120); Zinc oxide AS® (Cosmetic grade, K.S. Pearl corporation, Incheon City, Korea)
38. Zinc oxide and triethoxycaprylylsilane (ZnT200); Z-coteHP1® (Cosmetic grade, BASF, Ludwigshafen, Germany)

Apparatus

1. Analytical balance 4 Digits (Precisa®300A, Becthai Bangkok Equipment & Chemical Co., Ltd., Bangkok, Thailand)
2. Analytical balance 5 Digits (Mettler®AT201, Mettler-Toledo GmbH, Laboratory & Weighing Technologies, Zürich, Switzerland)
3. Color spectrophotometer (CM-700d®, Konica Minolta, New Jersey, United states)

4. Homogenizer (Charn Intertech Co., Ltd, Bangkok, Thailand)

5. Hydrophilic membrane filter 0.22 µm (Durapore®, Merck Millipore, Darmstadt, Germany)

6. Micropipette (Bio-Rad Laboratories, Sydney, Australia)

7. pH meter (Sevenmulti™, Mettler Toledo, Ho Chi Minh city, Vietnam)

8. Poly methyl methacrylate (PMMA) plate, roughness value SA = 6 µm, size 5 cm × 5 cm (Helioplate® HD 6, Helioscreen, Creil, France)

9. Quartz plate, size 5 cm × 2.5 cm (The sun chemical Co., Ltd., Bangkok, Thailand)

10. Rheometer (DV-III, AMETEK Brookfield, Middleboro, United states)

11. Solar simulator (Suntest® CPS+, Atlas material testing technology GmBH, linsengericht, Germany)

12. Sonicator Bath (Elma®, Transsonic 829/H, Lebanon)

13. Transmission electron microscope (Tecnai® 12, Philips, Amsterdam, Netherland)

14. Ultraviolet transmittance analyzer (UV-2000S®, Labsphere, North Sutton, United states)

15. UV-VIS spectrophotometer (UV-1800®, Shimadzu, Kyoto, Japan)

16. Vortex (Scientific industries Inc., New York, United states)

Methodology

The scope of the thesis is summarized in **Figure 7**.

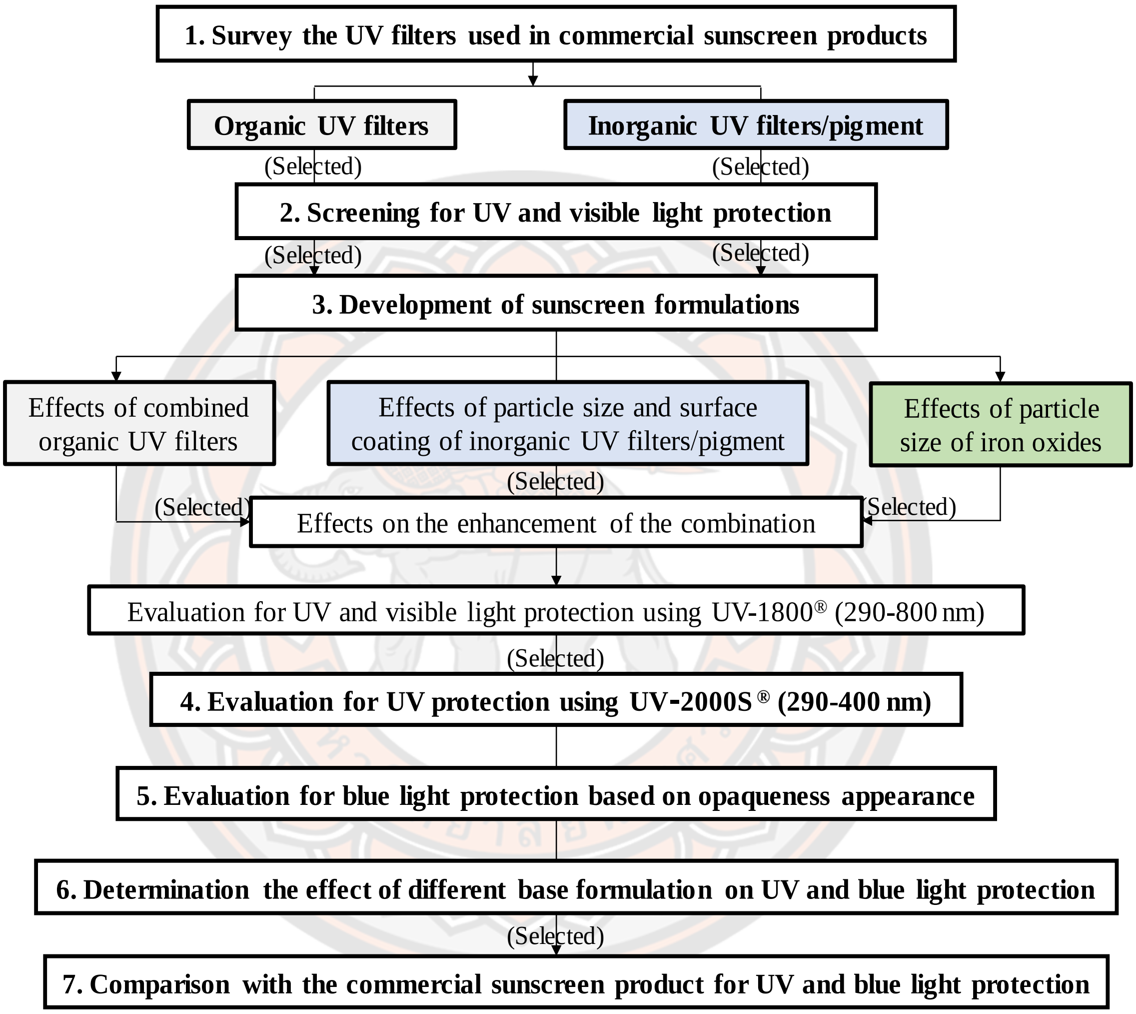

Figure 7 Flow chart summary of the scope of the thesis.

Part 1: Survey the UV filters frequently used in commercial sunscreens

Based on the Notification of the Ministry of Health, Thailand B.E. 2560, there are 28 UV filters (26 organic and 2 inorganic UV filters) are allowed to be used in sunscreen products (1). However, not all of them are used in commercial products. Therefore, the frequently used UV filters in commercial sunscreens were investigated. The survey was performed from May to June 2019 at hypermarkets in Phitsanulok, Thailand. The products which were intended to be applied to the skin to prevent adverse effects caused by sunlight, generally known as sunscreens were focused in this part. The products recruited must show the following signs on the label: SPF and UVA seal or PA rating system. The information recorded included trade name, manufacturers, claimed protection (i.e. SPF and UVA seal or PA plus signs) and lists of UV filters. The frequency of usage for each UV filter was calculated by dividing the frequency of occurrence of a UV filter in commercial sunscreens by the total number of sunscreens in the survey (Equation 1). After that, the UV filters which showed high frequency of usage were selected for further studies.

$$\%\text{ frequency of usage of each UV filter} = \frac{\text{the frequency of occurrence of a UV filter}}{\text{total number of surveyed products}} \times 100 \quad \text{(Eq.1)}$$

Part 2: Screening for ultraviolet and visible light protective ability of the selected organic UV filters, inorganic UV filters and inorganic pigments

After surveying, the organic and inorganic UV filters frequently used in commercial sunscreens were selected. As generally known, organic and inorganic UV filters are compounds used to reduce the amount of UV light penetrating into the skin. They function by absorbing or reflecting UV radiation. However, their protective ability against visible light has not been widely published. Therefore, the frequently used organic and inorganic UV filters listed from the survey were screened not only for the UV protective ability but also for the visible light protective ability.

Inorganic pigments are chemicals functioning as colorants. Examples of the inorganic pigments used in cosmetic products are white titanium dioxide and zinc oxide, and various colored iron oxides. These compounds were also investigated in this study.

1. Organic UV filters

The selected organic UV filters were determined for UV and visible light protective ability. The samples were prepared by dissolving each organic UV filter in ethanol and diluted to the optimum concentration, giving an absorbance around 0.3-1. Then, the absorbance spectra between 200-800 nm of all samples were recorded using a UV-Vis spectrophotometer (UV-1800®; Shimadzu, Kyoto, Japan). In addition, UVB, UVA, and visible light protective ability were evaluated through, maximum absorption wavelength (λ_{max}), A (1%, 1cm), critical wavelength (λ_C), and visible protection wavelength (λ_{Vis}), respectively. Area under the curve (AUC) for the total wavelength between 290-800 nm as well as separate ranges of UVB, UVA, blue light, visible light wavelength was also calculated. Details of the calculations are in Part 2, Topic 3.

2. Inorganic UV filters and pigments

In the case of inorganic UV filters, only titanium dioxide (TiO_2) and zinc oxide (ZnO) are allowed to use in commercial sunscreen products according to Thai FDA regulation (1). In addition, only names of inorganic UV filters were indicated on the products label. No information of crystalline structure, particle size, and coating agent were given. Therefore, both TiO_2 and ZnO having two different particle sizes (i.e. small size (UV filter grade) and large size (pigment grade)) and having different coating agents were recruited into the study. The selection criteria of them were based on the EC regulation *(*Details in Chapter II*)*.

Again, the selected inorganic UV filters and pigments were determined for UV and visible light protective ability by using the UV-Vis spectrophotometry. Each sample was individually prepared by dispersing in ethanol and diluted to the optimum concentration. After that, the sample was sonicated in a sonicator bath (Elma®, Transsonic 829/H, Lebanon) for 10 minutes. Then, the transmission spectra between 200-800 nm of all samples were scanned and recorded using UV-1800® spectrophotometer. Their efficacy of UVB, UVA, and visible light protection were evaluated through critical wavelength (λ_C), visible protection wavelength (λ_{Vis}), respectively. Area under the curve (AUC) for the total wavelength between 290-800 nm as well as separate ranges of UVB, UVA, blue light and visible light wavelength was also calculated. Details of the calculations are in Part 2, Topic 3.

3. Determination of ultraviolet and visible light protective efficiency

Various parameters were used to indicate the efficacy of the selected UV filters in UV and visible light protection. These parameters are shown by following:

3.1 Maximum absorption wavelength (λ_{max})

Lambda max (λ_{max}) was the wavelength in the absorbance spectra at which the highest peak is shown. It was used to classify types of organic UV filters into UVB, UVA, or UVB/A filters. UVB filters should have λ_{max} in the range of 290-320 nm. UVA filters should have λ_{max} in the range of 320-400 nm. On the other hand, UVB/A filters should have λ_{max} in both range of UVB and UVA wavelengths. The λ_{max} of Vis filters should fall in the range between 400-800 nm.

3.2 A One One A (1%, 1cm)

A (1%, 1cm) was calculated from maximum absorbance of UV filters, which prepared at concentration 1% W/V and measured by cuvette had the path length of light in 1 cm. It depended on λ_{max} of each UV filter.

3.3 Critical wavelength (λ_C)

λ_C was calculated from 90% of the summation of AUC of absorbance spectrum from wavelength between 290 to 400 nm. The UV filter having $\lambda_C \geq 370$ nm can be classified as UVB/A filter or UVA filter. λ_C was calculated using Equation 2.

$$\lambda_C = 0.9 \int_{290}^{400} \text{Abs}\,(\lambda)\cdot \text{d}\,(\lambda) \qquad \text{(Eq. 2)}$$

Where Abs (λ) is absorbance of samples at wavelength 290-400 nm, d (λ) is wavelength interval, which is 1 nm.

3.4 Visible protection wavelength (λ_{Vis})

λ_{Vis} was a parameter indicating the efficacy of visible light protection for this thesis. It was modified from critical wavelength equation and calculated from 90% of the summation of AUC at wavelength between 290-800 nm (Equation 3). If λ_{Vis} of a filter ≥ 400 nm, it was classified as a Vis filter.

$$\lambda_{Vis} = 0.9 \int_{290}^{800} \text{Abs}\,(\lambda)\cdot \text{d}\,(\lambda) \qquad \text{(Eq. 3)}$$

Where Abs (λ) is absorbance of samples at wavelength 290-800 nm, d(λ) is wavelength interval, which is 1 nm.

3.5 Area under the curve (AUC)

AUC was calculated from the summation of absorbance value from minimum wavelength (λ_{min}) to maximum wavelength (λ_{max}) of the specified region, including UVB (290-320nm), UVA (320-400 nm), blue light (400-450 nm), and visible light (400-800 nm) wavelength (Equation 4).

$$\text{AUC} = \int_{\lambda\text{min}}^{\lambda\text{max}} \text{Abs}\,(\lambda)\cdot \text{d}\,(\lambda) \qquad \text{(Eq. 4)}$$

Part 3: Development of sunscreen products for ultraviolet and visible light protection

1. Preparation of base cream

The compositions of base cream are shown in **Table 7**. The preparation of base cream was performed as follows; the ingredients in the oil phase were melted based on their melting point. The wax having highest melting point was first melted and the lowest melting point was last added (i.e. stearic acid, glyceryl stearate (and) PEG-100 stearate, sorbitan monostearate, and cetylstearyl alcohol). Then the liquid oil ingredients (Caprylic capric triglyceride and C12-15 alkyl benzoate) were added and mixed. For aqueous phase, carbopol was dispersed separately in water and neutralized with triethanolamine to form a gel. Glycerin and tetrasodium EDTA were dissolved in water before adding to the carbopol. Both oil and aqueous phases were separately heated to 70-75°C. After reaching the desired temperature, the aqueous phase was poured slowly into the oil phase while constantly homogenized (Charn Intertech Co., Ltd, Bangkok, Thailand) at 2000 rpm. The resulting base cream was continuously homogenized until it cooled down to 40°C. Then, phenoxyethanol was incorporated and homogenized until the base cream became homogenous.

Table 7 The compositions of base cream.

	Ingredients	%W/W	Function
Oil phase	Caprylic capric triglyceride	7.00	Dispersing agent
	C12-15 alkyl benzoate	5.50	Dispersing agent
	Cetylstearyl alcohol	1.00	Thickening agent
	Glyceryl stearate (and) PEG-100 stearate	4.25	Emulsifier
	Stearic acid	1.00	Stiffening agent
	Sorbitan monostearate	0.75	Emulsifier
Aqueous phase	Glycerin	3.00	Humectant
	Carbopol 940	0.08	Gelling agent
	Triethanolamine	0.50	Neutralizing agent with Carbopol
	Tetrasodium EDTA	0.04	Chelating agent
	Phenoxyethanol	0.40	Preservative
	Water	q.s.to 100	-

2. Effects of combined organic UV filters

From the screening of organic UV filters, the filters showed the highest protective ability against UV and visible light radiation were selected. Then, various combinations of these filters were formulated in form of sunscreen formulation. The incorporation of organic UV filters in the base cream was dependent on their nature. In the case of solid organic UV filter, it was melted into the oil phase. However, in the case of aqueous suspensions organic UV filter, it was dispersed into the water phase. The concentration of organic UV filters was used at the level of legislation range. After that, these formulations were evaluated for the protective efficiency against UV and visible light radiation using the UV-1800® spectrophotometer as described in Part 3, Topic 5.

3. Effects of particle size and surface coating of inorganic UV filters and pigments

The selected inorganic UV filters and pigments with various particle size and coating agents were individually incorporated into the base cream. Each of them was dispersed in the liquid oil (C12-15 alkyl benzoate and caprylic capric triglyceride) before adding into the melted oil ingredients. The concentration of them was fixed at 10%W/W, which is the commonly used concentration. The UV and visible light protective ability of the prepared formulations were evaluated using the UV-1800® spectrophotometer as described in Part 3, Topic 5.

4. Effects of iron oxides on the enhancement of ultraviolet and visible light protection of sunscreen creams

Iron oxides can be alternatively added to the white sunscreens for providing a foundation effect in the sunscreens and improving greater cosmetic acceptability. The iron oxides were selected based on the particle size and color used in foundation colored sunscreens. In addition, they must be listed in the EU regulation (56).

4.1 Effects of particle size of iron oxides

Firstly, the selected iron oxides having two different particle sizes were individually determined for the effects of UV and visible light protection. Each iron oxide was incorporated into the base cream at 1%W/W and was dispersed in the liquid oil (C12-15 alkyl benzoate and caprylic capric triglyceride) before adding into the melted oil ingredients. The UV and visible light protective ability of the prepared formulations were evaluated using UV-1800® spectrophotometer as described in Part 3, Topic 5. The iron oxides with a certain size that showed better UV and visible light protection were selected to blend for further studies.

4.2 Effects of iron oxides in combination with organic UV filters and/or inorganic UV filters/pigments

Various colored iron oxides with a certain particle size showing better UV and visible light protection were selected and combined to obtain colors fitting to Asian skin-tone. Then, the mixture of colored iron oxides was further combined with the selected organic UV filters and/or inorganic particles (UV filter or pigment grade). The effects of iron oxides on the enhancement of UV and visible light protection were determined through SPF, UVAPF, $\lambda_{C,}$ and PPF values.

To incorporate iron oxides, organic UV filters and/or inorganic UV filters/pigments into base cream. The iron oxides were firstly incorporated into the sunscreens by blending individual color into the liquid oil and following it with the dispersing of the inorganic particles and continuous stirring until it became homogeneous. The addition of organic UV filters was prepared same as details above. Again, the UV and visible light protective ability of the prepared formulations were evaluated using UV-1800® spectrophotometer as described in Part 3, Topic 5.

5. Determination of ultraviolet and visible light protective efficiency of developed sunscreens using UV-1800® spectrophotometer

The method for evaluating the efficacy of developed sunscreens for UV and visible light protection was performed as follow: To prepare the samples, each sample was accurately weighed and was dropped on a quartz plate (5 cm × 2.5 cm) at 1.3 mg/cm^2. Then, the sample was spread over the whole surface of the plate using a fingertip (pre-saturated with the sample prior to spreading). The plate was dried in the dark for 15 minutes. The sample plate was prepared in three replicates. After that, their UV and visible light absorptive ability were measured using a UV-1800® spectrophotometer at wavelength between 200 to 800 nm. The obtained absorbance values were calculated SPF, UVAPF, and PPF values as described below.

5.1 Sun protection factor (SPF)

SPF is a value indicating to the efficacy of samples in UVB protection (Equation 5).

$$\mathrm{SPF} = \frac{\int_{290\ \mathrm{nm}}^{400\ \mathrm{nm}} E(\lambda)\cdot I(\lambda)\cdot d(\lambda)}{\int_{290\ \mathrm{nm}}^{400\ \mathrm{nm}} E(\lambda)\cdot I(\lambda)\cdot 10^{-\mathrm{Abs}(\lambda)}\cdot d(\lambda)} \qquad \text{(Eq.5)}$$

Where E (λ) is erythema action spectrum, I(λ) is spectral irradiance (W/m^2/nm) at wavelength 290-400 nm, Abs(λ) is Mean of absorbance value of samples at wavelength 290-400 nm, d(λ) is wavelength interval, which is 1 nm.

5.2 UVA protection factor (UVAPF)

UVAPF is a value indicating to the protective efficiency of samples in UVA radiation (Equation 6).

$$\text{UVA-PF} = \frac{\int_{320\ \text{nm}}^{400\ \text{nm}} P(\lambda)\cdot I(\lambda)\cdot d(\lambda)}{\int_{320\ \text{nm}}^{400\ \text{nm}} P(\lambda)\cdot I(\lambda)\cdot 10^{-\text{Abs}(\lambda)}\cdot d(\lambda)} \qquad \text{(Eq.6)}$$

Where P (λ) is persistent pigment darkening action spectrum, I(λ) is spectral irradiance (W/m^2/nm) at wavelength 320-400 nm, Abs(λ) is Mean of absorbance value of samples at wavelength 320-400 nm, d(λ) is wavelength interval, which is 1 nm.

5.3 Porphyrin protection factor (PPF)

PPF is a value indicating the efficacy of samples in blue light protection. The measurement and calculation of PPF value was applied from the method proposed by Teramura et al. (as details in Chapter II). Briefly, PPIX was dissolved in dimethyl sulfoxide and diluted to a final concentration of 0.0025 mg/mL. The absorption of PPIX solution was measured using a UV-1800® spectrophotometer at wavelength between 400-450 nm. The obtained absorbance values of PPIX solution was used to calculate PPF by using Equation 7.

$$\text{PPF} = \frac{\int_{400\ \text{nm}}^{450\ \text{nm}} PP(\lambda)\cdot I(\lambda)\cdot d(\lambda)}{\int_{400\ \text{nm}}^{450\ \text{nm}} PP(\lambda)\cdot I(\lambda)\cdot 10^{-\text{Abs}(\lambda)}\cdot d(\lambda)} \qquad \text{(Eq.7)}$$

Where PP (λ) is Mean of absorbance value of protoporphyrin IX solution, I (λ) is the standard spectral irradiance of the solar source based on an air mass of 1.5G (received from IEC60904-3), Abs (λ) is Mean of absorbance value of samples at wavelength 400-450 nm, d (λ) is wavelength interval, which is 1 nm.

5.4 Visible protection wavelength (λ_{Vis})

λ_{Vis} was a parameter indicating the protective efficiency of visible light (Details in Equation 3).

Part 4: UV protective efficiency of developed sunscreens using UV-2000S® ultraviolet transmittance analyzer

The obtained SPF, UVAPF, and λ_C values from the previous measurement using UV-1800® spectrophotometer were only used to evaluate for preliminary screening during the sunscreen development. The developed sunscreens were again evaluated for their efficacy in UVB and UVA protection for providing the practically values that could claim on the product’s label. The details of evaluation methods were following:

4.1 Evaluation of SPF

As described in Chapter II, a standard *in vitro* SPF method is not available. The in-house method was used to evaluate the SPF value. The measurement and the preparation of samples were proceeded by modifying from incorporation of many recommendations issued by ISO 24443:2012 (Details are shown below). The resulting SPF value was automatically calculated using UV-2000S® ultraviolet transmittance analyzer (UV-2000S®, Labsphere, North Sutton, United States) at wavelength between 290 to 400 nm.

4.2 Evaluation of UVAPF

UVAPF method was proceeded according to ISO 24443:2012. The selected sunscreen was weighted by dropping on roughened side of PMMA plate (Helioplate® HD 6, Helioscreen, Creil, France) (size 5 cm × 5 cm) at application rate of 1.3 mg/cm^2. Pre-saturated with the small amount of sample on a fingertip (without fingercot), then was immediately spread over the whole plate using a fingertip. The sample plate was dried for 30 minutes in the dark. The sample plate was prepared in four replicates. After that, the sample plates were placed on the sample stage of UV-2000S® and then moved to nine different positions to measure the absorption of UVA light at wavelength between 320 to 400 nm. For baseline measurement, the glycerin treated plate was used in the subsequence UVAPF measurement. The resulting UVAPF$_0$ and UVAPF were automatically calculated from the software.

UVAPF$_0$ is the indicated value of the UVA protective efficiency measured before the irradiating of samples (Equation 8).

$$\mathrm{UVAPF_0} = \frac{\int_{320\ \mathrm{nm}}^{400\ \mathrm{nm}} \mathrm{P}(\lambda) \cdot \mathrm{I}(\lambda) \cdot \mathrm{d}(\lambda)}{\int_{320\ \mathrm{nm}}^{400\ \mathrm{nm}} \mathrm{P}(\lambda) \cdot \mathrm{I}(\lambda) \cdot 10^{-\mathrm{Abs}(\lambda)\mathrm{C}} \cdot \mathrm{d}(\lambda)} \qquad \text{(Eq.8)}$$

Where P(λ) is persistent pigment darkening action spectrum, I(λ) is spectral irradiance (W/m^2/nm) at wavelength 320-400 nm, Abs(λ) is Mean of absorbance value of samples before UV exposure at wavelength 320-400 nm, C is the coefficient of adjustment, d(λ) is wavelength interval, which is 1 nm.

C value (coefficient of adjustment) is a value obtained from the adjustment of *in vitro* calculated SPF are equal to *in vivo* SPF (SPF_{label}). C value is generated by the software and calculated by following Equation 9. C value should fall within range between 0.8 to 1.6.

$$SPF_{In\ vitro,\mathrm{adjust}} = SPF_{\mathrm{label}} = \frac{\int_{290\ \mathrm{nm}}^{400\ \mathrm{nm}} E(\lambda)\cdot I(\lambda)\cdot d(\lambda)}{\int_{290\ \mathrm{nm}}^{400\ \mathrm{nm}} E(\lambda)\cdot I(\lambda)\cdot 10^{-\mathrm{Abs}(\lambda)C}\cdot d(\lambda)} \quad \text{(Eq.9)}$$

Where SPF_{label} is SPF value measured from *in vivo* SPF method, E(λ) is erythema action spectrum, I(λ) is spectral irradiance ($W/m^2/nm$) at wavelength 290-400 nm, Abs(λ) is Mean of absorbance value of samples before UV exposure at wavelength 290-400 nm, d(λ) is wavelength interval, which is 1 nm.

Then, the sample plates were irradiated through xenon arc lamp from solar simulator (Suntest CPS+, Atlas Material Testing Technology GmBH, Linsengericht, Germany). The irradiation dose (D) is derived from $UVAPF_0$ and calculated using Equation 10. After that, the sample plates were again measured and calculated UVAPF after irradiation (Equation 11).

$$D = UVAPF_0 \times 1.2\ J/cm^2 \quad \text{(Eq.10)}$$

$$UVAPF = \frac{\int_{320\ \mathrm{nm}}^{400\ \mathrm{nm}} P(\lambda)\cdot I(\lambda)\cdot d(\lambda)}{\int_{320\ \mathrm{nm}}^{400\ \mathrm{nm}} P(\lambda)\cdot I(\lambda)\cdot 10^{-\mathrm{Abs}(\lambda)C}\cdot d(\lambda)} \quad \text{(Eq.11)}$$

Where P(λ) is persistent pigment darkening action spectrum, I(λ) is spectral irradiance ($W/m^2/nm$) at wavelength 320-400 nm, Abs(λ) is mean absorbance value of samples after UV exposure at wavelength 320-400 nm, C is the coefficient of adjustment, d(λ) is wavelength interval, which is 1 nm.

The UVAPF value of a sunscreen should be at least one third of the labelled SPF and λ_C must be equal to or greater than 370 nm. The sunscreen achieved both requirements indicated the ability to protect against UVA ray and could specify the UVA seal sign.

UVA reference sunscreen S2 (from Annex E, ISO24443:2012) (50).

S2 was used as a reference for the purposes of test procedure validation of UVA protection. Formulation of S2 was modified from UVA reference sunscreen of ISO24443:2012. The ingredients are shown in **Table 8**. The mean and acceptance rang for S2 used for the purposes of validating the test procedures of this test method are shown in **Table 9**.

Table 8 The compositions of reference sunscreen S2.

Compositions	**%W/W**
Aqueous phase	
Water	52.43
Propylene glycol	1.00
Xanthan gum	0.60
Carbopol 940	0.15
Disodium EDTA	0.08
Triethanolamine	0.23
Oil phase	
Octocrylene	3.00
Butylmethoxy dibenzoylmethane	5.00
Ethylhexyl methoxycinnamate	3.00
Bis-ethylhexyloxyphenol methoxyphenyl triazine	2.00
Cetyl alcohol	1.00
Steareth-21	2.50
Steareth-2	3.00
Dicaprylyl carbonate	6.50
Decyl cocoate	6.50
Phenoxyethanol	1.00
Cyclopentasiloxane	2.00

Table 9 The mean and acceptance rang of the reference sunscreen S2 (50).

Reference sunscreen	**Mean**	**Mean**	**Acceptance limits**	
Formulation	SPF	UVAPF	Lower limit	Upper limit
S2	16.0	12.7	10.7	14.7

Part 5: Determination the effects of base formulations

The combination of organic UV filters, inorganic UV filters and inorganic pigments in the developed sunscreens selected were prepared in different bases. The base formulations were mousse and lotion. The compositions of the two base formulations are shown in **Table 10**. The protective efficiency of the formulated sunscreens was evaluated by determining PPF value using a UV-1800® spectrophotometer and by determining SPF, UVAPF, and λ_C values using a UV-2000® transmittance analyzer.

In addition, the absorptive effectiveness in the blue light (400-450 nm) of a sunscreen was proved to correlate with the translucent or opaque appearance of the sunscreens (12). Therefore, in this part protective efficiency of the cream, mousse, and lotion formulations against blue light, the most harmful component of visible light, was evaluated through the measurement of translucency parameter (TP). To prepare the sample plates, the selected sunscreens were weighed and applied on quartz plates at 1.3 mg/cm^2. After that, the applied sample plates were measured L^*, a^*, b^* values against black (L^*_{SB}, a^*_{SB}, b^*_{SB}) and white (L^*_{SW}, a^*_{SW}, b^*_{SW}) backgrounds using CM-700d® spectrophotometer (Konica Minolta, New Jersey, United States). The empty plates were also measured L^*, a^*, b^* in black background (L^*_{EB}, a^*_{EB}, b^*_{EB}) and white background (L^*_{EW}, a^*_{EW}, b^*_{EW}). Then, these values were calculated TP according equation 12-13 (TP_S applied plate, TP_E empty plate). In addition, they were also calculated in the difference ($\Delta TP = TP_E - TP_S$) for enhancement the precision in the comparison of measured TP (Equation 14).

$$TP_S = \sqrt{(L^*_{SB} - L^*_{SW})^2 + (a^*_{SB} - a^*_{SW})^2 + (b^*_{SB} - b^*_{SW})^2} \quad \text{(Eq.12)}$$

Where TP_S is TP value of applied sample plates, L^*_{SB} or L^*_{SW}; a^*_{SB} or a^*_{SW}; b^*_{SB} or b^*_{SW} are L^*, a^*, b^* values of applied sample plates against black and white background respectively.

$$\mathrm{TP_E} = \sqrt{(L^*_{EB} - L^*_{EW})^2 + (a^*_{EB} - a^*_{EW})^2 + (b^*_{EB} - b^*_{EW})^2} \quad \text{(Eq.13)}$$

Where TP_E is TP value of the empty plate, L^*_{EB} or L^*_{EW}; a^*_{EB} or a^*_{EW}; b^*_{EB} or b^*_{EW} are L^*, a^*, b^* values of empty plate against black and white background respectively.

$$\Delta \mathrm{TP} = \mathrm{TP_E} - \mathrm{TP_S} \quad \text{(Eq.14)}$$

Cream, mousse, and lotion formulations were assessed the viscosity and the rheological profile using a Brookfield cone and plate type rheometer (DV-III, AMETEK Brookfield, Middleboro, United states) under experiment conditions including 25.0 ± 1.0 °C, 0.5 gram of sample, and CP51-CP52 spindles.

Table 10 The compositions of bases cream, mousse, and lotion.

Function	Compositions	Cream	Mousse	Lotion
			(%W/W)	
Dispersing agent	C12-15 Alkyl Benzoate	5.50	-	6.00
	Caprylic/Capric Triglyceride	7.00	-	2.00
	Hexyl Laurate	-	-	5.00
	Cyclomethicone	-	13.00	-
	Squalene	-	11.00	-
Thickener	Cetylstearyl alcohol	1.00	-	-
	Stearic acid	1.00	-	-
	Caprylic/capric triglyceride and stearalkonium hectorite and propylene carbonate	-	5.00	-
	Cyclopentasiloxane (and) Dimethicone Crosspolymer	-	39.00	-
	Carbopol 940	0.08	-	0.20
Emulsifier	Glyceryl stearate (and) PEG-100 stearate	4.25	-	-
	Sorbitan monostearate	0.75	-	-
	PEG-60 Hydrogenated Castor Oil	-	-	1.20
	Cremophore A25	-	-	1.00
	Cremophore A6	-	-	0.80
	Polyglyceryl-3 Diisostearate	-	-	2.00
Humectant	Glycerin	3.00	-	-
	Propylene glycol	-	-	4.00
Neutralizer	Triethanolamine	0.50	-	0.14
Chelating agent	Disodium EDTA	0.04	0.04	0.04
Preservative	Phenoxyethanol	0.40	0.40	0.40
Antioxidant	Vitamin E acetate	0.15	0.15	0.15
	Water	q.s.to 100	q.s.to 100	q.s.to 100

Part 6: Comparison the effectiveness of the developed sunscreen with commercial sunscreen products for the protection against blue light radiation

The developed sunscreen in the base formulation yielding the highest SPF, UVAPF, $\lambda_{C,}$ and PPF was selected. Their protection efficiency against blue light through PPF value was compared with the available commercial sunscreens. The criteria for selecting of commercial sunscreens to this study were following:

1. The products claimed to protect blue light on the label.
2. The products contained selected organic UV filters, inorganic UV filters and/or inorganic pigments.
3. The products contained or did not contain organic UV filters (which were studied in Part 2 of this thesis) and/or inorganic UV filters and/or inorganic pigments.
4. All selected products should have expiry date more than two years after manufacturing date.

Statistical Analysis

1. The statistics difference of the Mean of each sample was compared using one-way analysis of variance (ANOVA) followed by Tukey’s test for multiple comparisons (SPSS Statistic 22.0, International business machine Corporation, New York, USA). Level *p* less than or equal 0.05 was considered significant. The results were expressed as mean ± standard deviation (SD).

2. The reliability of SPF and UVAPF values measured from UV-2000S® were analyzed by 95%CI (95% confidence interval). 95%CI should less than 17% of mean SPF or UVAPF. If 95%CI was greater than 17% of the mean value, the test of that product should add plates until 95%CI was less than 17% of the Mean (50). 95%CI was calculated by following Equation 16.

$$95\%\text{CI} = \frac{(100\times \text{C})}{\text{Mean UVAPF}} \qquad \text{(Eq.16)}$$

$$\text{C} = \frac{(t\ \text{value})\times \text{S.D.}}{\sqrt{\text{n}}}$$

Where S.D. is standard deviation, n is total number of plates used, *t* is *t* value from the two-sided student-*t* distribution (**Table 11**).

Table 11 Two-sided student -*t* distribution.

n	4	5	6	7	8
t value	3.182	2.776	2.571	2.447	2.365

3. The reproducibility of results measured from UV-1800® spectrophotometer was analyzed using %CV (%Coefficient of variation). %CV was defined as the ratio of the standard deviation (S.D.) to Mean (Equation 17). %CV of the samples should not be higher than 20% (51).

$$\%\text{CV} = \frac{\text{S.D.}}{\text{Mean}} \times 100 \qquad \text{(Eq.17)}$$

CHAPTER IV

RESULTS AND DISCUSSION

Part 1: Survey the UV filters frequently used in commercial sunscreens

The survey for the UV filters frequently used in commercial sunscreens was performed in 89 products. The SPF value claimed on the labels was found to be ranging from 30 to 50+ and 56 out of 89 products claimed SPF 50+. The UVA protection was declared in 83 products using various signs, including PA system (67 products), UVA seal (13 products), and Boots star rating (3 products). The 89 surveyed products were found to contain 1 to 9 UV filters (**Figure 8**). Among these, the usage of 4-6 filters in one product was often found while the usage of 1, 7 or 9 filters in one product was found the least. In these surveyed products, 47 products (52.8% of total products) contained only organic UV filters, 4 products (4.5%) contained only inorganic UV filters and the remaining (42.7%) contained both organic and inorganic UV filters.

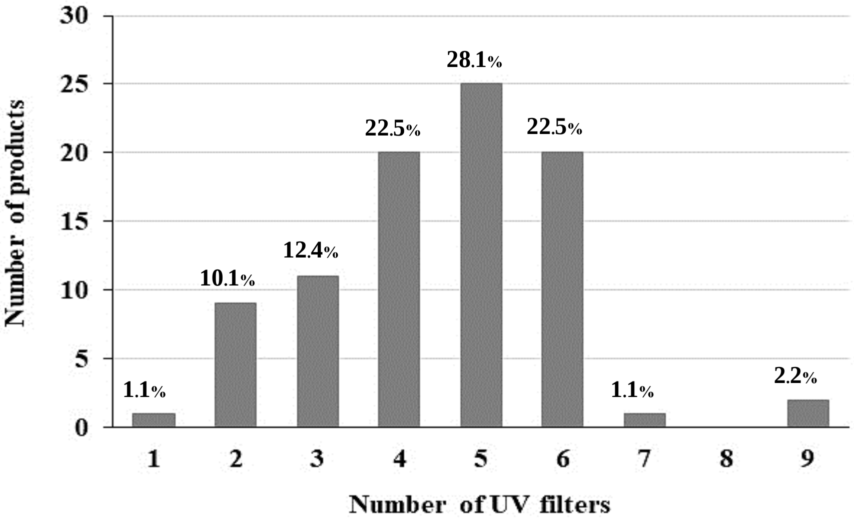

Figure 8 Graph showing number of commercial sunscreen products containing 1–9 UV filters. The percentage shown was calculated based on the total number of product surveyed.

In Thailand, 26 kinds of organic UV filters and 2 kinds of inorganic UV filters were permitted to use in sunscreens (1). However, not all of these filters were used in the commercial products. From this survey, it was found that only 18 UV filters were used and their usage frequency ranking from the highest to the lowest was as follows (**Figure 9**): 1) Butyl methoxydibenzoylmethane (BMDM), 2) Ethylhexyl methoxy-cinnamate (EHMC), 3) Bis-Ethylhexyloxyphenol Methoxy-phenyl Triazine (BEMT), 4) Octocrylene (OCR), 5) Titanium dioxide (TiO_2), 6) Ethylhexyl salicylate (EHS), 7) Homosalate (HMS), 8) Diethylamino hydroxybenzoyl hexyl benzoate (DHHB), 9) Phyenylbenzimidazole sulfonic acid (PBSA), 10) Zinc oxide (ZnO), 11) Ethylhexyl triazone (EHT), 12) Benzophenone-3 (BZ-3), 13) Methylene bis-benzotriazolyl tetramethylbutylphenol (MBBT), 14) Terephthalylidene dicamphor sulfonic acid (TDSA), 15) Drometrizole trisiloxane (DTS), 16) 4-methyl-benzylidene camphor (4-MBC), 17) Diethylhexyl butamido triazone (DHBT) and 18) Polysilicone-15 (PS-15).

From this list, only 11 filters were selected as shown in black bar of **Figure 9**. PBSA was not selected into the study. This is due to it possesses high melting point (234°C) and low water solubility. Its water solubility must be enhanced by neutralizing with suitable base (e.g. triethanolamine, sodium hydroxide) to pH-value of around 7 and a sunscreen formulation containing PBSA must be buffered at this pH-value. At pH below 6.5, it may revert to acid form, resulting in crystallization. Moreover, it was also reported that the hydrophilic property of PBSA caused the penetration through rat skin in higher amount than BZ-3 and BMDM (57). It has been reported that benzophenones, including BZ-3, commonly caused contact allergic dermatitis and photocontact dermatitis (58-60). BZ-3 also known as oxybenzone, is absorbed after applying on the skin and can be detected in urine and plasma of human (3). The EC’s Scientific Committee on Cosmetic Products and Non-Food Products (SCCP) reduced the maximum authorized concentration of BZ-3 as a UV filter in sunscreen products from 10%W/W to 6%W/W. In addition, it is allowed to use as a light stabilizer for all types of cosmetic products only up to 0.5% w/w and the warning “contains Benzophenone-3” must be indicated on the label (61). TDSA and DTS, known as Mexoryl SX and Mexoryl XL, are patented by L’Oreal Paris and sunscreens containing these filters are limited L’ Oreal and its brands. For 4-MBC, it has been reported to exhibit estrogenic effects and endogenous reproductive hormone levels in humans (62, 63). It also has carcinogenic effect by increasing the proliferation of breast cancer cell (64). 4-MBC is banned in the USA. PS-15 was the least used UV filter in the 89 products surveyed. It is used in leave on hair products with the benefit in UV protection against fading of hair color (65). Therefore, it was not often found in sunscreens. PS-15 was approved as UV filters in only the Europe and Asia, but not in the USA.

Apart from the 11 UV filters selected based on the surveyed, Tris-biphenyl triazine (nano) (TBPT) was also included into the study. TBPT is a new generation and the first micronized UV filter approved for use in sunscreens under the regulations of EU, Thailand, and Japan at the maximum authorized concentration of 10%W/W (44). It can protect the sunlight at wavelength range from UVB to UVAII by absorbing and scattering UV radiation (66). The study of Couteau et al. (67) have been reported that the protective efficiency of TBPT in UVB and UVA regions was comparable to BEMT and DHHB, respectively.

Moreover, apart from BEMT (powder form) which was included in this study, Bis-Ethylhexyloxyphenol methoxyphenyl triazine (and) polymethyl methacrylate (BEMT AQ) which was in the form of suspension was also included. BEMT AQ consists of encapsulation of BEMT in acrylates/C12-22 alkyl methacrylate copolymer. It is developed for mixing into aqueous phase and thus reducing of UV filters load in oil phase of formulation. It helps to improve the sensory of formulation with non-sticky texture.

In summary, the total of 13 UV filters were selected for further studies. Among these filters, there are 11 organic UV filters, including BMDM, EHMC, BEMT, OCR, EHS, HMS, DHHB, EHT, MBBT, TBPT and BEMT AQ and 2 inorganic UV filters, including TiO_2 and ZnO.

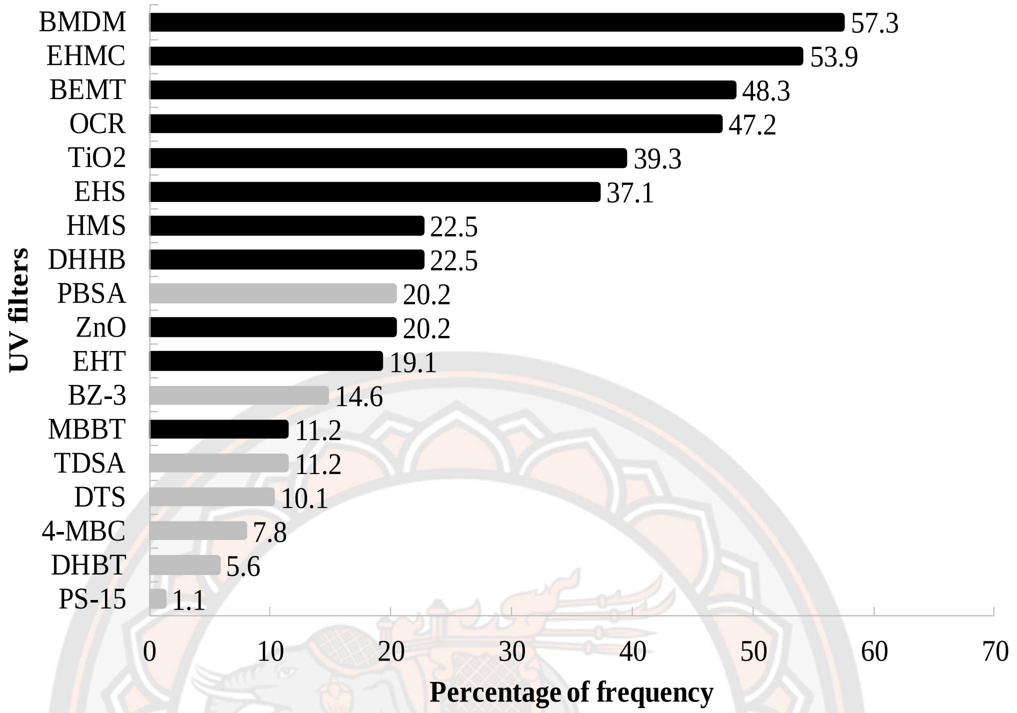

Figure 9 The ranked usage frequency of UV filters in commercial sunscreens, as obtained from a survey during May to June 2019 at hypermarkets in Phitsanulok (Thailand). Black bar were the UV filters included in the study and grey bar were the excluded UV filters.

Part 2: Screening for ultraviolet and visible light protective ability of the selected organic UV filters, inorganic UV filters and pigment

1. Organic UV filters

The selected eleven organic UV filters (i.e. BMDM, EHMC, BEMT, OCR, EHS, HMS, DHHB, EHT, MBBT, TBPT, and BEMT AQ) were screened for the ability of UV and visible light protection. They were shown different protection through their absorbance spectra (**Figure 10**). Each sample provided the highest peak (maximum absorption) at different wavelength region based on their types of organic UV filters. It was observed that only TBPT provided the absorption extending from UV to visible light wavelength (290-800 nm).

The protective ability of these selected organic UV filters was also demonstrated through various parameters including maximum absorption wavelength (λ_{max}), A (1%, 1cm), critical wavelength (λ_C) (**Table 12**) and visible protection wavelength (λ_{Vis}) (**Figure 12**).

λ_{max} was used to classify the types of organic UV filters into UVB, UVA, or UVB/A filters. If the λ_{max} of a filter falls in the range of UVB wavelength (290-320 nm), it is classified as a UVB filter. On the other hand, if the λ_{max} of a filter falls in the range of UVA wavelength (320-400 nm), it is classified as a UVA filter. The results of this part were correlated with other publications (68, 69). EHMC, EHS, EHT, HMS, and OCR were found to be UVB filters, while BMDM and DHHB were found to be UVA filters. Interestingly, TBPT showed λ_{max} in the UVB wavelength region. Moreover, it was the only organic UV filter, which could absorb light in visible light wavelength (400-800 nm). On the other hand, BEMT, BEMT AQ, and MBBT provided the λ_{max} in both UVB and UVA wavelength regions. Therefore, they were classified as UVB/A filters.

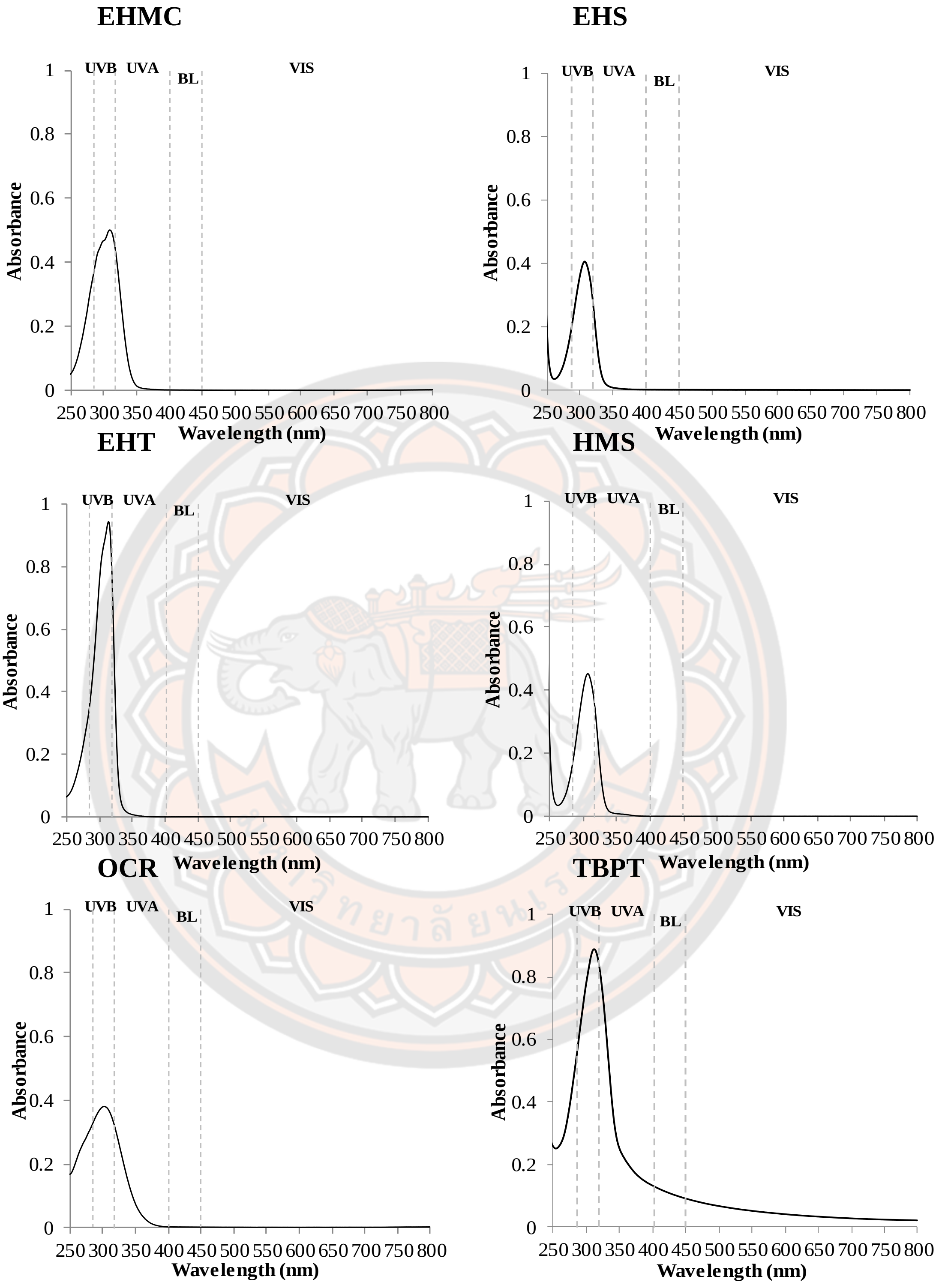

Figure 10 The absorbance spectra of selected organic UV filters; EHMC, EHS, EHT, HMS, OCR, TBPT, BMDM, DHHB, BEMT, BEMT AQ, and MBBT were carried out using UV-1800$^{®}$ spectrophotometer. The samples were prepared in ethanolic solution at 0.005-0.02 mg/ml.

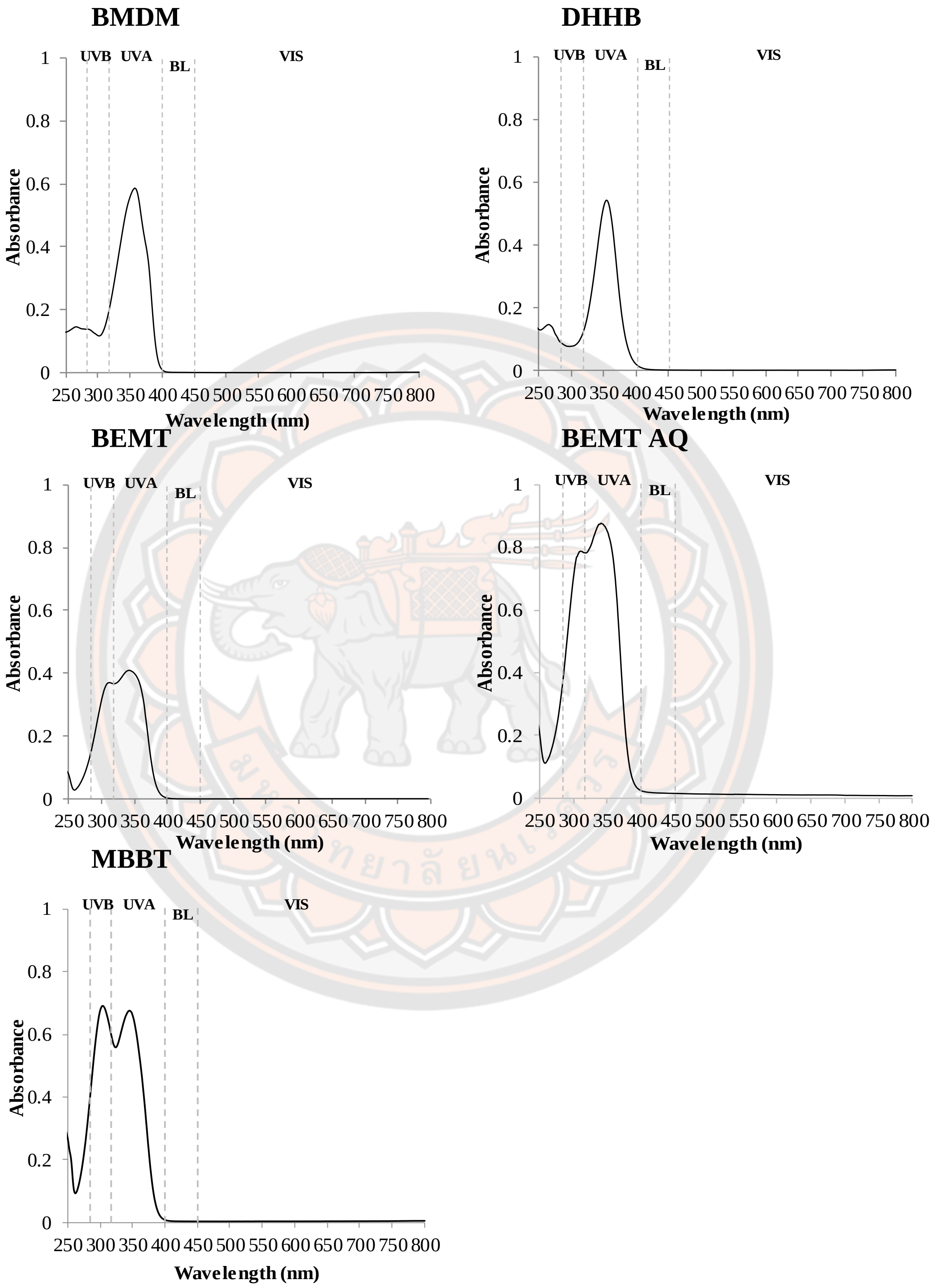

Figure 10 (Continued).

A (1%, 1cm) value indicates the absorption coefficient of an organic UV filter. Among those UVB filters, EHT showed the highest A (1%, 1cm) value, indicating the greatest protection in UVB radiation compared with other UVB filters. Comparing between UVA filters, BMDM showed higher protective efficiency against UVA radiation than DHHB. The remaining organic UV filters (BEMT, BEMT AQ, and MBBT) were UVB/A filters, they showed A (1%, 1cm) values in both UVB and UVA wavelengths.

In addition, the samples were also evaluated the breadth of protection at cover wavelength from 290-400 nm by λ_C values. The filters had λ_C values at least wavelength 370 nm, they provided broad protection cover entire UV wavelength (**Figure 11**). BMDM, and DHHB (UVA filters) showed λ_C values higher than wavelength 370 nm due to their high proportion of absorption in long wavelength region (UVA wavelength; 320-400 nm). The same results as BEMT, BEMT AQ, and MBBT, their absorptive ability in both UVB and UVA wavelengths led to obtain λ_C value greater than wavelength 370 nm.

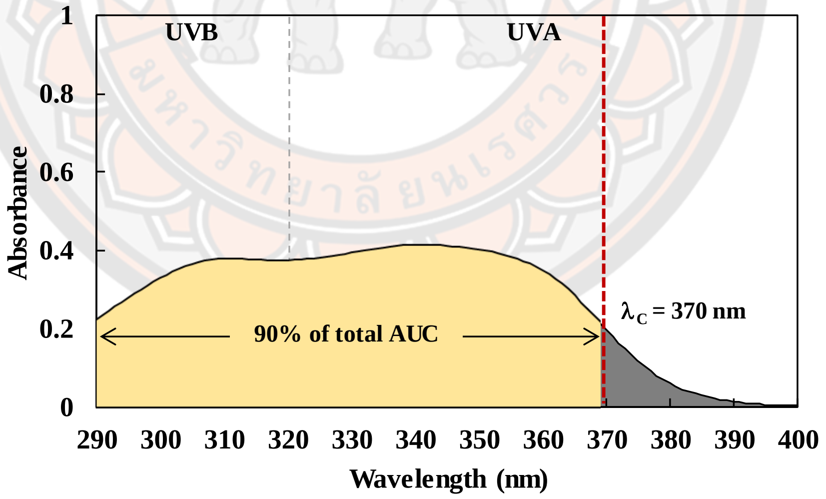

Figure 11 Breadth of UV protection determined from critical wavelength (λ_C), which is wavelength at 90% of area under the curve (AUC) of absorbance spectrum from 290 to 400 nm. The filters obtained λ_C value at least 370 nm that filters can provide broad protection cover entire UV wavelength.

Table 12 Maximum absorption wavelength (λ_{max}), A (1%, 1cm), critical wavelength (λ_C) and types of selected organic UV filters. The samples were prepared in ethanolic solution at 0.005-0.02 mg/ml based on active.

Samples	λ_{max} (nm)	A (1%, 1cm)	λ_C (nm)	Type
EHMC	309	999.7±13.4	336	UVB filter
EHS	306	203.2±4.5	332	UVB filter
EHT	314	1,890.5±17.6	330	UVB filter
HMS	306	226.3±6.9	331	UVB filter
OCR	303	379.5±17.0	349	UVB filter
TBPT	312	888.5±46.8*	367	UVB filter
BMDM	357	1,174.6±13.8	385	UVA filter
DHHB	354	1,083.9±33.9	381	UVA filter
BEMT	311	738.3±8.9	373	UVB/A filter
	342	821.5±10.5		
BEMT AQ	311	744.3±23.7*	373	UVB/A filter
	342	828.7±27.6*		
MBBT	304	681.1±17.6*	373	UVB/A filter
	345	668.8±14.1*		

*A (1%, 1cm) values of suspension samples were calculated based on active.

The visible light protective ability of selected organic UV filters was shown by visible protection wavelength (λ_{Vis}) (**Figure 12**). As details previously, λ_{Vis} was a parameter indicating the efficacy of a filter in visible light protection. It was adjusted from the calculation of critical wavelength, which become as 90% of the summation of AUC at wavelength between 290 to 800 nm. Interestingly, the results showed that only TBPT obtained λ_{Vis} value at wavelength higher than 400 nm, suggesting that it could act as a Vis filter. TBPT suspension is a particulate organic UV filter (particle size less than 100 nm). The compositions of TBPT suspension are shown in Chapter III (materials) and the structure of TBPT is shown in **Figure 13**. It can absorb or scatter as function of its particles (70). These characteristics may be led to TBPT had visible light attenuating properties.

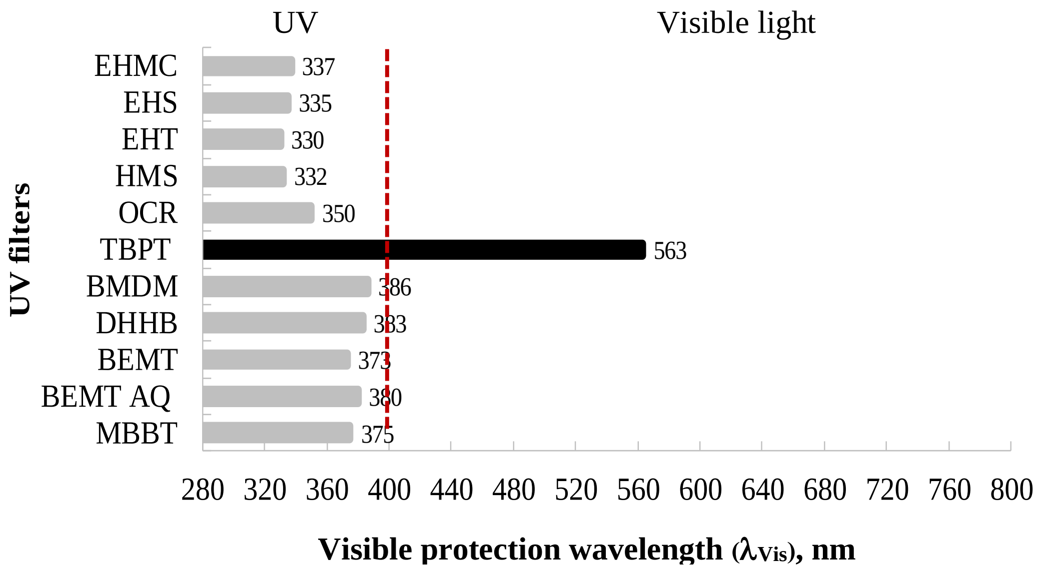

Figure 12 Visible protection wavelength (λ_{Vis}) of selected 11 organic UV filters, Black bar was Vis filters showing $\lambda_{Vis} \geq 400$ nm, Grey bar was organic UV filters showing $\lambda_{Vis} < 400$ nm. The samples were prepared in ethanolic solution at 0.005-0.02 mg/ml.

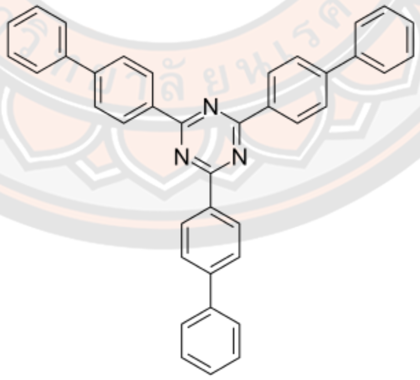

Figure 13 Structure of Tris-biphenyl triazine (TBPT) (67).

From the screening for UV and visible light protective ability of the selected organic UV filters, each type of them was selected for determining the effect of combination of various filters in further studies. EHT was selected as a UVB filter Although, BMDM showed higher efficacy of UVA protection than DHHB, it has been reported to be unstable under exposure of UV radiation and when combined with titanium dioxide (71). Therefore, DHHB was selected as a UVA filter. BEMT was selected as a UVB/A filter. BEMT in the form of powder and suspension (BEMT AQ) gave no different absorptive efficiency A (1%, 1 cm). Therefore, BEMT, was selected for further studies. Lastly, TBPT was selected as a Vis filter.

2. Inorganic UV filters and pigments

TiO_2 and ZnO are allowed for use as inorganic UV filters in sunscreens. In cosmetic industry, they are available in a variety range of primary particle sizes and coating agents. Several studies have been reported that the particle size of TiO_2 and ZnO influenced to their efficacy of UV and visible light protection. TiO_2 and ZnO having size between 200-400 nm known as pigment was shown to be the best for scattering efficiency against visible light radiation (39, 72). However, this size range caused thick, white, and opaque appearance upon application. Therefore, nanosize inorganic particles with size less than 100 nm (i.e. UV filter) is generally used in commercial sunscreens. The nanosize particles can provide a translucent appearance on application, which make the greater cosmetic acceptability and also provide the better effective protection against UV radiation (39).

The surface coated inorganic UV filters and pigments are widely used in commercial sunscreen products. They can minimize the photocatalytic effect by capturing ROS and preventing contact between TiO_2 surface and oxygen or medium (40) and affect to the properties of inorganic particles such as hydrophobicity, dispersibility, and wettability. The coating agent are often used including triethoxycrprylylsilane, dimethicone, hydrogen dimethicone, silica, stearic acid, and aluminium hydroxide.

From these reasons, TiO_2 and ZnO having particle size in range between 200 to 300 nm (pigment grade) and size less than 100 nm (UV filter grade) were included in this study. In addition, TiO_2 and ZnO having various coating agents and uncoated were also included. The selection of these inorganic particles was based on different particle size with same coating agents and the same particle size with different coating agents. Their characteristics were selected according the criteria of EC regulation and are detailed in **Table 13**. All of them were cosmetic grade materials for using in sunscreens.

These ten selected inorganic UV filters and pigments were determined for the protective efficiency against UV and visible light radiation. As described previously, λ_C was calculated from 90% of the summation of AUC of absorbance spectrum from wavelength 290 - 400 nm. The λ_C of all ten selected inorganic UV filters and pigments showed $\lambda_C \geq 370$ nm (**Table 14**), indicating that they could protect both UVB and UVA radiations. λ_{Vis} was a parameter used to indicate visible light protection. It was modified from critical wavelength equation and calculated from 90% of the summation of AUC at 290-800 nm. From the results show in **Table 14**, it was observed that all samples yielded $\lambda_{Vis} \geq 590$ nm. Therefore, these samples could act as Vis filters.

The transmittance spectra of all samples were shown extending from UVB to visible light wavelength regions (290-800 nm) (**Figure 14**). The four TiO_2 samples (i.e. TT60, TD35, T250, TT300) were showed better light protection, especially against visible light, compared to all ZnO samples. This result may be due to the difference between the RI of TiO_2 (2.700) or ZnO (2.000) particles and the medium (RI of ethanol = 1.362) (40). ZnO possesses lower RI than TiO_2, resulting in a lower ability of visible light scattering. In addition, some studies have been reported that the visible light scattering property of ZnO was minimized at particle size less than 200 nm (73), thereby transmission of light was increased.

Table 13 The characteristic of inorganic UV filters/pigments selected into the study.

Samples	Crystalline form/ Compositions	Coating agent	Primary Particle size*	Category
T35	Rutile/Titanium dioxide	Uncoated	35 nm	UV filter
TD35	Rutile, Titanium dioxide and aluminium hydroxide and hydrated silica and dimethicone	Dimethicone	35 nm	UV filter
TT60	Rutile/Titanium dioxide and aluminium hydroxide and triethoxycaprylylsilane	Triethoxy caprylyl silane	60 nm	UV filter
T250	Rutile/Titanium dioxide and aluminium hydroxide	Uncoated	250 nm	Pigment
THD250	Rutile/Titanium dioxide and aluminium hydroxide and hydrogen dimethicone	Hydrogen dimethicone	250 nm	Pigment
TT300	Rutile/Titanium dioxide and aluminium hydroxide and triethoxycaprylylsilane	Triethoxy caprylyl silane	300 nm	Pigment
ZT20	Wurtzite/Zinc oxide and triethoxycaprylylsilane		20 nm	UV filter
ZHD100	Wurtzite/Zinc oxide and hydrogen dimethicone		100 nm	UV filter
ZT120	Wurtzite/Zinc oxide and triethoxycaprylylsilane		120 nm	UV filter
ZT200	Wurtzite/Zinc oxide and triethoxycaprylylsilane		200 nm	Pigment

*Particle size reported from the manufacturer; particle size less than 100 nm denote nanosize and size 100-1000 nm denote submicronsize.

Samples code: First T = TiO_2, Z = ZnO, Second D, T, or HD = Coating agents, Number = particle size.

Table 14 Critical wavelength (λ_C) and visible protection wavelength (λ_{Vis}) of the selected titanium dioxide and zinc oxide with various particle sizes and coating agents. The samples were prepared in ethanolic solution at 0.02 mg/ml.

Samples	λ_C (nm)	λ_{Vis} (nm)
T35	389	738
TD35	384	638
TT60	385	593
T250	389	737
THD250	389	751
TT300	389	739
ZT20	384	590
ZHD100	388	715
ZT120	389	676
ZT200	385	609

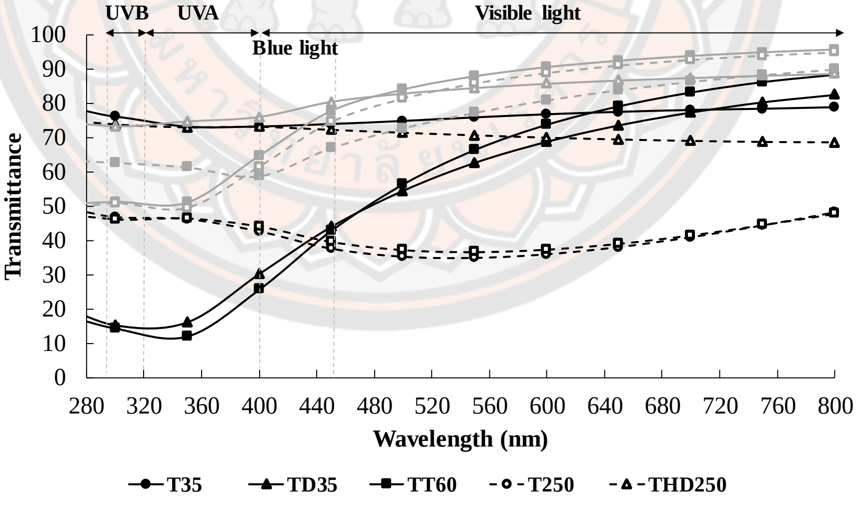

Figure 14 The UV-visible light transmittance spectra of individual TiO_2 (black line) and ZnO (grey line) with nanosize (solid line), submicronsize (dashed line), uncoated (circle), coated with dimethicone or hydrogen dimethicone (triangle), coated with triethoxycaprylylsilane (square). The samples were prepared in ethanolic solution at 0.02 mg/ml.

The area under the curve (AUC) in four wavelength ranges, including UVB (290-320 nm), UVA (320-400 nm), blue light (400-450 nm), and visible light (400-800 nm) for TiO_2 was further calculated (**Table 15**). It was observed that surface-coated nanosize TiO_2 (i.e.TD35 and TT60) produced higher AUC in both UVB and UVA wavelength ranges compared to the other four samples. These results indicated that TD35 and TT60 were suitable for protecting UVB and UVA radiation. Interestingly, uncoated nanosize TiO_2 (i.e. T35) showed poorer UVB and UVA protection than TD35 and TT60. It is generally known that the light scattering property of TiO_2 is influenced by particle size, crystalline form, RI of particles and surrounding medium, and dispersion of particles (72). In this study, T35, TD35 and TT60 were nanosize particles in the rutile crystalline form and the same medium was used for preparing of all samples. The difference among these three TiO_2 was surface property. It has been reported that the coating using silicon dioxide (SiO_2) or aluminium oxide (Al_2O_3) could reduce photoreactivity and thus less reactive oxygen species (ROS) were produced (74, 75). On the other hand, the coating agents such as dimethoxydiphenylsilane, triethoxycaprylylsilane, dimethicone and simethicone etc. have been shown to improve the dispersibility of TiO_2 in medium (76). Therefore, it may be possible that uncoated TiO_2 (T35) forms agglomerate through the attraction of van der waals force between the particles, resulting to reduce the amount of surface area available to absorb light (77).

The scattering property of TiO_2 with larger size shifts toward longer wavelength. The submicronsize TiO_2 (i.e. T250 and TT300), except THD250, showed high AUC in visible light wavelength (400-800 nm), suggesting the better visible light protection. This can be explained by the fact that submicronsize, rutile TiO_2 (known as pigment) hardly absorbs any light in the visible light range. In addition, it can effectively scatter visible light because it has a high RI (2.700) and thus it showed whitish and opaque appearance. The optimum scattering is proofed with TiO_2 particle diameter (D) equal half of the wavelength (λ) of the light ($D=\lambda/2$). Therefore, at visible light wavelength (400-800 nm), the size range between 200-400 should have excellent ability to scatter light (39, 72). In the case of THD250, submicronsize TiO_2 coated with hydrogen dimethicone, it possessed translucent appearance after dispersing in ethanol. The translucent samples have been reported to show lower ability of visible light protection (12).

Blue light is a subset of the visible light spectrum and it is known to cause of photoaging, induce abnormal pigmentation, resulting in age spots or melasma (5, 10). From **Table 15**, TT60 showed the highest protection against blue light, followed by TD35. Although T250 and TT300 provided a slightly lower protection against blue light, they offered protection against visible light two times higher than TT60 and TD35 samples.

Table 15 Area under the curve in UV-visible light wavelength of individual titanium dioxide with various particle size and coatings. The samples were prepared in ethanolic solution at 0.02 mg/ml.

Samples	**Area under the curve (AUC) (n=3)**				
	UVB	**UVA**	**Blue light**	**Visible light**	**Total area**
	290-320 nm	**320-400 nm**	**400-450 nm**	**400-800 nm**	**290-800 nm**
Titanium dioxide					
T35	3.6 ± 0.3^{e}	10.8 ± 0.9^{k}	6.7 ± 0.6^{q}	43.2 ± 1.2^{x}	57.7 ± 1.5
TD35	25.1 ± 0.2^{a}	57.1 ± 0.7^{g}	21.0 ± 0.4^{m}	78.3 ± 0.9^{u}	160.5 ± 1.6
TT60	25.7 ± 0.2^{a}	66.2 ± 0.1^{f}	23.3 ± 0.1^{l}	72.1 ± 0.6^{v}	164.6 ± 0.8
T250	9.8 ± 0.4^{b}	27.2 ± 0.9^{h}	19.9 ± 0.7^{m}	167.4 ± 2.6^{s}	204.5 ± 3.6
THD250	3.7 ± 0.2^{e}	10.6 ± 0.3^{k}	6.9 ± 0.1^{q}	61.5 ± 0.4^{w}	75.8 ± 0.9
TT300	10.0 ± 0.1^{b}	26.8 ± 0.3^{h}	18.9 ± 0.2^{n}	158.1 ± 1.8^{t}	195.0 ± 2.2
Zinc oxide					
ZnT20	8.8 ± 0.1^{c}	23.5 ± 0.3^{i}	7.1 ± 0.1^{q}	22.8 ± 0.3^{z}	55.1 ± 0.5
ZHD100	6.4 ± 0.3^{d}	19.2 ± 0.8^{j}	10.4 ± 0.4^{o}	44.9 ± 1.4^{x}	70.5 ± 2.5
ZT120	8.8 ± 0.3^{c}	24.3 ± 0.5^{i}	8.1 ± 0.1^{p}	26.7 ± 0.5^{y}	59.8 ± 1.3
ZT200	3.8 ± 0.2^{e}	10.2 ± 0.4^{k}	5.1 ± 0.1^{r}	27.7 ± 0.7^{y}	41.7 ± 1.2

Note: Different alphabet in each column are statistically different of data ($p<0.05$).

Part 3: Development of sunscreen products for ultraviolet and visible light protection

After the organic UV filters as well as TiO_2 and ZnO (UV filter and pigment grade) were individually investigated for protective ability of UV and visible light, these filters were incorporated in a base cream and again evaluated for the UV and visible light protective efficiency.

3.1 Effects of combined organic UV filters

From the survey, it was observed that almost all of the commercial sunscreen products consisted of a combination of more than one organic UV filters for enhancing the efficacy of UV protection. The degree of UV protection is directly related to the amount and types of UV filters. This part of the study was therefore performed to determine the effect of the combination of selected organic UV filters for UV and visible light protection. The compositions of the combined organic UV filters prepared in sunscreen formulation are shown in **Table 16**.

Table 16 The compositions of formulations containing combined organic UV filters (FCO1- FCO5) prepared in base cream.

Samples	Amount of filters (%W/W)				Total amount of filters (%w/w)
	UVB	UVA	UVB/A	VIS	
	EHT	DHHB	BEMT	TBPT*	
FCO1	-	-	5	2.5	7.5
FCO2	2.5	5	-	2.5	10.0
FCO3	2.5	-	5	2.5	10.0
FCO4	-	5	5	2.5	12.5
FCO5	2.5	5	5	2.5	15.0

*Concentration based on active.

Samples code: F=Formulation, C=Combination, O=Organic UV filters.

All combined organic UV filters resulted the absorption by the absorbance spectra, they showed the protective efficiency covering from UV to visible light wavelength (290-800 nm) (**Figure 15**).

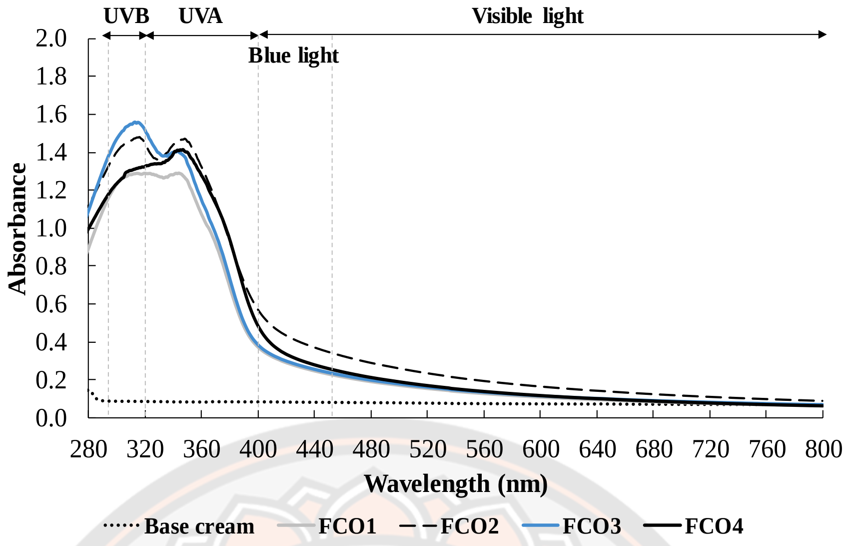

Figure 15 The absorbance spectra of base cream and formulations containing combined organic UV filters (FCO1- FCO5) in UV and visible light wavelength using UV-1800® spectrophotometer.

The efficacy of the formulations containing various combination of organic UV filters for UV and visible light protection was also demonstrated by AUC values (**Table 17**). FCO5 showed the highest AUC in all wavelength ranges, indicating the best in protection both UV and visible light. This was not surprising because FCO5 contained the highest total amount of organic UV filters. However, AUC for UVB (290-320 nm) and total wavelength ranges (290-800 nm) of FCO2 was higher than that of FCO4, even total amount of organic UV filters was lower. This is also not surprising because these two formulations had the different filters, which are EHT and BEMT. FCO2 contains 2.5% EHT while FCO4 contains 5% BEMT. As shown previously, EHT was the UVB filter with A (1%, 1cm) value of 1,890.5 ± 17.6 at 314 nm and BEMT was the UVB/A filter with A (1%, 1cm) value of 738.3 ± 8.9 at 311 nm and 821.5 ± 10.5 at 342 nm. These results indicated that EHT possesses more than two-times higher efficacy of absorption in UVB wavelength (290-320 nm) than BEMT does. Comparing between FCO2 and FCO5, the addition of BEMT (UVB/A filter) helped to enhance protection of UVA and blue/visible light. However, the synergistic effect of the combined selected organic UV filters in UV and visible light protection was not observed.

Table 17 Area under the curve in UV-visible light wavelength of base cream and formulations containing combined organic UV filters (FCO1- FCO5).

Samples	**Area under the curve (AUC) (n=3)**				
	UVB	**UVA**	**Blue light**	**Visible light**	**Total area**
	290-320 nm	**320-400 nm**	**400-450 nm**	**400-800 nm**	**290-800 nm**
Base cream	2.6 ± 0.1^{c}	6.6 ± 0.3^{h}	4.0 ± 0.2^{l}	28.9 ± 1.5^{p}	38.1 ± 1.9^{u}
FCO1	37.6 ± 1.7^{b}	78.8 ± 4.7^{g}	14.8 ± 0.6^{k}	58.3 ± 2.6^{o}	174.8 ± 8.0^{t}
FCO2	43.5 ± 2.4^{a}	90.3 ± 4.1^{e}	17.8 ± 2.3^{j}	66.7 ± 8.4^{n}	200.5 ± 12.0^{r}
FCO3	44.1 ± 3.5^{a}	85.6 ± 5.2^{f}	15.4 ± 1.4^{k}	59.8 ± 4.6^{o}	189.5 ± 8.9^{s}
FCO4	37.5 ± 2.4^{b}	89.7 ± 5.4^{e}	17.5 ± 1.8^{j}	63.3 ± 4.6^{n}	190.5 ± 11.0^{s}
FCO5	46.7 ± 2.1^{a}	104.1 ± 4.7^{d}	19.2 ± 1.5^{i}	70.7 ± 6.4^{m}	221.4 ± 9.7^{q}

Note: Different alphabet in each column are statistically different of data ($p<0.05$).

The obtained absorbance values were used in the calculation of SPF, UVAPF, λ_{C}, PPF and λ_{Vis} values to compare the efficacy of FCO1–FCO5 for UV and visible light protection (**Table 18**). FCO5 showed the highest SPF, UVAPF, and PPF, indication the highest protection against UV and visible light radiation. Focus on SPF, formulations containing EHT (UVB filter) i.e. FCO5, FCO3, and FCO2, gave higher SPF than those without EHT (i.e. FCO1 and FCO4). Although FCO4 contained BEMT (UVB/A filter), it possessed A (1%, 1cm) only half that of EHT at same UVB wavelength. For UVAPF, the formulations contained both DHHB and BEMT gave higher UVAPF (FCO5 and FCO4) than the formulation contained only DHHB (FCO2) or BEMT (FCO3). These results correlated with their A (1%, 1cm). As shown previously, TBPT was the only organic UV filters showed visible light protection. Therefore, it was added to all formulations and the PPF values were ranging from 2.1 ± 0.1 to 2.8 ± 0.3.

Table 18 Sun protection factor (SPF), UVA protection factor (UVAPF), critical wavelength (λ_C), porphyrin protection factor (PPF) and visible protection wavelength (λ_{Vis}) values of base cream and formulations containing combined organic UV filters (FCO1- FCO5).

Samples	SPF	UVAPF	λ_C (nm)	PPF	λ_{Vis} (nm)
Base cream	1.2 ± 0.0^e	1.2 ± 0.0^j	388	1.2 ± 0.0^o	740
FCO1	19.3 ± 2.6^d	10.9 ± 1.2^i	377	2.1 ± 0.1^n	602
FCO2	29.0 ± 3.4^c	14.6 ± 1.5^h	377	2.3 ± 0.2^m	608
FCO3	33.4 ± 3.7^b	12.0 ± 1.2^h	376	2.1 ± 0.1^n	584
FCO4	20.3 ± 2.1^d	16.1 ± 1.9^g	380	2.4 ± 0.2^l	582
FCO5	37.1 ± 3.8^a	22.9 ± 2.5^f	380	2.8 ± 0.3^k	581

Note: Different alphabet in each column are statistically different of data ($p<0.05$).

3.2 Effects of particle size and surface coating of inorganic UV filters and pigments

From the results of Part 2 Topic 2, TiO_2 showed better performance than ZnO. Therefore, it was selected into the study of this Part. The UV filter TiO_2 (i.e. T35, TD35, TT60) and the pigment TiO_2 (i.e. T250, THD250, TT300) were studied.

Firstly, these inorganic particle samples were individually incorporated into the base cream. The transmission spectra and area under the curve of base cream and formulations containing individual TiO_2 with various particle size and coating agents are shown in **Figure 18** and **Table 19,** respectively. The samples with lower transmittance values have shown greater protection due to the samples absorbed or scattered of incident light.

The study on effects of particle size on UV protection demonstrated that nanosize TiO_2 (i.e. FTT60, FTD35, FT35) showed better protection than submicronsize TiO_2 (i.e. FT250, FTT300, FTHD250) at UV wavelengths. These results are in agreement with the previous measurement, which the inorganic particles were dispersed in ethanol. TiO_2 not only scatters UV light but it also absorbs light at UV wavelength. The nanosize TiO_2 can absorb UV light stronger than those having submicronsize (**Figure 16**). In addition, TiO_2 absorbs light by excitation of a valence band electron (e^-) to the conduction band, leaving a hole in the valence band (h^+). The discrete energy levels of band called "band gap". Base on quantum size effect theory, band gap increases with decreasing the size of nanostructure, the smaller particles have a larger band gap energy, means that more energy is required to excite an electron (40) (**Figure 17**). Thus, UV light which has higher frequency and lower wavelength is better be absorbed by small-size TiO_2.

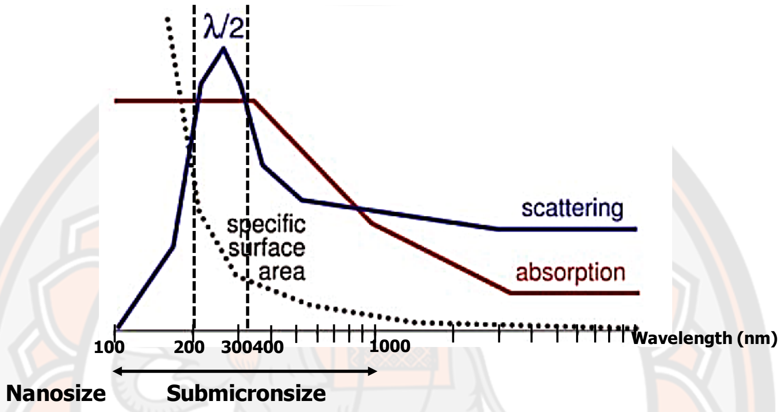

Figure 16 Visible light scattering or absorption of particle diameter between 0.1 to 10 micrometre (100 to 10000 nanometre) (78).

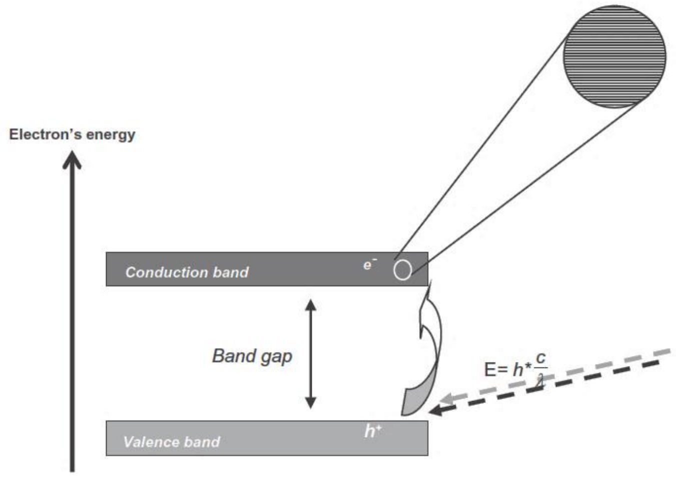

Figure 17 The band gap in a semiconducting material. Upon light absorption of minimally the band gap energy, a valence band electron (e−) is excited to the conduction band leaving a hole in the valence band (h+) (40).

The light absorption of nanosize TiO_2 may occur in the chemical compositions of molecules that are in the shell of particles (coating agents). Focusing on nanosize TiO_2, the effect of surface coating seemed to show less effect on UV and visible light protection. FTT60 formulation was the sunscreen cream containing TiO_2 coated with 4%W/W trethoxycaprylylsilane and having size 60 nm, FTD35 formulation was the cream containing TiO_2 coated with 3%W/W dimethicone (size 35 nm). AUC of these two formulations in UV-visible light wavelength regions were not significantly different. However, they provided better UV and visible light protection than FT35 formulation, the cream containing uncoated TiO_2 (**Table 19**). However, FT35 formulation was resulted in better UV and visible light protection than the previous results, preparing in ethanol. This may be due to dispersion of T35 particles in the process of cream preparation was performed using dispersing agents (i.e. C12-15 alkyl benzoate and caprylic capric triglyceride) before mixing with other ingredients in the formulation. This technique is generally used in sunscreen production. It helps to reduce the agglomeration of particles and provide superior protection of TiO_2.

For submicronsize TiO_2, uncoated FT250 showed significantly better protection against UV and blue/visible light than coated TiO_2, i.e. FTT300 and FTHD250, respectively. Comparing with nanosize TiO_2, submicronsize TiO_2 provided poorer protection against UVB radiation, but the protection was gradually increased in blue/visible light wavelengths. FT250 and FTT300 showed the significantly better blue/visible light protection than the other nanosize TiO_2 formulations. These results can be explained by high efficiency property of submicronsize T250 and TT300 in scattering the visible light (as details above). In addition, the reflectance of TiO_2 also depends on the surface coating.

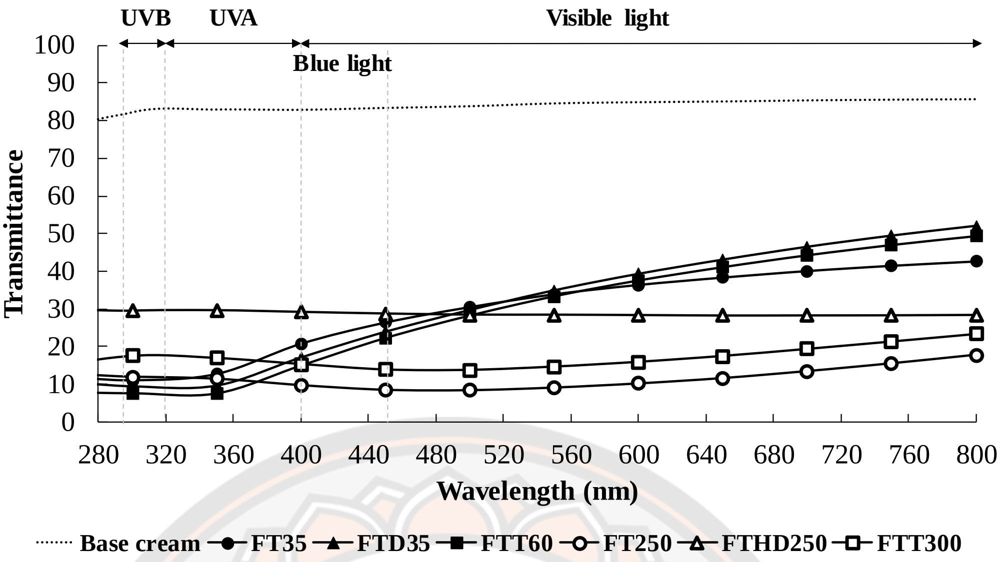

Figure 18 **The transmittance spectra of base cream and formulations containing individual TiO_2 with various particle size and coating agents in UV-visible light wavelength. Nanosize (solid line) and submicronsize (dashed line). The samples were prepared in base cream at 10%W/W and measured the transmission using a UV-1800® spectrophotometer.**

Table 19 **Area under the curve of base cream and formulations containing individual titanium dioxide with various particle size and coating agents in UV-visible light wavelength.**

Samples	Area under the curve (AUC) (n=3)				
	UVB	UVA	Blue light	Visible light	Total area
	290-320 nm	320-400 nm	400-450 nm	400-800 nm	290-800 nm
Base cream	2.6 ± 0.1^{e}	6.6 ± 0.3^{i}	4.0 ± 0.2^{o}	28.8 ± 1.5^{t}	38.1 ± 1.8^{x}
FT35	28.5 ± 1.6^{b}	66.5 ± 3.5^{g}	31.3 ± 1.4^{m}	189.5 ± 9.0^{s}	284.5 ± 13.0^{w}
FTD35	32.3 ± 1.0^{a}	79.2 ± 2.7^{f}	35.4 ± 1.4^{l}	185.2 ± 8.1^{s}	296.7 ± 11.3^{w}
FTT60	32.7 ± 1.3^{a}	81.0 ± 2.6^{f}	36.3 ± 2.2^{l}	189.6 ± 11.1^{s}	303.3 ± 12.5^{w}
FT250	27.6 ± 1.1^{b}	76.4 ± 3.2^{f}	52.1 ± 2.1^{j}	383.1 ± 16.7^{p}	487.1 ± 21.0^{u}
FTHD250	15.9 ± 0.6^{d}	42.8 ± 1.5^{h}	27.5 ± 0.9^{n}	229.7 ± 10.6^{r}	288.4 ± 12.4^{w}
FTT300	22.5 ± 1.3^{c}	61.8 ± 3.4^{g}	42.1 ± 2.7^{k}	317.3 ± 20.7^{q}	401.6 ± 24.6^{v}

Note: Different alphabet in each column are statistically different of data ($p<0.05$).

The efficacy of sunscreen creams containing individual titanium dioxide with different sizes and coatings on UVB, UVA, and blue/visible light protection were also assessed through parameters including SPF, UVAPF, λ_C, PPF, and λ_{Vis} values respectively (**Table 20).** Sunscreens containing nanosize coated TiO_2 (i.e. FTD35, FTT60) provided superior ability of UVB and UVA protection as shown by the highest values of SPF and UVAPF. Increasing particle size to submicronsize TiO_2 (i.e. FT250, FTHD250, FTT300) resulted to decrease SPF and UVAPF values. For PPF values, T250 was shown the best protection in blue light region, followed by FTT300 and FTHD250. FTHD250 provided the least in AUC of UV and blue light wavelength, corresponding with the lowest SPF, UVAPF, and PPF values.

Table 20 Sun protection factor (SPF), UVA protection factor (UVAPF), critical wavelength (λ_C), porphyrin protection factor (PPF), and visible protection wavelength (λ_{Vis}) of base cream and formulations containing individual titanium dioxide with various particle size and coating agents.

Samples	SPF	UVAPF	λ_C (nm)	PPF	λ_{Vis} (nm)
Base cream	1.2 ± 0.0^{e}	1.2 ± 0.0^{j}	388	1.2 ± 0.0^{p}	740
FT35	9.0 ± 1.0^{b}	6.8 ± 0.6^{h}	386	4.5 ± 0.3^{n}	722
FTD35	12.2 ± 1.0^{a}	10.1 ± 0.8^{f}	386	5.5 ± 0.4^{m}	700
FTT60	12.7 ± 1.2^{a}	10.8 ± 0.8^{f}	386	5.8 ± 0.4^{m}	706
FT250	8.4 ± 0.7^{b}	8.9 ± 0.8^{g}	389	10.7 ± 1.0^{k}	735
FTHD250	3.4 ± 0.1^{d}	3.4 ± 0.2^{i}	388	3.5 ± 0.2^{o}	747
FTT300	6.0 ± 0.7^{c}	5.9 ± 0.6^{h}	389	6.8 ± 0.6^{l}	739

Note: Different alphabet in each column are statistically different of data ($p<0.05$).

3.3 Effects of iron oxides on the enhancement of ultraviolet and visible light protection of sunscreen creams

3.3.1 Effects of particle size of iron oxides

As details previously, colored sunscreens gave better protection against visible light than white sunscreens (11, 14, 52). The foundation colored sunscreen was aimed to prepare for enhancement in the protective efficiency and to reduce the cosmetically undesired opaqueness of TiO_2. Therefore, iron oxides having yellow, red, and black color were chosen. Again, iron oxides with two size ranges (i.e. 200 nm and ≥ 1,500 nm) were included in the study to observe the effect of the particle size on UV and visible light protection. All samples of iron oxides chosen were coated with triethoxycaprylylsilane. Their characteristics are shown in **Table 21**.

Table 21 The characteristics of iron oxides selected into the study.

Samples	Compositions/Coating agent	Primary Particle size*
IYT-200	Yellow iron oxide and Triethoxycaprylylsilane	200 nm
IRT-200	Red iron oxide and Triethoxycaprylylsilane	200 nm
IBT-200	Black iron oxide and Triethoxycaprylylsilane	200 nm
IYT-1500	Yellow iron oxide and Triethoxycaprylylsilane	1500 nm
IRT-1700	Red iron oxide and Triethoxycaprylylsilane	1700 nm
IBT-3000	Black iron oxide and Triethoxycaprylylsilane	3000 nm

*Particle size reported from manufacturer; particle size 200 nm denote submicronsize and size ≥1500 denote micronsize.

Samples code: I = Iron oxide, Y or R or B = Yellow or red or black color, T = Triethoxycaprylylsilane which was a coating agent, Number = particle size.

The selected iron oxides were individually incorporated in base cream at 1%W/W. Their abilities for UV and visible light protection were measured using UV-1800® spectrophotometer. The obtained results were shown by the transmittance spectra (**Figure 19**) and area under the curve values (**Table 22**). It was found that, comparing between the same color, iron oxides having submicronsize yielded better protection in all wavelengths compared with those having micronsize (i.e. IYT-200>IYT-1500; IRT-200>IRT-1700; and IBT-200>IBT3000). These results are in agreement with the finding of Dondi et al. (78), suggesting that the scattering efficiency goes down (transmission value increases) as the particle diameter of iron oxides increases (**Figure16**). As details above, the optimal diameter of particles provided the highest scattering efficiency of visible light is between 200-400 nm.

Apart from the scattering property, the protection efficiency of iron oxides also depends on the selective absorption in different wavelength of visible light (79). For the effects of color, yellow iron oxides showed the highest absorption (lowest transmittance) in both UV and blue light wavelengths compared to red and black iron oxides, respectively (**Figure 19**). On the other hand, red iron oxide also showed higher protection in visible light wavelength compared to yellow iron oxide. Black iron oxide showed the lowest, consistent protection in all wavelength region between 290–800 nm.

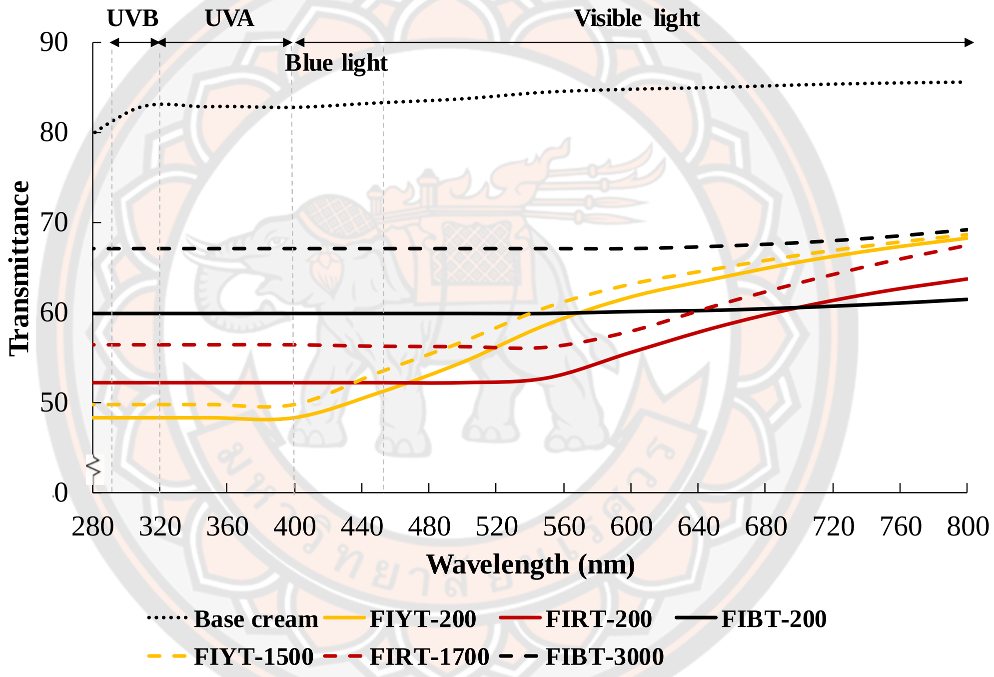

Figure 19 The transmittance spectra of base cream and formulations containing individual colored iron oxides with two different size ranges in UV and visible light wavelength. The two different size range of iron oxides including submicronsize (solid line) and micronsize (dashed line) were incorporated in base cream at 1%W/W and the spectra were measured using a UV-1800® spectrophotometer.

Table 22 Area under the curve of base cream and formulations containing individual colored iron oxides with two different size ranges in UV and visible light wavelength. The samples were prepared in base cream at 1%W/W.

Samples	Area under the curve (AUC) (n=3)				
	UVB	**UVA**	**Blue light**	**Visible light**	**Total area**
	290-320 nm	**320-400 nm**	**400-450 nm**	**400-800 nm**	**290-800 nm**
Base cream	2.59 ± 0.09^{d}	6.61 ± 0.29^{i}	4.00 ± 0.19^{p}	28.85 ± 1.48^{u}	38.06 ± 1.85^{z}
FIYT-200	9.34 ± 0.59^{a}	24.71 ± 1.53^{e}	15.33 ± 0.92^{j}	89.30 ± 4.85^{r}	123.35 ± 6.93^{w}
FIRT-200	8.54 ± 0.50^{a}	22.15 ± 1.09^{f}	14.36 ± 0.83^{k}	100.75 ± 5.84^{q}	131.45 ± 6.50^{v}
FIBT-200	7.01 ± 0.39^{b}	18.51 ± 1.02^{g}	11.50 ± 0.80^{n}	88.98 ± 5.97^{r}	114.50 ± 7.26^{x}
FIYT-1500	8.69 ± 0.40^{a}	22.48 ± 1.30^{f}	13.49 ± 0.65^{l}	78.02 ± 4.76^{s}	109.19 ± 4.83^{x}
FIRT-1700	7.22 ± 0.52^{c}	18.84 ± 1.20^{g}	12.22 ± 0.75^{m}	89.24 ± 6.53^{r}	115.30 ± 8.06^{x}
FIBT-3000	5.16 ± 0.36^{b}	13.77 ± 0.98^{h}	8.63 ± 0.57^{o}	66.18 ± 4.34^{t}	85.11 ± 5.50^{y}

Note: Different alphabet in each column are statistically different of data ($p<0.05$).

SPF, UVAPF, $\lambda_{C,}$ and PPF of individual iron oxide in base cream was also calculated and show in **Table 23**. These results clearly suggested that iron oxides themselves have no ability to contribute protection of UVB, UVA, and blue/visible light through SPF, UVAPF, and PPF respectively. λ_{C} of all samples including base cream was not difference and showed higher than wavelength 370 nm. However, color iron oxides have been reported that their combination in inorganic sunscreen products can enhance the protective ability by increasing of visible light scattering (80). Therefore, YT-200, RT-200, and BT-200 were selected to incorporate in the foundation colored sunscreens in the further study. Different ratios of the selected iron oxides were prepared to obtain color for providing the sunscreens have color fitting to skin-tone of Asian.

Table 23 Sun protection factor (SPF), UVA protection factor (UVAPF), critical wavelength (λ_C), porphyrin protection factor (PPF), and visible protection wavelength (λ_{Vis}) of base cream and formulations containing individual colored iron oxides with two different size ranges in UV and visible light wavelength. The samples were prepared in base cream at 1%W/W.

Samples	SPF	UVAPF	λ_C (nm)	PPF	λ_{Vis} (nm)
Base cream	1.22 ± 0.01^d	1.21 ± 0.01^h	388	1.20 ± 0.01^o	740
FIYT-200	2.03 ± 0.11^a	2.02 ± 0.10^e	388	2.01 ± 0.10^i	722
FIRT-200	1.93 ± 0.07^a	1.92 ± 0.07^e	388	1.94 ± 0.07^j	733
FIBT-200	1.72 ± 0.06^b	1.70 ± 0.07^f	388	1.70 ± 0.07^m	743
FIYT-1500	1.92 ± 0.09^a	1.90 ± 0.08^e	388	1.88 ± 0.09^k	726
FIRT-1700	1.73 ± 0.10^b	1.72 ± 0.10^f	389	1.75 ± 0.10^l	733
FIBT-3000	1.46 ± 0.07^c	1.46 ± 0.06^g	388	1.47 ± 0.06^n	743

Note: Different alphabet in each column are statistically different of data ($p<0.05$).

3.3.2 Effects of iron oxides in combination with inorganic UV filter and pigments

The blended iron oxides were combined with all TiO_2 samples for the development of colored sunscreens. The effects of blended iron oxides in combination with nanosize and submicronsize TiO_2 in the enhancement of UV and visible light protection were observed. The compositions of each formulations are shown in **Table 24**.

From results, FTHD250-R was excluded because the incompatibility between THD250 (coated with hydrogen dimethicone) and blended iron oxides (coated with triethoxycaprylylsilane) in the preparation process.

The protection efficacy of the formulations against UV and blue/visible light was demonstrated through the transmittance spectra in UV and visible light wavelength (**Figure 20**), AUC (**Table 25**) as well as SPF, UVAPF, λ_C, and PPF values (**Table 26**). The results were clearly shown that blended iron oxides themselves did not provide good protection against blue/visible light. However, when the blended iron oxides were combined with nanosize TiO_2 (i.e. FT35-R, FD35-R, FTT60-R), the enhancement of UV and blue/visible light protection was observed. The enhancement of visible light protection may be due to the addition of submicronsize blended iron oxides having optimal scattering size (size 200 nm) to such formulations containing nanosize TiO_2, which greatly increased the pathlength of scattered visible light.

On the other hand, adding the blended iron oxides to formulation containing T250 (uncoated TiO_2, size 250 nm) did not change the UV and blue/visible light protective efficacy of the formulation. This may cause from the similar particle size range of blended iron oxides (size 200 nm) and T250. In addition, their RI is in the same range. The blended iron oxides composed of yellow iron oxide (RI = 2.300), red iron oxide (RI= 2.910), black iron oxide (RI = 2.420) and RI of rutile TiO_2 equal to 2.700. In the case of FT300 and FTT300-R (F7), the slight enhancement in UV and blue light protective efficiency was shown.

Table 24 The compositions of formulations containing the combination of single titanium dioxide and blended iron oxides.

#F	**Compositions**	**Amount of filters (%W/W)**						
		T35	**TD35**	**TT60**	**T250**	**THD250**	**TT300**	**Blended iron oxides***
F1	Blended iron oxides (R)	-	-	-	-	-	-	2.5
F2	FT35-R	10.0	-	-	-	-	-	2.5
F3	FTD35-R	-	10.0	-	-	-	-	2.5
F4	FTT60-R	-	-	10.0	-	-	-	2.5
F5	FT250-R	-	-	-	10.0	-	-	2.5
F6	FTHD250-R	-	-	-	-	10.0	-	2.5
F7	FTT300-R	-	-	-	-	-	10.0	2.5

*The mixture of YT-200, RT-200, and BT-200

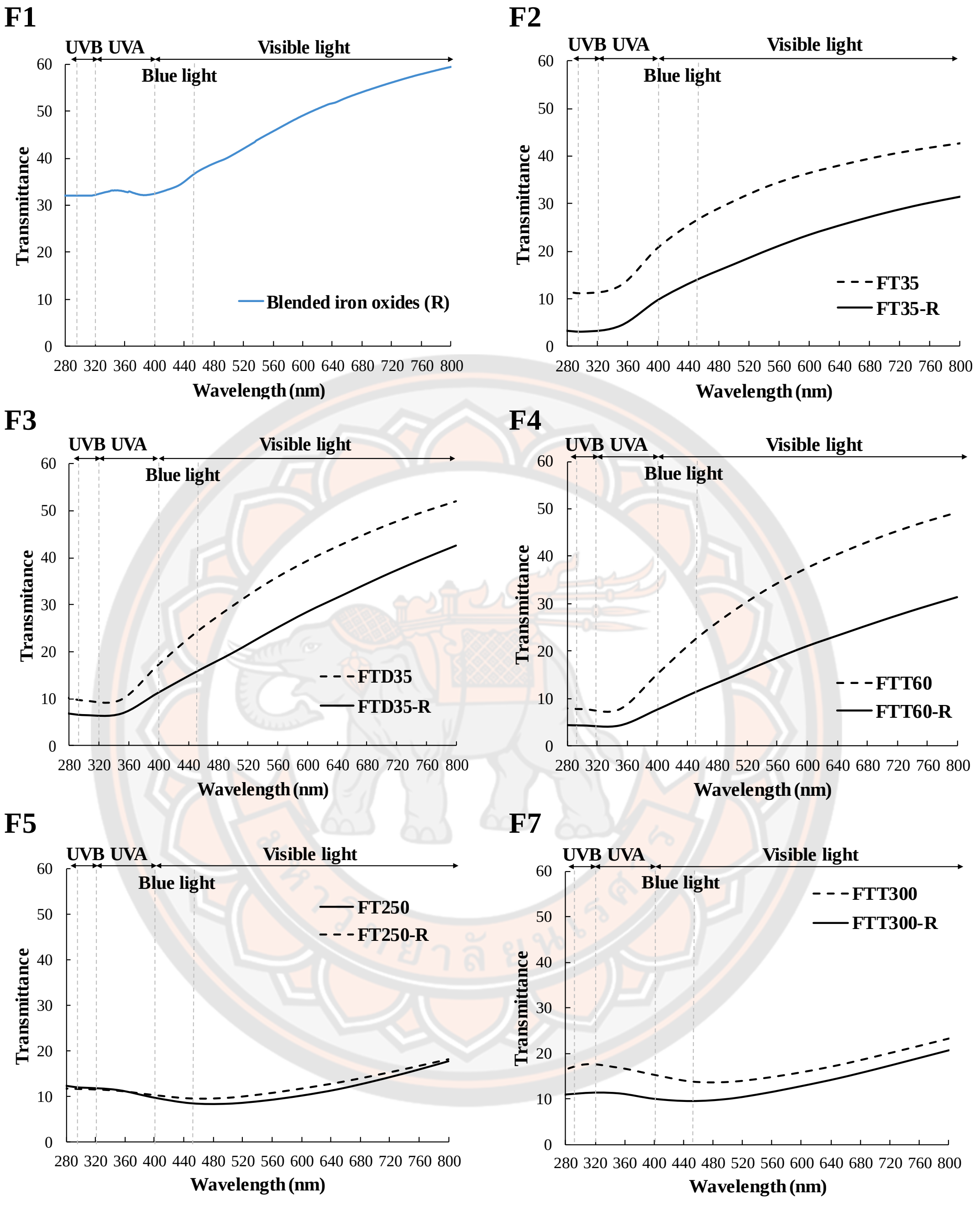

Figure 20 The transmittance spectra of the combination of titanium dioxide and blended iron oxides (solid line) and single titanium dioxide (dashed line) in UV and visible light wavelength. The samples were prepared in base cream at 10%W/W titanium dioxide and 2.5%W/W blended iron oxides and the spectra were measured using a UV-1800® spectrophotometer.

Table 25 Area under the curve of the combination of titanium dioxide and blended iron oxides in UV and visible light wavelength. The samples were prepared in base cream at 10%W/W titanium dioxide and 2.5%W/W blended iron oxides.

#F*	Area under the curve (AUC) (n=3)				
	UVB	UVA	Blue light	Visible light	Total area
	290-320 nm	320-400 nm	400-450 nm	400-800 nm	290-800 nm
Blend iron oxides (R) (F1)	14.6 ± 0.9^{d}	38.7 ± 2.2^{h}	23.8 ±1.4^{l}	137.2 ± 8.1^{q}	190.5 ± 10.8^{v}
FT35-R (F2)	42.9 ± 3.2^{a}	97.3 ± 6.4^{e}	45.1 ± 2.4^{j}	257.7 ± 16.2^{o}	397.9 ± 22.9^{t}
FTD35-R (F3)	35.8 ± 3.4^{b}	87.2 ± 7.7^{f}	40.8 ± 2.2^{k}	221.1 ± 16.2^{p}	344.1 ± 26.6^{u}
FTT60-R (F4)	41.7 ± 1.6^{a}	104.6 ± 4.4^{e}	51.4 ± 2.0^{i}	272.5 ± 15.6^{n}	418.9 ± 20.4^{s}
FT250-R (F5)	27.3 ± 1.7^{c}	74.1 ± 4.8^{g}	49.1 ± 3.3^{i}	353.3 ± 22.6^{m}	454.7 ± 29.1^{r}
FTT300-R (F7)	28.7 ± 1.1^{c}	78.1 ± 3.2^{g}	50.7 ± 1.1^{i}	358.7 ± 14.5^{m}	465.5 ± 18.7^{r}

Table 26 Sun protection factor (SPF), UVA protection factor (UVAPF), critical wavelength (λ_{C}), porphyrin protection factor (PPF), and visible protection wavelength (λ_{Vis}) of formulations F1, F2-F5, and F7.

#F*	SPF	UVAPF	λ_{C} (nm)	PPF	λ_{Vis} (nm)
Blend iron oxides (R) (F1)	3.1 ± 0.2^{d}	3.0 ± 0.2^{i}	389	3.1 ± 0.2^{n}	723
FT35-R (F2)	29.3 ± 1.2^{a}	18.1 ± 1.7^{f}	386	8.8 ± 0.9^{l}	719
FTD35-R (F3)	15.2 ± 1.8^{b}	12.7 ± 1.3^{g}	386	7.1 ± 0.6^{m}	707
FTT60-R (F4)	25.7 ± 2.3^{a}	21.0 ± 1.4^{e}	386	11.3 ± 1.2^{j}	709
FT250-R (F5)	8.1 ± 0.9^{c}	8.3 ± 0.9^{h}	389	9.4 ± 1.3^{l}	735
FTT300-R (F7)	9.2 ± 0.8^{c}	9.5 ± 0.8^{h}	389	10.3 ± 0.4^{k}	733

Note: Different alphabet in each column are statistically different of data ($p<0.05$).

According to the results shown above, among the formulations containing blended iron oxides and nanosize TiO_2, FTT60-R showed to be the best in terms of UVAPF and PPF values, indicating the highest protection efficacy against UVA and harmful blue light (the highest energy on the visible light spectrum). Critically focusing on the results, although FTT300-R did not yield better protection efficacy against UVB, UVA, and blue light compared to FTT60-R, it offered higher protection in the wavelengths ranging from 450–800 nm. In addition, TT300 has the same coating as TT60 and also the blended iron oxides. Therefore, these two formulations, i.e. FTT60-R and FTT300-R, were selected for further studies.

In this study, the sunscreen products developed in this study have aimed at SPF 50+ and UVA seal certification (i.e. UVAPF at least 1/3 of the labelled SPF and the λ_c equal or greater than 370 nm). More importantly, the protection of blue light was also aimed to achieve. From the above results, among 11 organic UV filters investigated, TBPT was the only filter which offered the protection in UV and also visible light.

Therefore, the selected sunscreen formulations (FTT60-R and FTT300-R) were combined with TBPT. The compositions of FTT60-R and FTT300-R formulations mixed with TBPT are shown in **Table 27**.

Table 27 The compositions of FTT60-R and FTT300-R formulations with and without Tris-biphenyl triazine (TBPT).

#F	Compositions	Amount of filters (%W/W)				Total amount of filters (%w/w)
		TT60	TT300	Blended iron oxides*	TBPT**	
F4	FTT60-R	10.0	-	2.5	-	12.5
F7	FTT300-R	-	10.0	2.5	-	12.5
F8	FTT60-R+TBPT	10.0	-	2.5	2.5	15.0
F9	FTT300-R+TBPT	-	10.0	2.5	2.5	15.0

*Blended iron oxides were the mixing of YT-200, RT-200 and BT-200.

**Concentration of active in suspensions.

Again, the protection efficacy of the formulations against UV and blue/visible light was demonstrated through the AUC (**Table 28**) as well as SPF, UVAPF, λ_C, PPF, and λ_{Vis} values (**Table 29**). Mixing TBPT into both formulations provided better protection against UVB, UVA, and blue/visible light. Previous results showed that FTT300-R exhibited weak UVB and UVA protection compared to FTT60-R. However, this property was greatly improved when adding with TBPT.

Table 28 Area under the curve of FTT60-R and FTT300-R formulations with and without Tris-biphenyl triazine (TBPT) in UV and visible light wavelength.

#F	**Area under the curve (AUC) (n=3)**				
	UVB	**UVA**	**Blue light**	**Visible light**	**Total area**
	290-320 nm	**320-400 nm**	**400-450 nm**	**400-800 nm**	**290-800 nm**
FTT60-R (F4)	41.7 ± 1.6^{b}	104.6 ± 4.4^{e}	51.4 ± 2.0^{h}	272.5 ± 15.6^{k}	418.9 ± 20.4^{o}
FTT300-R (F7)	28.7 ± 1.1^{c}	78.1 ± 3.2^{f}	50.7 ± 1.1^{h}	358.7 ± 14.5^{j}	465.5 ± 18.7^{m}
FTT60-R +TBPT (F8)	49.2 ± 1.7^{a}	114.7 ± 3.4^{d}	52.2 ± 2.4^{h}	281.3 ± 10.5^{k}	445.1 ± 14.0^{n}
FTT300-R+ TBPT (F9)	41.4 ± 2.4^{b}	104.2 ± 6.0^{e}	59.6 ± 3.7^{g}	422.7 ± 27.6^{i}	568.3 ± 35.7^{l}

Table 29 Sun protection factor (SPF), UVA protection factor (UVAPF), critical wavelength (λ_C), porphyrin protection factor (PPF) and visible protection wavelength (λ_{Vis}) of formulations F4, F7-F9.

#F	**SPF**	**UVAPF**	**λ_C (nm)**	**PPF**	**λ_{Vis} (nm)**
FTT60-R (F4)	25.7 ± 2.3^{b}	21.0 ± 1.4^{e}	386	11.3 ± 1.2^{h}	709
FTT300-R (F7)	9.2 ± 0.8^{c}	9.5 ± 0.8^{f}	389	10.3 ± 0.4^{h}	733
FTT60-R+TBPT (F8)	45.2 ± 4.7^{a}	27.2 ± 2.8^{d}	386	12.2 ± 1.5^{h}	703
FTT300-R+TBPT (F9)	24.6 ± 2.9^{b}	19.8 ± 2.6^{e}	387	15.0 ± 1.6^{g}	734

Note: Different alphabet in each column are statistically different of data ($p<0.05$).

FTT60-R+TBPT (F8) was selected to further investigation optimum of each active ingredients because it yielded high values of SPF, UVAPF, and optimum value of PPF. In this study, TT60 was tested in two concentration levels, i.e. middle (12.5%W/W) and the highest (25%W/W) level of legislation ranged. For TBPT, it was prepared at concentration 7.5%W/W and 10% W/W (highest level). All samples contained same concentration of blended iron oxides (2.5%W/W). The compositions of these combinations are shown in **Table 30**.

Table 30 The compositions of formulations F4, F8 and F10 – F13.

#F	Compositions	Amount of filters (%W/W)			Total amount of filters (%W/W)
		TT60	Blended iron oxides	TBPT*	
F4	FTT60-R	10.0	2.5	-	12.5
F8	FTT60-R+TBPT	10.0	2.5	2.5	15.0
F10	12.5TT60-R	12.5	2.5	-	15.0
F11	25TT60-R	25.0	2.5	-	27.5
F12	7.5TBPT-R	-	2.5	7.5	10.0
F13	10TBPT-R	-	2.5	10	12.5

*Concentration of active in suspensions.

Again, the protection efficacy of all formulations against UV and blue/visible light was demonstrated through the AUC (**Table 31**) as well as SPF, UVAPF, λ_C, PPF, and λ_{Vis} values (**Table 32**). Comparing among F4 (FTT60-R) and F13 (10TBPT-R), it was clearly demonstrated that TT60 provided great impact on UVA and blue light protection, compared with TBPT at the same concentration. The results of F8 (FTT60-R+TBPT) and F10 (12.5FTT60-R) showed that FTT60-R combined with TBPT could achieve superior protection covering UV and visible light. F11 (25FTT60-R) showed the highest AUC values in both UVB and UVA regions due to it was mainly composed of TT60 at 25%W/W, which is the highest concentration of legislation ranged. However, F11 possessed an opaque and whitish appearance, thus may reduce cosmetic acceptability. Although, F13 (10TBPT-R) contained TBPT at the highest concentration (10%W/W), it showed lower AUC values than F8 (FTT60-R+TBPT) in all wavelength ranges.

Table 31 Area under the curve of formulations F4, F8 and F10-F13 in UV and visible light wavelength.

#F	Area under the curve (AUC) (n=3)				
	UVB	**UVA**	**Blue light**	**Visible light**	**Total area**
	290-320 nm	**320-400 nm**	**400-450 nm**	**400-800 nm**	**290-800 nm**
FTT60-R (F4)	41.7 ± 1.6^{d}	104.6 ± 4.4^{h}	51.4 ± 2.0^{m}	272.5 ± 15.6^{q}	418.9 ± 20.4^{v}
FTT60-R +TBPT (F8)	49.2 ± 1.7^{b}	114.7 ± 3.4^{g}	52.2 ± 2.4^{l}	281.3 ± 10.5^{q}	445.1 ± 14.0^{u}
12.5TT60-R (F10)	42.8 ± 1.7^{d}	105.0 ± 3.3^{h}	50.8 ± 1.7^{m}	278.5 ± 12.0^{q}	426.0 ± 15.0^{v}
25TT60-R (F11)	65.4 ± 3.4^{a}	165.5 ± 6.8^{f}	79.7 ± 4.7^{k}	440.8 ± 36.5^{p}	671.7 ± 43.9^{t}
7.5TBPT-R (F12)	39.5 ± 2.6^{e}	84.3 ± 6.1^{j}	31.1 ± 2.9^{o}	149.7 ± 14.5^{s}	273.5 ± 21.0^{x}
10TBPT-R (F13)	45.3 ± 4.5^{c}	97.1 ± 9.2^{i}	36.7 ± 3.9^{n}	179.0 ± 21.6^{r}	321.4 ± 34.9^{w}

Note: Different alphabet in each column are statistically different of data ($p<0.05$).

As details in Chapter II, there is no official parameters to evaluate the protective efficiency against blue light of sunscreens. Moseley et al. (52) have compared the level of visible light protection of new colored sunscreens and commercial sunscreens (Sun E45) using photosensitivity protection factor. They resulted that the new colored sunscreens (containing 5% ZnO, 4% TiO_2 (pigment), iron oxides) provided the photosensitivity protection factor in range between 5.4-9.6, while Sun E45 (containing TiO_2 (microfine)) showed PPF 4.1. The study of Teramura et al. (11) have been shown the ability in blue light protection of the combination of commercial sunscreens (make-up base, power and liquid foundation), compared with the conventional sunscreen using porphyrin protection factor (PPF). The combination of make-up base with a powder as well as with a liquid foundation at thickness of 0.2, 0.4, and 0.6 mg/cm^2 resulted in PPF of 3.2-7.4 and 3.0-6.6, respectively. The conventional sunscreen applied at a thickness of 0.5, 1.0, and 2.0 mg/cm^2 resulted in

PPF of 1.3-2.0, that was significantly lower PPF values than those of combination. In this study, the colored sunscreen developed provided PPF values 12.2 ± 1.5, thus this formulation was more effective in blue light protection.

However, theses SPF, UVAPF and λ_C values obtained from measurement using UV-1800$^{\circledR}$ spectrophotometer were only used for preliminary screening during sunscreen development. F4, F8, F10-F13 were again investigated the UVB and UVA protection by UV-2000S$^{\circledR}$ ultraviolet transmittance analyzer in the next study.

Table 32 Sun protection factor (SPF), UVA protection factor (UVAPF), critical wavelength (λ_C), porphyrin protection factor (PPF) and visible protection wavelength (λ_{Vis}) of formulations F4, F8 and F10–F13.

#F	SPF	UVAPF	λ_C (nm)	PPF	λ_{Vis} (nm)
FTT60-R (F4)	25.7 ± 2.3^{d}	21.0 ± 1.4^{h}	386	11.3 ± 1.2^{m}	709
FTT60-R+ TBPT (F8)	45.2 ± 4.7^{b}	27.2 ± 2.8^{g}	386	12.2 ± 1.5^{l}	703
12.5FTT60-R (F10)	26.0 ± 1.2^{d}	21.3 ± 1.1^{h}	386	11.9 ± 0.9^{m}	714
25FTT60-R (F11)	156.4 ± 16.9^{a}	122.5 ± 8.9^{f}	386	44.5 ± 6.0^{k}	703
7.5TBPT-R (F12)	20.4 ± 2.4^{e}	10.3 ± 0.9^{j}	382	4.3 ± 0.4^{o}	688
10TBPT-R (F13)	34.4 ± 5.1^{c}	15.7 ± 2.2^{i}	383	6.1 ± 0.8^{n}	678

Note: Different alphabet in each column are statistically different of data ($p<0.05$).

Part 4: UV protective efficiency of developed sunscreens using UV-2000S® ultraviolet transmittance analyzer

This part aimed to investigate the level of UVB, and UVA protection of selected formulation samples based on the measurement of the transmission of UVB and UVA radiation through a sunscreen film. The measurements were performed by using UV-2000S®, which computes SPF, UVAPF, and λ_C values from the internationally recognized methods in its software. Therefore, F4, F8, F10-F13 were again measured these parameters to confirm the efficacy of UVB and UVA protection. The obtained SPF, UVAPF, and λ_C values are shown in **Table 33-34**.

For SPF values, it can be observed that SPF values were in range of 22.2 ± 0.6 to 5.63 ± 2.7 (**Table 33**). Among all formulation samples, F8 achieved the highest SPF value that mean F8 provided greater protective efficiency in UVB radiation than other formulation samples. According to the regulation of Thai food and drug administration, the measured SPF values above 50 could specify SPF 50+ on the label of sunscreen products (46). For UVAPF values of all formulation samples obtained after irradiation, they resulted in ranging from 11.3 ± 0.5 to 30.4 ± 0.9 that F8 possessed the highest UVAPF value (**Table 34**).

In addition, the UVA protection should have a correlation with the UVB protection to provide a complete measurement of broad-spectrum protection. European commission has been issued UVA seal sign, which can be shown on the label if ratio of UVAPF/SPF ≥ 0.33 and $\lambda_C \geq 370$ nm (as details above). The results were shown that four formulation samples (i.e. F4, F8, F10-F11) provided the ratio of UVAPF/SPF greater than 0.33 and had λ_C higher than 370 nm, according to EC proposed criterion (**Table 34**). In contrast, F12 and F13 (7.5TBPT-R and 10TBPT-R) showed λ_C of greater than 370 nm, but they achieve UVAPF/SPF ratio ≤ 0.33, therefore they did not meet the EC requirement. These may be due to the protection against UVA and UVB radiation of these samples were not balanced, they possessed high protective ability in UVB wavelength but having low protection in UVA wavelength, resulting to UVAPF/SPF was less than 0.33. In order to reach the balance of UVB and UVA protection, a combination of UV filters is important consideration for the formulation of sunscreens, UV filters should have different maximum absorption to cover entire UVB and UVA wavelength and to fulfill those requirement (81). The test procedure including the preparation of samples of this part were verified by the measurement of reference sunscreen formulation (S2). The UVAPF value of it was 13.0 ± 0.0, which was between the acceptance range (10.7 to 14.7) of ISO24443 (50).

Table 33 UVB protection of formulations F4, F8 and F10–F13, measured using in-house method and a UV-2000S® ultraviolet transmittance analyzer.

#F	SPF
FTT60-R (F4)	22.2 ± 0.6^{d}
FTT60-R+ TBPT (F8)	63.5 ± 2.7^{a}
12.5FTT60-R (F10)	26.7 ± 1.6^{d}
25FTT60-R (F11)	33.7 ± 2.3^{c}
7.5TBPT-R (F12)	37.2 ± 3.5^{c}
10TBPT-R (F13)	60.6 ± 5.3^{a}

Table 34 UVA protection of formulations F4, F8 and F10–F13, measured using ISO 24443:2012 method and a UV-2000S® ultraviolet transmittance analyzer.

#F	SPF	$UVAPF_0$	UVAPF	UVAPF/ SPF	λ_C (nm)	Broad-spectrum protection
F4	22*	14.7 ± 0.5	13.4 ± 0.5^{d}	0.6	385	Pass
F8	64*	33.8 ± 1.1	30.4 ± 0.9^{a}	0.5	385	Pass
F10	27*	17.1 ± 0.7	15.3 ± 0.5^{c}	0.6	386	Pass
F11	34*	23.5 ± 0.3	21.4 ± 1.3^{b}	0.6	385	Pass
F12	37*	12.4 ± 0.5	11.3 ± 0.5^{e}	0.3	381	Fail
F13	60*	13.2 ± 0.7	11.7 ± 0.9^{e}	0.2	379	Fail
S2	16**	15.3 ± 0.1	13.0 ± 0.0	0.8	381	Pass

Note: Different alphabet in each column are statistically different of data ($p<0.05$).

*Obtained from In-house *in vitro* SPF method, **Obtained from *in vivo* SPF method.

Part 5: Determination the effect of base formulations

Currently, several forms of sunscreens such as emulsion, lotion, spray, gel etc. are available in the market. This part aimed to investigate the effect of bases cream, mousse, and lotion in which the selected filters (i.e. Triethoxycaprylylsilane-treated TiO_2 having size 60 nm, blended iron oxides, and TBPT) were incorporated.

As described above, the area under the curve in blue light wavelength (400-450 nm) of sunscreens was proved to correlate with their translucent or opaque appearance (12). Therefore, the different of bases cream, mousse and lotion on the blue light protection was evaluated through the measurement of translucency parameter (TP). The results showed that base formulations greatly affected the protection ability against UV and blue light. The appearance of bases cream, mousse and lotion are shown in **Table 35.**

Table 35 The appearance of bases cream, mousse, and lotion.

Characteristic	Cream	Mousse	Lotion
Appearance	White Creamy	Airy, Silky	Glossy, Like-yoghurt
			

Among three formulations, lotion formulation showed the highest PPF values (47.8 ± 5.3), following by mousse and cream formulation (**Table 36**). The scattering property is directly related to the relative refractive index, which is determined by the contrast between the RI of the particles (N_p) and the RI of the surrounding medium (N_m) (Formula=N_p/N_m) (82). Therefore, the differences in scattering efficiency against blue light of various formulations having the same filters may be explained by the differences in RI of the base formulations. From **Table 39**, it was shown that both bases and formulations in form of lotion was more transparency than mousse and cream, respectively. RI of a medium is equal to the ratio of the speed of light traveling in air and the speed of light traveling in that medium. Light can travel in translucency medium with faster speed than in opaque medium. Therefore, RI of medium in the form of lotion is lower than mousse and cream, respectively. The lowest refractive index of lotion results in the big difference in RI between filters (i.e. triethoxycaprylylsilane-treated TiO_2, blended iron oxides and TBPT) and the surrounding medium. Thus, the highest scattering efficiency against blue light is obtained.

In addition, the efficacy of cream, mousse, and lotion in UVB and UVA protection were expressed by SPF and UVAPF values respectively (**Table 37-38**). It was observed that lotion formulation exhibited similar both SPF and UVAPF values with cream formulation, while mousse formulation showed the lower values in both of SPF and UVAPF values. Mousse contained the components of silicone group (i.e. cyclomethicone, cyclopentasiloxane (and) dimethicone crosspolymer) more than 50%, thus it possessed higher viscosity (**Figure 21**) than the other formulations. The incorporation of inorganic particles in a highly viscous formulation may be nonuniformly distribution and the aggregation of particles is possible to somewhat (83). This can affect to the function of inorganic particle’s ability of UV absorption due to the aggregated particles will reduce the amount of surface area available to absorb UV radiation (77).

Table 36 Porphyrin protection factor (PPF), indicating blue light protective efficacy of cream, mousse, and lotion formulations containing triethoxycaprylylsilane-treated TiO_2 having size 60 nm, blended iron oxides, and TBPT

Samples	PPF
Cream (F8)	12.2 ± 1.5^c
Mousse	20.8 ± 2.7^b
lotion	47.8 ± 5.3^a

Table 37 Sun protection factor (SPF), indicating UVB protective efficacy of cream, mousse, and lotion formulations containing triethoxycaprylylsilane-treated TiO_2 having size 60 nm, blended iron oxides, and TBPT. The SPF was measured using in-house method and a UV-2000S® ultraviolet transmittance analyzer.

Samples	SPF
Cream (F8)	63.5 ± 2.7^{a}
Mousse	41.4 ± 1.4^{b}
lotion	64.8 ± 4.8^{a}

Table 38 UVA protection factor (UVAPF), indicating UVA protection of cream, mousse, and lotion formulations containing triethoxycaprylylsilane-treated TiO_2 having size 60 nm, blended iron oxides, and TBPT. The UVAPF was measured using ISO 24443:2012 method and a UV-2000S® ultraviolet transmittance analyzer.

Samples	SPF	$UVAPF_0$	UVAPF	UVAPF /SPF	λ_C (nm)	Broad-spectrum protection
Cream (F8)	64*	33.8 ± 1.1	30.4 ± 0.9^{a}	0.5	385	Pass
Mousse	41*	16.3 ± 0.2	15.8 ± 0.2^{b}	0.4	381	Pass
Lotion	65*	33.6 ± 1.7	31.0 ± 0.8^{a}	0.5	384	Pass
UVAPF reference (S2)	16**	15.3 ± 0.1	13.0 ± 0.0	0.8	381	Pass

Note: Different alphabet in each column are statistically different of data ($p<0.05$).

*Obtained from In-house *in vitro* SPF method

**Obtained from *in vivo* SPF method.

Table 39 Transparency parameter (TP) of cream, mousse, and lotion formulations in both with and without UV and Vis filters.

Samples	TP	ΔTP
Base cream	50.4 ± 0.2	19.5 ± 0.3
Base mousse	55.2 ± 0.5	14.7 ± 0.3
Base lotion	62.2 ± 0.1	7.7 ± 0.2
Cream	20.8 ± 0.0	49.0 ± 0.2
Mousse	25.2 ± 1.1	44.7 ± 1.0
Lotion	32.0 ± 0.4	37.9 ± 0.7

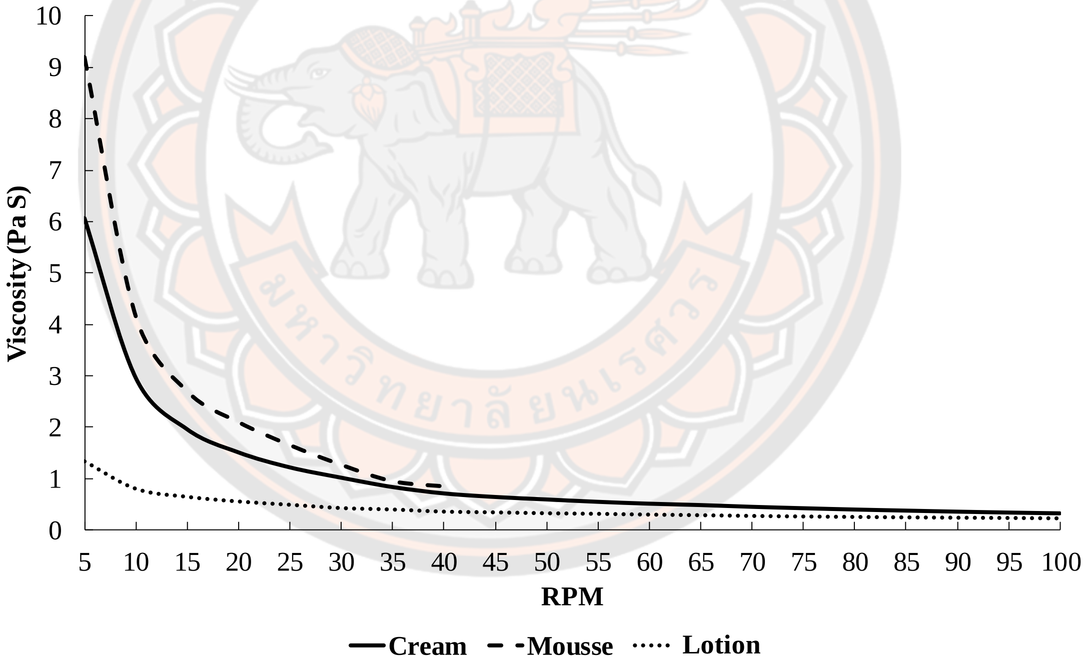

Figure 21 The viscosity of cream, mousse, and lotion formulations containing triethoxycaprylylsilane-treated TiO_2 having size 60 nm, blended iron oxides, and TBPT. The viscosity was measured using Brookfiled DV IIT equipped with CP-51 for cream and lotion, CP-52 for mousse.

Part 6: Comparison the effectiveness of the developed sunscreen with commercial sunscreen products for the protection against blue light radiation

As there are no criteria for blue light protection, in this study the effectiveness of the developed sunscreen for the protection against blue light radiation was compared with commercial sunscreen products through PPF values. The SPF and UVAPF were not determined for the commercial products because the determination methods for SPF and UVAPF of these products were unknown.

From the previous results, colored sunscreen in base lotion which contained the combination of triethoxycaprylylsilane-treated TiO_2 having size 60 nm, blended iron oxides and TBPT showed the best ability for the protection of blue light. Thus, it was selected to compare for the PPF value with the commercial products. The criteria for selecting of commercial sunscreens to this study were described in Chapter II. The details of the selected commercial products having the characteristics according to the specified conditions are shown in **Table 40.**

The results found that the sunscreens developed in this study (i.e. Lotion) showed the highest PPF value, compared to the other commercial products (**Table 41**). It is suggested that lotion foundation colored sunscreen possesses more efficient in blue light protection than the commercially available sunscreens in the market.

Table 40 Details specified on the labels of the five commercial sunscreens claimed to protect blue light radiation.

Commercial sunscreens	UVB protection	UVA protection	Visible light protection	Compositions	
				Organic UV filters	Inorganic UV filters/pigments
Com1	SPF50+	PA+++	Claim to protect HEV	EHMC, OCR, BEMT	TiO_2, ZnO, Red, yellow, black iron oxides
Com 2	SPF 50+	UVA	Claim to protect HEV	BMDM, EHS, BEMT, EHT, PBSA	TiO_2 (nano)
Com 3	SPF 50+	PA+++	Claim to protect HEV	EHMC, EHS, BEMT, BMDM, BZ-3	-
Com 4	SPF 50+	PA++++	Claim to protect HEV	-	Micronized TiO_2 and ZnO
Com 5	SPF 50+	PA+++	Claim to protect HEV	BMDM, EHMC, MBBT, OCR, BZ-3	TiO_2 (nano)

Table 41 Porphyrin protection factor (PPF), indicating blue light protective efficacy of the lotion formulation compared with the selected commercial sunscreen products and measured using a UV-1800® spectrophotometer.

Samples	PPF
Lotion	47.8 ± 5.3^{a}
Com 1	9.6 ± 0.5^{b}
Com 2	4.1 ± 0.4^{c}
Com 3	1.5 ± 0.0^{e}
Com 4	2.7 ± 0.2^{d}
Com 5	3.1 ± 0.1^{d}

Note: Different alphabet in each column are statistically different of data ($p<0.05$).

CHAPTER V

CONCLUSION

Protection against UVB (290-320 nm) and UVA (320-400 nm) light have been studied for a long time. However, recently the damaging effects of visible light (400-800 nm) and ways to protect against it have also gained interest. Visible light accounts for almost half of sunlight, and it can penetrate more deeply into the skin than UVB and UVA can, reaching lower layers of the skin. Once in contact to the skin, it stimulates a production of free radicals, proinflammatory cytokines, and MMP-1, all of which result in photoaging. Multiple exposure to visible light has been shown to induce abnormal pigmentation, resulting in age spots or melasma. The portion of the visible light spectrum having the highest energy is referred to as blue light (400-450 nm). A clinical study performed on human skin showed that blue light irradiation is a main cause of abnormal pigmentation. It has also been implicated in skin conditions such as EPP, solar urticaria, and chronic actinic dermatitis. These skin disorders can limit the outdoor activity and decrease quality of life of photosensitivity patients. Given these deleterious effects, protection against sunlight should consider not only UVB and UVA light but also blue/visible light.

Although the protection of UV and visible light have been studied as previous described, most of them did not provided the detailed information about optimizing characteristic of inorganic UV filters/pigments for maximum blue/visible light protection. The characteristics influencing the efficacy of these compounds in blue/visible light protection are such as particle size and surface coating etc. These data are essential for the development of sunscreen products which could protect against blue/visible light. This study was therefore aimed to screen the protective efficiency of the organic and inorganic UV filters which are frequently used in commercial products. The inorganic pigments, including TiO_2, ZnO and iron oxides were also investigated.

Firstly, the frequently used UV filters in commercial sunscreen products were surveyed from May to June 2019 at hypermarkets in Thailand. From this survey, 18 UV filters were frequently used in the commercial products. Among of these UV filters, only 11 UV filters with safety, non-toxic, and non-patent were selected into the study including BMDM, EHMC, BEMT, OCR, TiO_2 EHS, HMS, DHHB, ZnO, EHT, and MBBT (rank from the highest to lowest frequency usage). In addition, the new generation of organic UV filters; TBPT and BEMT AQ were also included into the study, even though they were not found in any surveyed products.

Next, the selected organic UV filters were screened for UV and visible light protective ability. It was revealed that TBPT was only organic UV filter providing the absorptive efficiency extending from UV to visible wavelength (290-800 nm). However, combined of the selected organic UV filters did not provide satisfy protection against visible light. This study suggested that the combination of organic UV filters should consider the absorption coefficient or A (1%, 1cm), the amount and types of organic UV filters for achieving the desirable sunscreen formulation.

Further investigations were performed for the inorganic particles (i.e TiO_2 and ZnO) both UV filters (nanosize) and pigments (submicronsize). It was observed that, TiO_2 (i.e. TT60, TD35, T250, and TT300) samples showed the better visible light protection, compared to all ZnO (i.e. ZT20, ZHD100, ZT120, ZT200) samples. The difference between the RI of TiO_2 (2.700) particles and the surrounding medium (RI of ethanol = 1.362) as well as those of ZnO (RI = 2.000) influenced to the efficiency of them in visible light protection. ZnO possesses lower the difference of RI than TiO_2, resulting in lower ability of visible light scattering. Hence, TiO_2 was selected to study the effects of particle size and surface coating.

The study on effect of particle size of TiO2 for UV and visible light protection was shown that nanosize TiO2 having size 35 and 60 nm can absorb UV light stronger than submicronsize TiO2 having size 250 and 300 nm. The results are in agreement with the finding of Dondi et al. (78), suggesting that when the particle size of TiO_2 is nanosize, it is more predominate in light absorption. TiO_2 absorbs light by excitation of a valence band electron (e−) to the conduction band, leaving a hole in the valence band (h+). The discrete energy levels of band called “band gap. The smaller particles have a larger band gap energy that mean more energy is required to excite an electron. Thus, UV light which has higher frequency and lower wavelength is better be absorbed by small-size TiO_2.

The increased particle size to submicronsize TiO2 is responsible for its ability in visible light protection. The uncoated submicronsize TiO_2 having size 250 nm (FT250) showed significantly better protection against blue/visible light than coated submicronsize TiO2, (i.e. FTT300 and FTHD250). The results were proofed to correlate with Mie theory that the optimum scattering property is obtained when the particle diameter (D) equals half of the wavelength (λ) of the light (D=λ/2). Therefore, at visible light wavelength (400-800 nm), the size range between 200-400 should have excellent ability to scatter visible light. In comparison with nanosize TiO_2 (size 35 and 60 nm), it was observed that the uncoated FT250 and coated FTT300 also showed the better blue light protection in term of PPF values. However, these submicronsize TiO_2 resulted in lower SPF and UVAPF values than those nanosize TiO_2.

The effect of the particle size of yellow, red, and black iron oxides on UV and visible light protection were found that the scattering efficiency goes down as the size of particle increases to micronsize. In addition, the results clearly suggested that iron oxides themselves have no ability to contribute protection of UVB, UVA, and blue/visible light.

The effect of surface coating of coated nanosize TiO_2 having size 35 and 60 nm seemed to show not significant difference on both UV and visible light protection. In contrast to uncoated nanosize TiO_2 (T35), it showed significantly poorer UVB and UVA protection than TD35 and TT60. The uncoated TiO_2 trend to form agglomerated particles, resulting to reduce the amount of surface area available to absorb light. This study has suggested that the dispersion of nanosize TiO_2 in suitable dispersing agents before mixing with other ingredients in formulations will decrease the agglomeration of particles and provide superior protection.

Although iron oxide is not classified as a UV filter, but its photoprotective action in visible light wavelength has motivated its use in foundation colored sunscreens. For improving the protective efficiency and the cosmetically undesired whiteness formulations, the blended iron oxides were combined with single TiO_2. The UV and visible light protection of all nanosize TiO_2 (T35, TD35, TT60) and coated submicronsize TiO_2 (TT300) can be enhanced by mixing them with blended iron oxides. The addition of blended iron oxides having optimal scattering particle size

(size 200 nm) to such white sunscreens greatly enhanced their photoprotective ability, due to the effect of scattering by increasing the mean path length of light.

The combination of color inorganic sunscreens was improved the UVB and UVA protection by the addition of organic UV filter. The addition of TBPT in the color sunscreens containing nanosize or submicronsize TiO_2 (i.e. FTT60-R, FTT300-R) can enhance superior protection in both UV and visible light wavelength ranges. This resulted to obtain the highest SPF and UVAPF values in colored sunscreen containing TT60 (size 60 nm) and also improved two-times of both SPF and UVAPF values in color sunscreen containing TT300 (size 300 nm). In addition, the varying concentration of each component of FTT60-R+TBPT (F8) was found that it was composed of an optimum component that can provide SPF, UVAPF similar to the target of this thesis (SPF 50+, UVAPF at least 1/3SPF, critical wavelength ≥ 370 nm) and optimum value of PPF vales. That components included nanosize TiO_2 (size 60 nm), blended iron oxides (size 200 nm), both coated with triethoxycaprylylsilane, and TBPT.

For providing the practically values that could claim on the product’s label. The degree of UVB, and UVA protection of selected formulations were measured using the internationally standard methods. The results were observed that F8 (FTT60-R+TBPT) possessed the highest SPF and UVAPF values and providing the requirement of EC (ratio of UVAPF/SPF greater than 0.33) and had λ_C higher than 370 nm. This study also suggested that the balancing of UVB and UVA protection of filters is important consideration for the formulation of sunscreens, the filters should have different maximum absorption to cover entire UVB and UVA wavelength and to fulfill EC requirement.

The effect of base formulations in which the selected UV and Vis filters (i.e. triethoxycaprylylsilane-treated TiO_2 having size 60 nm, blended iron oxides and TBPT) were incorporated. The appearance of bases cream was creamy, mousse was silky, and lotion was glossy and like-yoghurt. From visual observation, the formulations ranking from the most to the least translucent were lotion, mousse and cream. The translucency of the base formulations greatly affected the protective ability against blue light. As discussed above, this may be explained by the RI of the base formulation, which is equal to the ratio of the speed of light traveling in air and the speed of light traveling in that base. As light can travel in transparent base with faster speed than in opaque base. Therefore, RI of base in the form of lotion is lower than mousse and cream, respectively. The lowest RI of lotion resulted in the big difference in RI between filters and the base. Thus, the highest scattering efficiency against blue light is obtained.

Moreover, the lotion foundation colored sunscreen was more effective than commercial sunscreens available on the market in protecting the blue light. Finally, it is clear that different physicochemical properties of inorganic UV filters/pigments play a crucial role in their ability to protect against UV and blue/visible light. An understanding the effects of these different properties as described will be helpful in formulating the efficient foundation colored sunscreens in UV and blue/visible light protection. In addition, this thesis suggests that to maximize protection in the UV and blue/visible light wavelengths, the foundation colored sunscreens should be selected.

Suggestion for future studies

1. The RI is a factor influencing to the scattering ability in visible light. Hence, the RI of inorganic UV filters/pigments should be determined.

2. The method for evaluation of visible light protection has not yet been officially establish. The efficacy and safety of the developed sunscreen may be confirmed by performing in *in vivo* or in-use study.

REFERENCES

1. Thailand food and drug administration. Determination of UV filters that may be used as ingredients in sunscreen products. In: Ministry of public health, editor. 2017.

2. European commission. Cosmetic ingredient database (Cosing) - List of UV filters allowed in cosmetic products Annex VI of the regulation No 1223/2009, 2020.

3. Stiefel C, Schwack W. Photoprotection in changing times - UV filter efficacy and safety, sensitization processes and regulatory aspects. Int J Cosmet Sci. 2015; 37(1): 2-30.

4. Dupont E, Gomez J, Bilodeau D. Beyond UV radiation: a skin under challenge. Int J Cosmet Sci. 2013; 35(3): 224-32.

5. Liebel F, Kaur S, Ruvolo E, Kollias N, Southall MD. Irradiation of skin with visible light induces reactive oxygen species and matrix-degrading enzymes. J Invest Dermatol. 2012; 132(7): 1901-7.

6. Randhawa M, Seo I, Liebel F, Southall MD, Kollias N, Ruvolo E. Visible light induces melanogenesis in human skin through a photoadaptive response. PLoS One. 2015; 10(6): e0130949.

7. Mahmoud BH, Ruvolo E, Hexsel CL, Liu Y, Owen MR, Kollias N, et al. Impact of long-wavelength UVA and visible light on melanocompetent skin. J Invest Dermatol. 2010; 130(8): 2092-7.

8. Nahhas AF, Abdel-Malek ZA, Kohli I, Braunberger TL, Lim HW, Hamzavi IH. The potential role of antioxidants in mitigating skin hyperpigmentation resulting from ultraviolet and visible light-induced oxidative stress. Photodermatol Photoimmunol Photomed. 2019; 35(6): 420-8.

9. Nakashima Y, Ohta S, Wolf AM. Blue light-induced oxidative stress in live skin. Free Radic Biol Med. 2017; 108: 300-10.

10. Duteil L, Cardot-Leccia N, Queille-Roussel C, Maubert Y, Harmelin Y, Boukari F, et al. Differences in visible light-induced pigmentation according to wavelengths: a clinical and histological study in comparison with UVB exposure. Pigment Cell Melanoma Res. 2014;

27(5): 822-6.

11. Teramura T, Mizuno M, Asano H, Naru E, Kawara S, Kamide R, et al. Prevention of photosensitivity with action spectrum adjusted protection for erythropoietic protoporphyria. J Dermatol. 2018; 45(2): 145-9.

12. Schalka S, Sant'Anna AFA, Agelune CM, De Melo C. Pereira V. Sunscreen protection against visible light: a new proposal for evaluation. Surg. Cosmet. Dermatology. 2012; 3(4): 45-52.

13. Castanedo-Cazares JP, Hernandez-Blanco D, Carlos-Ortega B, Fuentes-Ahumada C, Torres-Alvarez B. Near-visible light and UV photoprotection in the treatment of melasma: a double-blind randomized trial. Photodermatol Photoimmunol Photomed 2014; 30(1): 35-42.

14. Martini APM, Maia Campos P. Influence of visible light on cutaneous hyperchromias: clinical efficacy of broad-spectrum sunscreens. Photodermatol Photoimmunol Photomed. 2018; 34(4): 241-8.

15. Biga LM, Dawson S, A. H, Hopkins R, Kaufmann J, Lemaster M, et al. Anatomy & physiology. Oregon State University, United states: Openstax; 2019.

16. Honari G, Maibach H. Applied dermatotoxicology. Honari, H.M. (Ed.). Boston: Academic press; 2014.

17. Shimizu H. Shimizu's textbook of dermatology. Hokkaido, Japan: Hokkaido University Press/Nakayama Shoten; 2007.

18. Kolarsick PAJ, Kolarsick MA, Goodwin C. Anatomy and physiology of the skin: Erratum. J Dermatol Nurs. 2011; 3(6): 366.

19. Svobodova A, Vostalova J. Solar radiation induced skin damage: review of protective and preventive options. Int J Radiat Biol. 2010; 86(12): 999-1030.

20. Murphery MB, Miao JH, Zito PM. Histology, stratum corneum. Statpearls publishing. 2019: 1-4.

21. Baranoski S, Ayello E, Levine JM, Leblanc K, Tomic-Canic M. Skin: An

essential organ. In wound care essentials: practice principles: Fourth Edition. Wolters kluwer health. 2015.

22. Holick MF. Biological effects of sunlight, ultraviolet radiation, visible light, infrared radiation and vitamin D for health. Anticancer Res. 2016; 36(3): 1345-56.

23. Tanaka Y, Motomura H, Jinno M. Biological defenses against ultraviolet, visible Light, and near-infrared exposure. Optics and Photonics Journal. 2016; 06(01): 8-14.

24. Krutmann J, Morita A, Chung JH. Sun exposure: what molecular photodermatology tells us about its good and bad sides. J Invest Dermatol. 2012; 132(3 Pt 2): 976-84.

25. Hönigsmann H. Erythema and pigmentation. Photodermatol Photoimmunol Photomed. 2002; 18(2): 75-81.

26. Matsumura Y, Ananthaswamy HN. Toxic effects of ultraviolet radiation on the skin. Toxicol Appl Pharmacol. 2004; 195(3): 298-308.

27. Brenner M, Hearing VJ. The protective role of melanin against UV damage in human skin. Photochem. Photobiol. 2008; 84(3): 539-49.

28. Assefa Z, Van Laethem A, Garmyn M, Agostinis P. Ultraviolet radiation-induced apoptosis in keratinocytes: on the role of cytosolic factors. Biochim Biophys Acta. 2005; 1755(2): 90-106.

29. D' Orazio J, Jarrett S, Amaro-Ortiz A, Scott T. UV radiation and the skin. Int J Mol Sci. 2013; 14(6): 12222-48.

30. Pittayapruek P, Meephansan J, Prapapan O, Komine M, Ohtsuki M. Role of matrix metalloproteinases in photoaging and photocarcinogenesis. Int J Mol Sci. 2016; 17(6).

31. Poon F, Kang S, Chien AL. Mechanisms and treatments of photoaging. Photodermatol Photoimmunol Photomed. 2015; 31(2): 65-74.

32. Sklar LR, Almutawa F, Lim HW, Hamzavi I. Effects of ultraviolet radiation, visible light, and infrared radiation on erythema and pigmentation: a review. Photochem Photobiol Sci. 2013; 12(1): 54-64.

33. Oplander C, Hidding S, Werners FB, Born M, Pallua N, Suschek CV. Effects of blue light irradiation on human dermal fibroblasts. J Photochem Photobiol B. 2011; 103(2): 118-25.

34. Gupta AK, Gover MD, Nouri K, Taylor S. The treatment of melasma: a review of clinical trials. J Am Acad Dermatol. 2006; 55(6): 1048-65.

35. Schalka S. New data on hyperpigmentation disorders. J Eur Acad Dermatol Venereol. 2017; 31(5): 18-21.

36. Regazzetti C, Sormani L, Debayle D, Bernerd F, Tulic MK, De Donatis GM, et al. Melanocytes sense blue light and regulate pigmentation through Opsin-3. J Invest Dermatol. 2018; 138(1): 171-8.

37. Ramanujam V-MS, Anderson KE. Porphyria diagnostics-part 1: a brief overview of the porphyrias. Curr Protoc Hum Genet. 2015; 86: 1-6.

38. Young AR, Claveau J, Rossi AB. Ultraviolet radiation and the skin: photobiology and sunscreen photoprotection. J Am Acad Dermatol. 2017; 76(3S1): S100-S9.

39. Manaia EB, Kaminski RCK, Corrêa MA, Chiavacci LA. Inorganic UV filters. Braz J Pharm Sci. 2013; 49: 201-9.

40. Smijs TG, Pavel S. Titanium dioxide and zinc oxide nanoparticles in sunscreens: focus on their safety and effectiveness. Nanotechnol Sci Appl. 2011; 4: 95-112.

41. Osterwalder U, Sohn M, Herzog B. Global state of sunscreens. Photodermatol Photoimmunol Photomed. 2014; 30(2-3): 62-80.

42. International organization for standardization. Cosmetics-sun protection test methods-*in vivo* determination of the sun protection factor (ISO 24444:2010). Geneva, Switzerland, 2010.

43. Miksa S, Lutz D, Guy C. New approach for a reliable *in vitro* sun protection factor method Part I: Principle and mathematical aspects. Int J Cosmet Sci. 2015; 37(6): 555-66.

44. European Commission. On the efficacy of sunscreen products and the claims made relating thereto. Off J Eur Union. 2006; 265: 39-43.

45. Department of health & human services. Labeling and effectiveness testing; sunscreen drug products for over-the-counter human use. Final rule. 2011; 76: 35620-65.

46. Thailand fod and drug administration. Labeling the sun protection value of sunscreen products. In: Ministry of public health, editor. 2017.

47. National industrial chemicals notification & assessment Scheme. Sunscreen products—evaluation and classification; Standards Australia (AZ/NZS 2604:2012). Sydney, Australia, 2012.

48. Japan Cosmetic Industry Association. Measurement standards for UVA protection efficacy. (JCIA:2013). Tokyo, Japan, 2013.

49. Pelizzo M, Zattra E, Nicolosi P, Peserico A, Garoli D, Alaibac M. *In vitro* evaluation of sunscreens: an update for the clinicians. ISRN Dermatol. 2012: 352135.

50. International organization for standardization. Determination of sunscreen UVA photoprotection *in vitro* (ISO 24443:2012). Geneva, Switzerland, 2012.

51. The European Cosmetic and Perfumery Association. *In vitro* method for the determination of the UVA protection factor and "critical wavelength" values of sunscreen products. Bruxelles, Belgium, 2011.

52. Moseley H, Cameron H, MacLeod T, Clark C, Dawe R, Ferguson J. New sunscreens confer improved protection for photosensitive patients in the blue light region. Br. J. Dermatol. 2001; 145: 789-94.

53. Delamour E, Miksa S, Lutz D. Are you ready to protect yourself from blue light ?. New *in vitro* method allowing the blue light protection assessment of sunscreens. Euro Cosmetics. 2017: 22-6.

54. Schalka S, de Paula Correa M, Sawada LY, Canale CC, de Andrade TN. A novel method for evaluating sun visible light protection factor and pigmentation protection factor of sunscreens. Clin Cosmet Investig Dermatol. 2019; 12: 605-16.

55. Rosen CF, Jacques SL, Stuart ME, Gange RW. Immediate pigment darkening: visual and reflectance spectrophotometric analysis of action spectrum. Photochem. Photobio.

1990; 51(5): 583-8.

56. European Commission. Cosmetic ingredient database (Cosing)-list of colorants allowed in cosmetic products (Reference number 135-137), 2019.

57. Shokri J, Hassanzadeh D, Ghanbarzadeh S, Arash Z, Farahani A, Adibkia K. The effect of beta-cyclodextrin on percutaneous absorption of commonly used Eusolex® sunscreens. Drug Res (Stuttg). 2013; 63(11): 591-6.

58. Wang SQ, Balagula Y, Osterwalder U. Photoprotection: a review of the current and future technologies. Dermatol Ther. 2010; 23(1): 31-47.

59. Heurung AR, Raju SI, Warshaw EM. Benzophenones. Dermatitis. 2014; 25(1): 3-10.

60. Lim HW, Arellano-Mendoza MI, Stengel F. Current challenges in photoprotection. J Am Acad Dermatol. 2017; 76(3S1): S91-S9.

61. European Commission. Commission regulation (EU) 2017/238, amending Annex VI to Regulation (EC) No 1223/2009, 2017.

62. Schlumpf M, Cotton B, Conscience M, Haller V, Steinmann B, Lichtensteiger W. *In vitro* and *in vivo* estrogenicity of UV screens. Environ Health Perspect. 2001; 109(3): 239-44.

63. Kullavanijaya P, Lim HW. Photoprotection. J Am Acad Dermatol. 2005; 52(6): 937-58; quiz 59-62.

64. Janjua N, Mogensen B, Andersson A-M, Petersen J, Henriksen M, Skakkebaek N, et al. Systemic absorption of the sunscreens benzophenone-3, octyl-methoxycinnamate, and 3-(4-Methyl-Benzylidene) camphor after whole-body topical application and reproductive hormone levels in humans. J Invest Derm. 2004; 123: 57-61.

65. Maillan P. UV protection of artificially coloured hair using a leave-on formulation. Int J Cosmet Sci. 2002; 24: 117-22.

66. Santos BAMC, da Silva ACP, Bello ML, Gonçalves AS, Gouvêa TA, Rodrigues RF, et al. Molecular modeling for the investigation of UV absorbers for sunscreens:

triazine and benzotriazole derivatives. J Photoch Photobio A. 2018; 356: 219-29.

67. Couteau C, Paparis E, Chauvet C, Coiffard L. Tris-biphenyl triazine, a new ultraviolet filter studied in terms of photoprotective efficacy. Int J Pharm. 2015; 487(1-2): 120-3.

68. Couteau C, Pommier M, Paparis E, Coiffard L. Study of the efficacy of 18 sun filters authorized in European Union tested *in vitro*. Pharmazie. 2007; 62: 449-52.

69. Shaath NA. Ultraviolet filters. Photochem Photobiol Sci. 2010; 9(4): 464-9.

70. Huglin D. Advanced UV absorbers for the protection of human Skin. Chimia. 2016; 70: 496-501.

71. Kockler J, Oelgemöller M, Robertson S, Glass DB. Influence of titanium dioxide particle size on the photostability of the chemical UV-Filters butyl methoxy dibenzoylmethane and octocrylene in a microemulsion. Cosmetics. 2014; 1(2).

72. Serpone N, Dondi D, Albini A. Inorganic and organic UV filters: Their role and efficacy in sunscreens and suncare product. Inorganica Chim Acta. 2007; 360: 794-802.

73. Mitchnick M, Fairhurst D, Pinnell S. Microfine zinc oxide (Z-Cote) as a photostable UVA/UVB sunblock agent. J Am Acad Dermatol. 1999; 40: 85-90.

74. Lorenz C, Tiede K, Tear SP, Boxall A, Goetz N, Hungerbühler K. Imaging and characterization of engineered nanoparticles in sunscreens by electron microscopy, under wet and dry conditions. Int J Occup Environ health. 2010; 16: 406-28.

75. Lewicka ZA, Benedetto AF, Benoit DN, Yu WW, Fortner JD, Colvin VL. The structure, composition, and dimensions of TiO_2 and ZnO nanomaterials in commercial sunscreens. J Nanopart Res. 2011; 13(9): 3607.

76. Bernauer U, Chaudhry Q, Coenraads PJ, Degen G, Dusinska M, Gawkrodger D, et al. SCCS Opinion on titanium Dioxide (nano form) COLIPA n S75 - SCCS/1516/13 (Reversion of 22 April 2014), 2014.

77. Tyner K, Wokovich A, Godar D, Doub W, Sadrieh N. The state of nano-sized titanium dioxide (TiO_2) may affect sunscreen performance. Int J Cosmetic Sci. 2011; 33: 234-44.

78. Dondi M, Blosi M, Gardini D, Chiara Z. Ceramic pigments for digital

decoration inks: an overview. Ceram Forum Int. 2012; 89: E59-E64.

79. Gueli A, Bonfiglio G, Pasquale S, Troja S. Effect of particle size on pigments colour. Color Res Appl. 2016; 42.

80. Kaye ET, Levin JA, Blank IH, Arndt KA, Anderson RR. Efficiency of opaque photoprotective agents in the visible light range. Arch Dermatol. 1991; 127(3): 351-5.

81. Moyal D. The development of efficient sunscreens. Indian J Dermatol VE. 2012; 78(7): 31-4.

82. Auger J-C, Martinez V, Stout B. Theoretical study of the scattering efficiency of rutile titanium dioxide pigments as a function of their spatial dispersion. J Coat Technol Res. 2009; 6: 89-97.

83. Changyong O, Yoon S, Kim E, Han J, Chung H, Jeong H-J. Non-destructive determination of TiO_2 concentration in cream formulation using Raman spectroscopy. J Pharm Biomed Anal. 2010; 53: 762-6.